UNIVERSIDAD POLITÉCNICA DE VALENCIA

Departamento de Ingeniería Mecánica y de Materiales

TESIS DE MASTER

Multibody Approach For Railway Dynamic Analysis

Presentada por: D. Ramy Elsayed Shaltout

Dirigida por: Dr. D. Luis Baeza González

Valencia, Julio de 2010

MASTER THESIS

Multibody Approach For Railway Dynamic Analysis

For obtaining

the title of

Official Master of Mechanical and Material Engineering

by

Ramy Elsayed Shaltout

In

Department of Mechanical and Material Engineering

Technical University of Valencia

Under supervision of

Dr. Luis Baeza González

Valencia, July 2010

TESIS DE MASTER

Multibody Approach For Railway Dynamic Analysis

---

que para la obtención

del título de

Master Oficial en Ingeniería Mecánica y Materiales

presenta

D. Ramy Elsayed Shaltout

en el

Departamento de Ingeniería Mecánica y de Materiales

de la Universidad Politécnica de Valencia

Dirigida por

Dr. D. Luis Baeza González

Valencia, Julio de 2010

Tesis Master

Multibody Approach For Railway Dynamic Analysis

Presentada por: D. Ramy Elsayed Shaltout

Dirigida por: Dr. D. Luis Baeza González

TRIBUNAL CALIFICADOR

Presidente: Dr. D. _____

Vocales: Dr. D. _____

Dr. D. _____

En Valencia, a de Julio de 2010.

Abstract

In the work presented, a computational tool used for the dynamic simulation of railway vehicle systems was developed using multibody systems formulations. The model based on the multibody techniques developed by Shabana. With respect to other exciting methodologies the proposed one make use of a combined frame of references that permit the use of independent coordinates, with out the possibility to have singularity configurations depending on the rotation sequence. The combined frame of references used as a base for the formulation and modeling of wheel-rail contact problem with high precision. The program was designed for considering with a flexible form the different configuration of railway vehicles. The main structure of the program has the ability of making changes for enhancement of the wheel-rail contact model or the implementation of dynamic structure of the track, which considered to be future aspects for a PHD dissertation. The model used was applied to make a simulation for single bogie , also for a complete vehicle with two bogies. The obtained results of the dynamic response for a defined track composed of, tangent segment, transition curve which take the form of a clothoid curve, and finally circular curve with constant radius. The calculations were made for different velocities, lower than the critical in which the vehicle responded in stable form, and higher than the critical at which the instability of the vehicle was studied.

Resumen

En este trabajo se ha llevado a cabo el desarrollo de una herramienta computacional para la simulación dinámica de vehículos ferroviarios. El modelo está basado en técnicas multicuerpo debidas a Shabana. Con respecto a otras metodologías existentes, la propuesta hace uso de un conjunto de sistemas de referencia que permite el uso de coordenadas independientes sin la posibilidad de configuraciones singulares debida a grandes giros. El conjunto de sistemas de referencia sirve de base para formular de manera precisa el problema de contacto rueda-carril. El programa está diseñado para considerar de forma flexible distintas configuraciones de vehículo así como diversas geometrías de trazado. La estructura del programa está abierta a cambios orientados a la mejora del modelo de contacto rueda-carril o a la implementación de la dinámica estructural de la vía, aspectos del modelado que serán hitos en el desarrollo de una futura tesis doctoral. Se han llevado a cabo simulaciones de un bogie y de un vehículo completo con bogies. Los resultados corresponden a la respuesta dinámica asociada al trazado de una vía definida por un tramo recto, clotoide de transición y plena curva. Los cálculos fueron realizados para velocidades subcríticas en las que el vehículo responde de forma estable, y supercríticas en la que se aprecia el fenómeno de inestabilidad dinámica.

Resum

En este treball s'ha dut a terme el desenvolupament d'una ferramenta computacional per a la simulació dinàmica de vehicles ferroviaris. El model està basat en tècniques multicossos desenvolupades per Shabana. Respecte a altres metodologies existents, la proposta fa ús d'un conjunt de sistemes de referència que permet l'ús de coordenades independents sense la possibilitat de configuracions singulars degudes a grans girs. El conjunt de sistemes de referència servix de base per a formular de manera precisa el problema de contacte roda- carril. El programa està dissenyat per a considerar de forma flexible distintes configuracions de vehicle així com diverses geometries de traçat. L'estructura del programa està oberta a canvis orientats a la millora del model de contacte roda-carril o a la implementació de la dinàmica estructural de la via, aspectes del modelatge que seran fites en el desenvolupament d'una futura tesi doctoral. S'han dut a terme simulacions d'un bogi i d'un vehicle complet amb bogis. Els resultats corresponen a la resposta dinàmica associada al traçat d'una via definida per un tram recte, clotoide de transició i plena corba. Els càlculs van ser realitzats per a velocitats subcrítiques en les que el vehicle respon de forma estable, i supercrítiques en la que s'aprecia el fenomen d'inestabilitat dinàmica.

Keywords

Multibody system Dynamics, Track parametrization, Railway Dynamics, Wheel-Rail Contact, Creep Forces.

Palabras Clave

Dinámica de sistemas de multicuerpos, Parametrización de la vía, Dinámica de vehículos ferroviarios, Contacto rueda-carril, Fuerzas tangenciales al contacto.

A mi familia

A mis amigos

Agradecimientos/ Acknowledgments

Agradecimientos/ Acknowledgments

En primer lugar quiero expresar mi agradecimiento a mi director Luis Baeza por su orientación, ayuda y apoyo durante la realización de esta Tesis, así como por dirigirme mediante sus amplios conocimientos y experiencia profesional. De él he aprendido que para llegar lejos en la investigación hay que trabajar de manera incansable. He sido un privilegiado al haberlo tenido como director de Tesina, habiéndome beneficiado de sus cualidades como profesor e investigador. Me ha proporcionado la inmensa motivación que ha de ser siempre el estado anímico de un investigador. Gracias por todo.

Quiero también mostrar mi agradecimiento en especial a los miembros del Área de Ingeniería Mecánica: Javier Fuenmayor, Juanjo, Paco, Alex, Javi, Pepe, y todos los professores del Máster. También doy las gracias a todos los compañeros del Máster. Quiero agradecer a mis amigos y compañeros del CITV y en especial a José, Fede, Rafa, Octavio, Enrique, Virginia, Héctor, Guillem, Fares y Justo por los momentos muy agradables que hemos tenido y las conversaciones tomando el café cada mañana. También doy las gracias a mis amigos del ITM, Lissette e Irma. Me habéis hecho sentir como si estuviera en casa, me habéis dado fuerza cuando la necesitaba. Los almuerzos, comidas y cenas que hemos compartido han sido momentos inolvidables.

Profundo agradecimiento también para Andrés Rovira, por su apoyo y consejos durante todo el tiempo que he pasado en Valencia, y por la experiencia que me ha aportado tanto en el trabajo como en la vida social. Gracias Andrés por todo el tiempo que hemos pasado conversando, por las rutas de bici que hemos hecho y por lo que vamos a hacer en el futuro.

Unas cuantas líneas son poco para mostrar mi aprecio hacia Mohamed y Antoine; doy gracias por haber tenido la suerte de contar con dos amigos como estos. Sus palabras eran como una guía para mí, mostrándome el camino. Siempre motivando, escuchando y esforzándose. A ellos les agradezco su preocupación, sus consejos y su

constante disposición a ayudar en el complejo camino que supone para un estudiante el inicio de una carrera investigadora. Nunca olvidaré lo que habéis hecho por mí. Muchas gracias.

I would like to thank all my Egyptian friends here in Valencia, Maher, Khaled, Ragab, Ali, Tarek. For all the moments that we have passed together and for the animation that they have given to me. many thanks for being beside me during the period that i have spent in Valencia, many thanks for all of you.
Finally i would like to say that my words would not be enough to transfer what I'm feeling inside me. My mother, with out you and your praying for me, i would not reach this level. My brothers, thanks for all your encouragements and animation during all this time.
To my friends Ahmed and Abd-El Rahaman, and all who have crossed my path during my lifetime, given me spiritual or intellectual guidance, appealed to my senses or my energy or my desire for adventures, or have otherwise challenged me to think in new ways, i thank you.

Contents

List of Figures

List of Tables

List of Symbols

Convention

a, A, γ	Scalar;
$\mathbf{a}$	Vector;
$\mathbf{A}$	Matrix;

Over script

$\bar{\mathbf{a}}$	Vector represented in Track frame of reference;
$\bar{\bar{\mathbf{a}}}$	Vector represented in Solid frame of reference;
$\dot{\mathbf{a}}$	First time derivative of a vector $\mathbf{a}$;
$\ddot{\mathbf{a}}$	Second time derivative of a vector $\mathbf{a}$;
$\tilde{\mathbf{a}}$	Skew-symmetric matrix;

Down script

$\underline{\mathbf{a}}$	Vector represented in Intermediate frame of reference;

Superscript

$\mathbf{a}^{\mathrm{T}}$	Transpose of a vector;
$\mathbf{A}^{\mathrm{T}}$	Transpose of a Matrix;

Subscript

a_r	Quantity referred to the rail;
a_w	Quantity referred to the wheel;
a_c	Quantity referred to the contact;
a_{CM}	Quantity referred to center of mass;

Latin Symbols

a,b	Longitudinal and transversal semi axis of the contact ellipse;
A,B	Geometrical functions related to the principle and transversal radii of curvature of the wheel and the rail;
$\mathbf{A}$	Transformation matrix from Track frame to Fixed frame;
$\mathbf{B}$	Transformation matrix from Solid frame to Track frame;
$\mathbf{B}_{zx}$	Transformation matrix from Intermediate frame to Track frame;
$C_{11}, C_{22}, C_{23}, C_{33}$	Creepage and spin coefficients from Kalker's theory;
$\mathbf{c}$	Damping coefficient;
$\mathbf{q}$, $\dot{\mathbf{q}}$, $\ddot{\mathbf{q}}$	Vectors of generalized coordinate, velocities and acceleration;
$\mathbf{Q}$	Generalized force vector;
E	Young's modulus;
G	Track gauge;
G	The combined shear modulus of rigidity of rail and wheel materials;
$\mathbf{k}$	Spring stiffness;
$\mathbf{K}$	Geometry parameter;
$\mathbf{I}$	Identity matrix;
$\boldsymbol{J}$	Inertia matrix;
J_{xx} J_{yy} J_{zz}	Moments of inertia with respect to the principal axes of a rigid body;
R	Radius of curvature;
X Y Z	Global reference frame;
$\mathrm{X_T Y_T Z_T}$	Track reference frame;
$\mathrm{X_S Y_S Z_S}$	Solid reference frame;
$\underline{\mathrm{X}}\,\underline{\mathrm{Y}}\,\underline{\mathrm{Z}}$	Intermediate reference frame;
$\mathbf{M}$	System mass matrix;
$\mathbf{M_c}$	Moment at the contact patch;
m	Rigid body mass;
$\boldsymbol{n}$	Principal unit normal vector;
$\boldsymbol{l}$	Principal unit longitudinal vector;
$\boldsymbol{t}$	Principal unit lateral vector;

Greek Symbols

δ	Indentation (or penetration) during contact;
γ	Conicity of the wheel profile;
$\boldsymbol{\omega}$	Solid angular velocity in the global frame of reference;
$\boldsymbol{\tau}$	Track angular velocity;
ν	Poisson's ratio;
κ	Curvature;
ξ_x	Longitudinal creepage;
ξ_y	Lateral creepage;
ξ_{sp}	Spin creepage;
ϕ	Roll angle;
θ	Pitch angle;
ψ	Yaw angle;

Abbreviations

CM	Centre of Mass;
MBS	MultiBody System;
K.E	Kinetic Energy;
DAE	Differential Algebraic Equations;
ODE	Ordinary Differential Equations;
F.O.R	Frame Of Reference;
I.P	Initial Position;

Chapter 1

Introduction

1.1 Introduction

Modeling and simulation in the field of railway dynamics is a complex interdisciplinary topic. The necessity for the enhancement of the performance of the railway vehicles and obtaining more safety and comfort conditions of the railway vehicles leads to more complex definition and description for all parameters affecting the model simulation of a railway vehicle systems. Then it was necessary to define a computational tool capable of the accurate description of such systems. The existing computational tools used in the dynamic analysis required not only in the purposes of enhancement of these systems including also facing the fast progress in the other means of transportation systems, but also for the design purposes and maintenance operations of the railway systems in order to avoid the time and material loses used in making prototypes for the studying of the simulation of parts and systems under study. Now it is easy to use the simulation solutions provided with the computational simulation programs to predict and make the necessary design modifications on the models before and during the operation of these parts in realistic working conditions of the railway systems. The aim of the work, is to introduce a computational tool used for the dynamic analysis of the railway systems with in the multibody system formulations, that consider the railway vehicles and rail guided systems as a connection of rigid bodies. In the presented work the dynamic include as a first stage, the track parameterizations and definition of the track geometry, the second stage is the dynamic analysis of the railway systems using the multibody formulations for rigid bodies, then a model of a railway vehicle was presented to validate the multibody program used in the dynamic simulation of the railway vehicle systems and the computational results obtained.

1.2 Work Motivation

The dynamic analysis of railway or other type of rail guided vehicles requires an accurate description of the track geometry. During the research and development of the new transportation solutions, the computational tools can be used to study problems related to the maintenance and operation of existing railway vehicles. The use of profiled- flanged steel wheels running on steel track in order to simultaneously support, guidance and traction was a brilliant concept in the early days in this industry. Nevertheless, the simplicity of the concept masked the complexity of the contact phenomenon [21, 24, 26]. The complex contact force developed in the wheel-rail interface strongly influence the dynamic behavior of the rail guided vehicle. Also the characteristics of the suspensions, the masses and inertia properties of the system elements, and the geometry of the track play an important rule in this issue. Such mentioned reasons and more reasons related to the ride comfort, wheel-rail wear and vehicle stabilities were a strong motivation for making such work presented. The main objective is to develop a computational program capable of making the simulation and dynamic analysis of railroad vehicles regarding the following topics.

- Development of a parameterized track model that allow the realistic analysis of the railroad guided vehicles.
- Definition of the mathematical formulations that describe and characterize the wheel-rail contact model.
- Definition of the creepage and calculation of the creepage forces and moments affecting the wheel-rail interaction model.
- Dynamic analysis of a railroad vehicle using multibody relations.
- Making dynamic simulation for a vehicle moving on the proposed track model in deferent operation scenarios.

1.3 Literature Review

Simulation of the dynamic behavior of railway vehicles is a complex topic in the railway dynamic field. Modern general-purpose softwares for the simulation of railway vehicle systems have included features that enable efficient dynamic analysis of the railway vehicles and vehicle-track interaction [4, 20, 30]. The dynamic behavior of railway vehicles relates to the motion or vibration of all the parts of the vehicle and is influenced by the vehicle design, particularly the suspension and the track on which the vehicle run. Due to this issue several models of simulation schemes were developed in which all the factors affecting the dynamics of a railway vehicle were studied, such as the model developed by S. Iwinicki and A. H. Wickens [10], in which a Matlab computer program was developed in order to validate the results obtained by experimental measurements from a 1/5 scale roller rig used to evaluate the design change of the vehicle suspension system in Manchester University. The model used

in the simulation and implemented in the Matlab code was, a four-axel vehicle with a body and two bogies has been used. Each bogie has a frame including two wheelsets. All the bogies and the wheelsets are assumed to be rigid bodies connected by massless suspension elements. The instability in 1/5 roller rig has clearly bean detected by the linear MATLAB program used and the model has provide more thorough re-examination of the effects of the errors due to the scaling and finite radius of the roller used, and usefulness of a roller rig analysis of railway behavior. During the last decades, the techniques using multibody approaches have evolved from manual graphics art to a highly specialized research field where the kinematics and dynamics of general mechanical systems are analyzed [20, 25, 29]. More efficient and reliable computer codes was developed to allow the formulation and the analysis of the dynamic behavior of a railway systems and solving the equations of motion of mechanical systems included with increasing the degree of complexity. Multibody computational methods can be used to simulate the dynamic effects of a vehicle components and the track, and the use of multibody algorithms which allow for the analysis of the non linear models, linearization schemes currently employed in railroad vehicle-track can be evaluated [26].

J. Pombo and J. Ambrósio [20, 23] has developed and implemented a computational tool suitable to study the dynamic behavior of rail guided vehicles in realistic operation conditions, an efficient multibody methodology was suggested and its computational implementation was discussed. The methodology proposed can be summarized in several points: the description of a three dimensional track model used for a roller coaster application [22, 23] and railway vehicle, obtaining realistic track conditions by definition and implementation of the track irregularities; development of a new methodology [21, 24] for the accurate prediction of the location of the contact points between the wheel and the rail surfaces; implementation of several creep force models in order to compute all the tangential forces at the contact patch defined in the wheel-rail interaction area; finally validation of the multibody code presented in this work with modeling of a railway vehicle used by Lisbon metro company, and its performance was studied in real operation conditions and in different operation scenarios. The numerical results obtained from the computational tool proposed and the results obtained from ADAMS/RAIL Computer package used to study and simulate the performance of two railway vehicles in real operation conditions, was compared with experimental tests made on the railway vehicles to validate the obtained results.

Shabana et al. [28] presented a non linear finite element formulation for modeling the rail structural flexibility in multibody railroad vehicle systems, it was considered to use two types of interpolations in the kinematic equations developed in the study;*the geometry interpolation* and the *deformation interpolation*. The coupling between the the rail deformation and geometry, contact coordinates, and non linear vehicle dynamics was considered. The main aim of the analysis was developing a new procedure that allows building complex track model used as an input to general purpose multibody computer program used in the dynamic analysis of railroad vehicle systems. This was achieved by the following consequence; first the track geometry was defined in a pre-processor computer program which produce an output *geometry file* including all information about the track elements of the space curve of the track

and the left and right rail in terms of position coordinates and rotations defined at the selected nodal points, then making a finit element model of the track in a finit element pre-processor computer based on the track material properties and geometry and the out put is a *finite-element*, finally the *geometry file* and the *finite-element* were used as an input to a general purpose multibody computer program in which the wheel-rail contact models are impelemented to study the dynamic behavior of the railroad vehicle.

E. Meli *et al.* [17] has developed a numerical model which reproduce the complete three-dimensional dynamics of a railway vehicle running on a generic track. The model has been developed with the objective of real-time implementation, in order to use the results to control the actuators of Hardware In the Loop(HIL) test rigs. The numerical model in the test rig has been realised in Matlab – Simulink^{TM} environment. The module was applied to a benchmark vehicle (The Manchester wagon). Comparison between the obtained results and the those obtained using a commercial multibody software package ADAMS/RAIL was shown. In the work presented by Meli et al, it was highlighted that the models used evaluate the deformation of the wheel and the rail in the contact zone by means of two different approaches. With respect to the existing models of railway multibody models, its features were more detailed modeling of wheel-rail contact problems.

The step of the track geometry description represents the first step in the solution of the dynamic analysis problem in which the pre-processing operation for the track geometry is made using the input data provided by the manufacturing or the industry to be the input for the track geometry program, then the output data generated in such step provided to the next step which include the multibody dynamic analysis program used to simulate the behavior of the rail guided vehicle. The track model used here in the dynamic simulation must be presented as a parameterized track in order to obtain the required information of the track and all the kinematic and dynamic parameters as a function of the parameter used here which is the distanc covered by the vehicle or the track length, there is two main approaches used in the parameterization of the track centerline, the first one uses a combination of analytical segments, straight, transition and plane curve segments to form the track model used in the analysis. The second approach depends on the use of piece wise cubic interpolation schemes to make an interpolation between provided data points representing the track to find the parameterized track centerline curve. In both approaches it was necessary to define the cant angle of the track to provide a complete definition of the track. In the methodology presented in the work, it was proposed to use analytical segments to form the presented track, the track model presented in this work consists of tangent or straight line segment, followed by transition curve segment, and finally the plane curve segment with constant radius R. The pre-processed data defined in the track geometry step was provided to a multibody program used for the dynamic analysis of the railroad vehicle, starting with the study and the analysis of a general solid moving along the proposed track. As a next step the analysis of wheelset moving along the track and then the combination between the two solids in the step of the definition of the train vehicle model proposed in the work in the proceeding context.

J. Pombo [22, 23] developed an appropriate methodology for the accurate description of the track centerline geometry, in the frame work of multibody dynamics. A pre-processing step was made to achieve the computational efficiency for the definition of spatial geometry of the centerline based on the data given by the user. Starting with the roller coaster application, four different interpolation schemes was used in the definition of the spatial track centerline. All the information and the data of the right and left rail was stored in a tabulated manner in which interpolation between the entires were made to obtain the required information. The application was extended to be used in the definition of railway track application in which the rail irregularities were implemented and piecewise interpolation schemes were used to parametrize the track irregularities as well as the input data, to obtain the track centerline as a function of the track length.
Shabana *et al.* [29] use an analytical track description defined by three step procedure: i)Projection, which define the planar curve obtained by projecting the track centerline onto the horizontal plane; ii) Development, which defines an elevation angle; iii) Super-elevation, which defines the track cant angle. In his formulation, a relationship between the arc-length of actual curve and arc-length of the projected curve is stated. Then, the track centerline is defined by providing information about the horizontal curvature as a function of the projected arc-length, the vertical development angle as a function of actual arc-length and the cant angle as a function of the projected arc-length. During the dynamic analysis, the rail space curve are obtained by means of absolute nodal coordinate formulation, leading to an isoparametric beam element that can be conveniently used to describe curved rigid and flexible rails. The method considered each rail as a separate body in order to account for relative motion. The method used by Shabana [28] in the definition of the track pre-processing step, basically depends on the definition of the *geometry file* produced , the input data for this program use the industry data such as the curvature, super-elevation and development. The out put data of the pre-processing stage was used in the next stage which is the development of a finite element pre-processor computer program. Description of the rail deformation was discussed which based on the finite element floating frame of reference formulation [25]. The use of this formulation allows for arbitrary rigid body displacement of the track structure, it also allows treating the two rails as one body or two separate bodies.
The fundamental component common to all conventional railway vehicles is the wheelset [20]. The movement of the wheelset over the track is characterized by a complex interaction [4, 26] where lateral translation as well as yaw and roll rotations are observed. The formulation of the problem of contact between the wheel and the rail is complex task and has been the subject of several investigations which presented different solutions [21, 24, 27]. Two approaches can be used for solving the problem of wheel-rail contact in railroad dynamics. The first is the commonly called constraint approach, in which non-linear kinematic contact constraint equations are introduced. In this approach, the contact surfaces are represented in a parametric form using the differential geometry methods. The coordinates of the contact points can be predicted online during the dynamic simulation by introducing surface parameters that describe the contact surface geometries. The second is the elastic approach, in which

the wheelset is assumed to have six degrees of freedom with respect to the rails. The local deformation of the contact surface at the contact point is allowed and the normal contact forces are defined using Hertz's contact theory or in terms of assumed stiffness and damping coefficients. This type of approach allows the separation between the wheel and the rail and allows multiple contact points to be managed. One of the main problems correlated with this approach is the definition of the contact point location online. In most elastic force models, the three-dimensional contact problem is reduced, for the sake of efficiency, to a two-dimensional problem when the location of the contact points is searched for. Both of these approaches allow the component of the contact force normal to the surfaces to be defined. In the constraint method these forces are calculated as the Lagrange multipliers that, together with the system generalized coordinates and the surface parameters time derivatives, constitute the unknown vector of the differential algebraic equation system that describes the vehicle dynamics. In the elastic approach the normal component of the contact force at the contact point is calculated as a function of the penetration between the surfaces. The contact problem can be divided into three distinct but correlated tasks: the contact geometry, the contact kinematics, and contact mechanics. Contact geometry is the problem of defining the location of the contact point on the profiled surfaces taking into account the geometric contact constraints which impose constraints upon the relative displacements and orientations of the contacting bodies. Contact kinematics defines the creepages (normalized relative velocities) at the point of contact. Contact mechanics determines the tangential creep forces and spin moment on the basis of three-dimensional rolling contact theories.

Shabana *et al.* [27] developed a new elastic force contact formulation for the dynamic simulation of the wheel-rail interaction. In this contact formulation, four surface parameters are introduced in order to be able to describe the geometry of the surfaces of the two bodies that come in contact. The method developed in the mentioned investigation exploits features of multibody computational algorithms that allow adding arbitrary first order differential equations. A differential equation associated with the rail arc length and expressed in terms of the wheel generalized co-ordinates and velocity is used to accurately predict the location of the points of contact between the wheel and the rail. This first order differential equation is integrated simultaneously with the dynamic equations of motion of the wheel-rail system, thereby defining the rail arc length traveled by the wheel. This arc length is used with an optimized search algorithm to determine all possible contact regions. Pombo [21, 24] presented a new general formulation for the accurate prediction of the location of the contact points on the wheel and rail surfaces. The mentioned model has been proposed and implemented in a general multibody program used in the dynamic analysis of railway vehicles. The coordinates of the contact points are predicted online during the dynamic analysis by introducing the surface parameters that describe the geometry of the contact surfaces. This method was applied to study specific problems inherent to the railway dynamics such as the two points of contact scenario. The methodology to look for the candidates for contact points is fully independent for the wheel tread and for the wheel flange. The used formulation also allowed for investigations related to hunting instability and prediction of wheel climbing, which are very important to

study derailment phenomena. The methodology used [20] for the parameterization of the wheel and rail surfaces and for the description of the wheel-rail contact phenomenon was general, since it was able to represent any spatial configuration of the wheels and rails and any wheel and rail profiles, even the ones obtained from direct measurements. Because the wheels are treated separately, the used approach allowed dealing with railway vehicles either with conventional wheelsets, like trains, or with independent wheels, such as in many of the trams in operation.
In the contact model used by E. Meli *et al.* [17] the contact point position is calculated offline by means of a procedure based on the simplex method. This procedure was used to generate a three dimensional lookup table used in the real-time simulation to find the position of the contact points as a function of wheelset-rail relative displacement, described by three coordinates (the lateral wheelset displacement, the roll and yaw wheelset angle). The procedure was numerically sufficiently efficient and allows multiple contact points to be managed. The method used here in solving the wheel-rail contact problem based on the elastic approach, in which the wheel is considered to have six DOF with respect to the rail and the normal contact forces are defined in terms of the indentation between the surfaces and using Hertz contact theory. The main problem encountered in when using the elastic approach, is the determination of the contact points. For sake efficiency, the three dimensional contact problem is usually reduced to a two dimensional problem [17] when searching for the contact points. In the dynamic analysis of railway vehicles, the evaluation of the wheel-rail contact forces is repeated many times. Then, short calculation time algorithm should be used taking the computational cost of the model implemented in the multibody computer program used in the analysis. The method used in the work here for calculating the tangential contact forces and moments is Kalker linear theory of rolling contact [12–15, 26], this theory based on the assumptions that the existence of small creepages and spin creep, and the area of slip is so small that its influence can be neglected. Under these assumptions, the adhesion zone is assumed to cover the entire area of contact. This method doesn't include the saturation effect of the friction force and, therefore, it is limited to cotact problems with small creepage values.
Due to the simplicity and computational implementation easiness, Cartesian coordinates are used [29] in this work to formulate the equations of motion of the multibody systems. No kinematic constraints are added to the formulation, to avoid the complexity produced from the Differential Algebraic Equations (DAE), also the instabilities in the integration process, produced from the substitution of the algebraic equations of the system by their counterpart (ODE), are avoided. Then the equations of motion developed in this work are set of Ordinary Differential Equations (ODE) solved by numerical integration algorithms. Two approaches are often used to formulate the dynamic equations of motion of a mechanical systems: the *Newtonian* and the *Lagrangian* approaches. In the *Newtonian* approach, vector mechanics is used to develop the dynamic equations, in this approach the equilibrium position of each body is first studied separately, and it can be used relatively for simple systems and is not suited for the analysis of complex systems such as railroad vehicles. In the *Lagrangian* approach, scalar quantities such as the virtual work and the kinetic and potential energies are used to develop the equations of motion of the body. In this case

there is no need to study the equilibrium of the bodies in the system separately [3, 29]. In this work the *Lagrangian* approach is used to develop the equations of motion of the multibody systems. The concept of the generalized coordinates is fundamental in the Lagrangian formulation of the equations of motion. For unconstrained motion proposed here in the formulation, six degrees of freedom are used for each body used in the multibody system; three coordinate are used to describe the translation of a point on the body and the other three are used to describe the orientation of the body frame of reference. The parameterization of the finite rotation used in this work is the set of Euler angles, where the orientation of a point on the the rigid body is defined using three successive rotations. To avoid singularity problems that may exist in the formulation, the final rotation in the successive rotations proposed was assigned to the higher values of rotation angles.

1.4 Scope and work organization

The main objective of the work is to develop An appropriate method using the multibody approach to make dynamic analysis for the railway vehicle system applications in deferent application scenarios using a general multibody program developed in MATLAB environment, to achieve the required tasks implemented in the computer program. The importance of the work can be illustrated in the demonstration of railway system application modeling and make the necessary analysis for the studied system to study the dynamic behavior of the railway vehicle. The work proposed here was presented in the following five chapters. In the analysis of the systems used in the multibody formulations used in this work, it was necessary to define all the reference frames used in the analysis and define all the transformations used to define a point in a specific reference frame to other one, all the transformation matrices and the reference frame descriptions was provided in chapter (2). The first stage for any dynamic analysis of railway vehicle is the presentation of the track, because of its important effect on the dynamic behavior of vehicle. Chapter (3) provide the description and the parametrization method used to describe the track geometry used in this work. The dynamic analysis of railway systems requires the construction of the equations of motion of the vehicle model and the accurate description of its kinematic structure. For this purpose, a full descriptions of the models used in the construction of the railway vehicle used in this work was described and implemented in the multibody formulations used in the work were defined in chapter (4), starting from the kinematic analysis of a general solid negotiating the designed track, then a definition of the conventional wheelset including the definition of the contact geometry and the development of the contact forces produced from the wheel-rail interaction. Chapter (5) include the description of the railway vehicle model defined in this work and all the dynamic analysis of railway vehicles are used and implemented in this chapter. Finally chapter (6) the obtained results were discussed for the studied model, overall conclusions and perspectives for future research that are a sequence of this work are suggested.

Chapter 2

Reference Frames Description

2.1 Introduction

In this chapter, the complete description of the reference frames is presented in order to give a detailed definition for all the variables and identities used in the mathematical representation of the models used in the dynamic simulation of the railway multibody systems. This chapter also include the definition of the systems of references used for the multibody computer program developed in this work. Each reference frame was clearly defined, starting from the fixed frame of reference, the track frame of reference which represent reference frame which follow the motion of the body [23, 29]. The local coordinate reference frame of each body is introduced to represent the position and orientation of each point on the body with respect to each local frame. The origin and orientation of each locale frame of reference was attached to the center of mass of the body. The transformation between the reference frames was defined by calculating the necessary transformation matrix required, using the Euler angles with the sequence of rotation that avoid the singularity problem [29]. Cartesian coordinates are supposed to be used in the formulation used the due to the simplicity of its implementation in the multibody program used in the dynamic analysis of the railway vehicles, rotation sequences was defined for the track frame of reference, as a successive rotation about Z-axis, followed by rotation about Y-axis and finally, a rotation about X-axis. But for the rotation sequences used for the solid bodies it was defined as a successive rotation about Z-axis, then about X-axis and finally, the pitch motion with a rotation with about Y-axis.

2.2 Reference frames

In this section we would like to define all the frame of references used in the formulations, giving more details about each frame of reference used and its combination with the overall system. Starting with the description of the system we use in the analysis of solid body as shown Fig. (2.1). we define three main reference frames , the first one is the fixed frame of reference (X Y Z) , the second one is the track frame of (X_T Y_T Z_T) reference and the last one is the solid frame of reference (X_S Y_S Z_S).

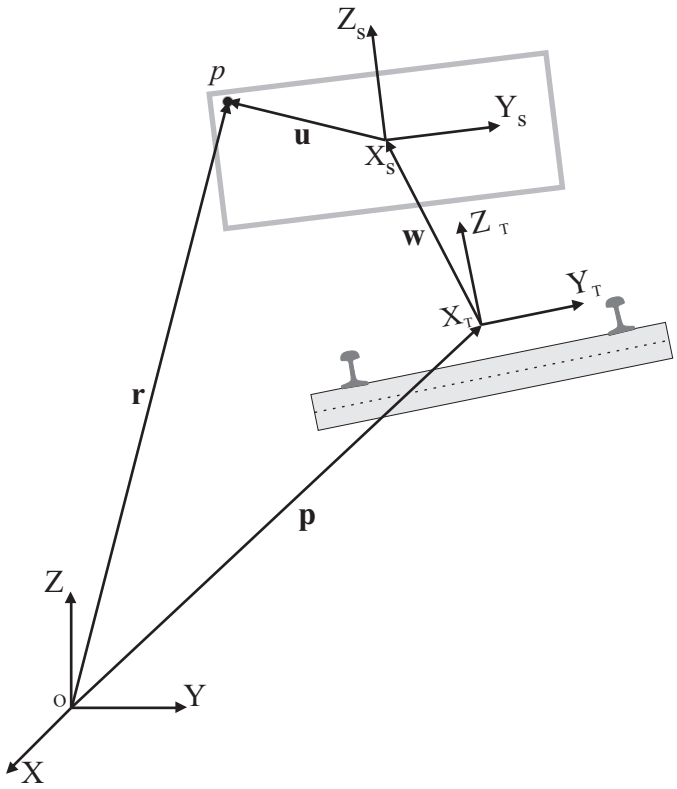

Figure 2.1. *Reference frames combination*

2.2.1 Fixed Reference Frame

A system that can be located at any fixed point with respect to the systems and bodies used in the analysis, which can be represented by a three orthogonal axes X, Y and Z, that are rigidly connected in one point called the origin O. This fixed frame of reference also called the global frame of reference. In this frame of reference all the measurable quantities that can define the configuration of the body can be represented with respect to it such as: displacement, velocities and accelerations. Fig. (2.2) shows a the global reference frame consists of three orthogonal axes Z, Y, and X. The Z-axis points to the vertical direction, X and Y-axis forming the horizontal plane. A vector **u** is defined by the three components that form u_x, u_y, and u_z. So the vector **u** can be written in terms of its components as follow:

$$\mathbf{u} = \begin{bmatrix} u_x & u_y & u_z \end{bmatrix}^{\mathrm{T}} \tag{2.1}$$

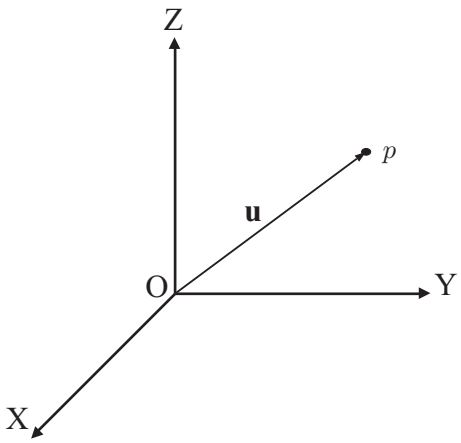

Figure 2.2. *Fixed Reference Frame*

2.2.2 Track Reference Frame

Track reference frame here was defined with three orthogonal coordinates axis X_T ,Y_T , and Z_T as shown in Fig. (2.3). The track reference frame was located at the track centerline presented between the left and right rail. The direction of the X_T-axis pointing to the longitudinal direction referring to the rolling direction of the moving body along the track, Z_T-axis pointing to the vertical direction normal to the track horizontal plane and the Y-axis located normal to the two other axes of the frame.

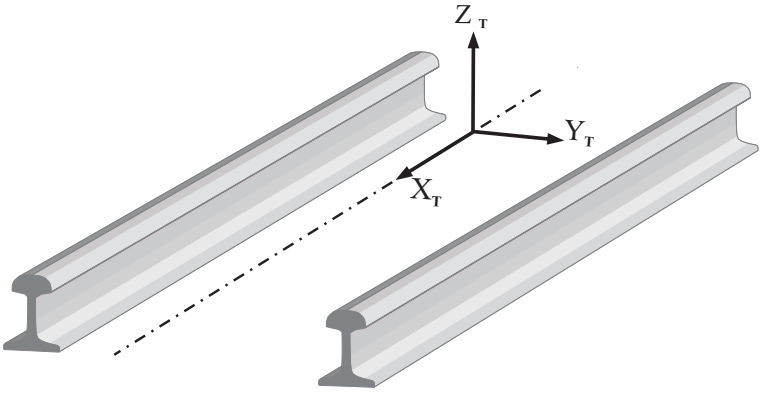

Figure 2.3. *Track Reference Frame*

A point p located in the track reference frame has a position vector which can be expressed in the local track frame of reference as shown in Fig(2.4).

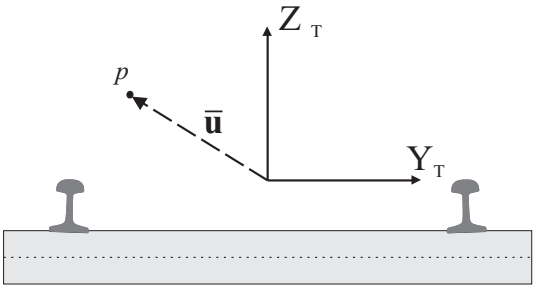

Figure 2.4. *Local position of point p in Track reference frame*

$$\bar{\mathbf{u}} = \begin{bmatrix} \bar{u}_x & \bar{u}_y & \bar{u}_z \end{bmatrix}^{\mathrm{T}} \tag{2.2}$$

In the expression, it was noted that the use of the upper bar sign, means that the vector presented in the track local reference frame. This notation here was used to distinguish the difference between the vectors presented in the track frame of reference and the global frame of reference.

2.2.3 Solid Reference Frame

As we present the track reference frame, here we define the solid reference frame represented by three orthogonal coordinate axes $\mathrm{X_S}$, $\mathrm{Y_S}$, and $\mathrm{Z_S}$. The solid frame of reference attached to the center of mass of the solid Fig. (2.5).
The local position vector of a point p located in the solid reference frame can be defined as:

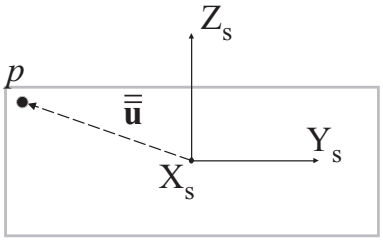

Figure 2.5. *Local position of point p in Solid reference frame*

$$\bar{\bar{\mathbf{u}}} = \begin{bmatrix} \bar{\bar{u}}_x & \bar{\bar{u}}_y & \bar{\bar{u}}_z \end{bmatrix}^{\mathrm{T}} \tag{2.3}$$

2.3 Reference Frame Transformation

In this part it was necessary to define how to make the transformation from one system to another in order to present the necessary formulations used in the frames transformation in the proceeding chapters.

2.3.1 Transformation from Track to Fixed reference frame

Fig. (2.6) shows the combination of the track frame (X_T Y_T Z_T) with the fixed or global reference frame (X Y Z). The global reference frame can be located at any fixed point selected by the user or the observer, and the track reference frame was located as it is appeared in the figure at the track centerline between the right and left rail.

A point p in the track reference frame can be defined by the position vector, which represent the location of point p with respect to the fixed reference frame (X Y Z) and by the global position vector $\mathbf{p}$, i.e.

$$\mathbf{r}_{\mathrm{p}} = \mathbf{p} + \mathbf{u} = \mathbf{p} + \mathbf{A}\,\bar{\mathbf{u}} \tag{2.4}$$

where $\mathbf{p}$, is the global position vector of the of origin O_T of the track reference frame, $\mathbf{u}$ is the global position vector of the point p with respect to the fixed frame of reference. $\mathbf{A}$ is the transformation matrix for the track that defines the orientation of the track (X_T Y_T Z_T) frame with respect to the fixed frame (X Y Z). This matrix can be written as [25]:

$$\mathbf{A} = \mathbf{A}_z\,\mathbf{A}_y\,\mathbf{A}_x \tag{2.5}$$

The selected sequence of rotation here was achieved by making three consecutive rotations a bout Z-axis and then rotation about Y-axis and finally rotation about

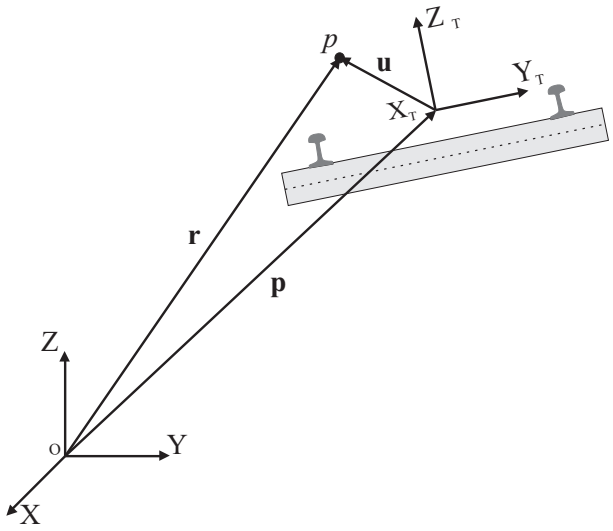

Figure 2.6. *Transformation from Solid to Track reference frame*

X-axis. For large rotation angles, the use of Euler angles in the calculation of the transformation matrix may cause singularity problems [4, 29]. To avoid this problems The selection of the rotation sequence for the track frame was chosen by making the largest rotation angle to be the final rotation, which is in our case here the rotation about X-axis representing the roll angle or the cant angle of the track [25]. The expression of the transformation matrix **A** illustrated in details in the included appendix.

2.3.2 Transformation from Solid to Fixed reference frame

The description of the transformation from the fixed frame of reference to the solid frame of reference illustrated here by defining the three main reference frames required to present the general solid which is in this case the body of the railway vehicle. Fig. (2.7) shows the sequence of the transformation, from the global to the track reference frame, afterwards transformation from track to solid reference frame. A point p located on the solid body can be defined by defining the position vector with respect to the global reference frame as:

$$\begin{aligned} \mathbf{r}_{\mathrm{p}} &= \mathbf{p} + \mathbf{w} + \mathbf{u} \\ &= \mathbf{p} + \mathbf{A}\,\bar{\mathbf{w}} + \mathbf{A}\,\mathbf{B}\,\bar{\bar{\mathbf{u}}} \end{aligned} \tag{2.6}$$

where $\bar{\mathbf{w}}$ is the position vector of the origin of the solid reference frame $\mathrm{O_s}$, with respect to the track reference frame, **B** is the transformation matrix required to define the orientation of the solid reference frame ($\mathrm{X_S\ Y_S\ Z_S}$) with respect to the track reference frame, and is the position vector of the point p with respect to the solid

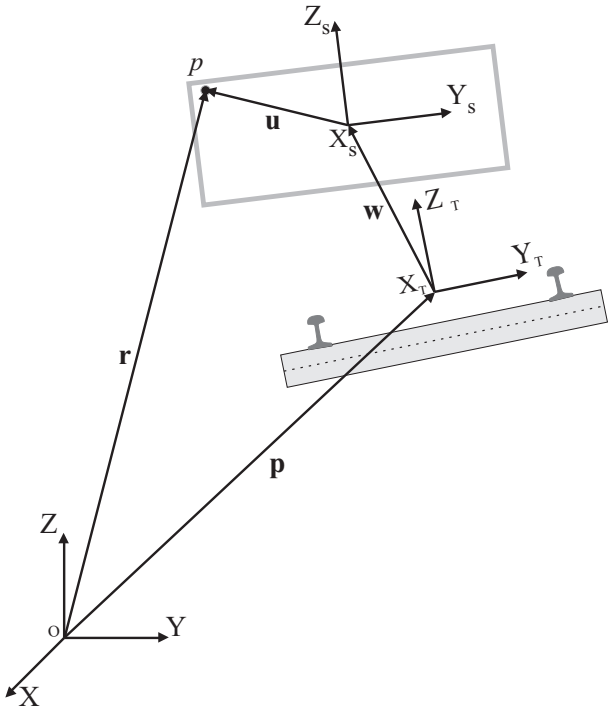

Figure 2.7. *Transformation from Solid to Fixed frame*

reference frame. The transformation matrix **B** of the solid is obtained by three consecutive rotations using Euler angles principle, but with the difference that the sequence of rotation in the case we have includes: a rotation about Z-axis with an angle θ_z, then a rotation about X-axis with an angle θ_x, and finally as the largest value for the rotation angles used in the transformation is the rotation about Y-axis with an angle θ_y which represent the rotation of the wheelset. The selection of the rotation sequence here used to avoid the singularity problems that may be appeared in case of dealing with high values for the rotation angles used during the motion.

2.4 Conclusions

To represent the previous idea for the transformation from one system to another, using the illustration Fig. (2.8) to define the transformation matrices used in the analytical presentation of the identities used in the formulations used in the dynamic simulation of the multibody system used in the analysis of the railway dynamics. It is appeared from the figure shown, the matrix **A** was used to define the orientation of the track reference frame with respect to the global reference frame, and the matrix **B** is used to define the orientation of the solid reference frame with respect to the track

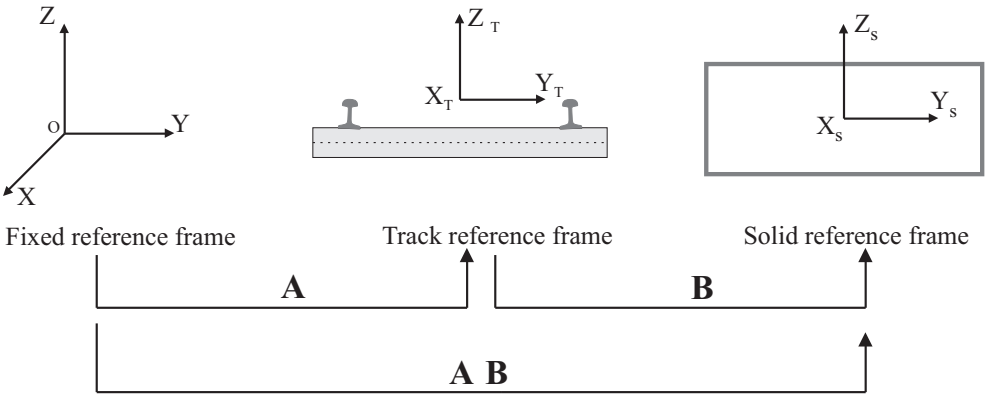

Figure 2.8. *Successive transformations between frame of references used*

reference frame. To define the orientation of the solid reference frame with respect to the global reference frame it was necessary to represent two successive transformation represented by the multiplication of the two matrices **A** and **B** respectively.

Chapter 3

Track Model

3.1 Introduction

The study of the railroad vehicle systems and the dynamic analysis of railway vehicle systems generally divided into two main stages. The first stage is a pre-processing stage at which the track geometry and the wheel and rail profiles are defined. The second stage is developing the equations of motion of the multibody vehicle system, in this stage all the parameters required to define the wheel and rail surfaces are defined as well as the track geometry parameters which enter the formulations of the contact conditions and the system equations of motion. Then as a first stage here in the methodology proposed for the analysis of a railroad vehicle, we have to define the track geometry and make modeling for the track to provide the required data in the next step of the dynamic analysis of the problem [29]. Any track irregularities can be perceived as deviations from the reference path parallel lines, representing the track rails, the introduction of the track irregularities is not considered here in the in this work. The track models for multibody analysis must be in the form of parameterized curves, where the nominal geometry is obtained as a function of a parameter associated to the track curve length [21, 23]. The parameterizations of the track can be done by two approaches, the first approach is the use of analytical segments for the track parametrization including the definition of the track generally done by putting together straight and circular curves interconnected by transition track segment that ensure the continuity of the first and second derivatives of the railway in the transition points. The second approach depends on the parametrization of the track using parametric curves such as Akima splines [1], shape reserved splines and piece wise cubic interpolation schemes. These methods require the definition of data points representing the track and provide the interpolation between these points to represent the parameterized track path. Undesired oscillations produced with using the mentioned interpolation schemes and this can be avoided in such case of the horizontal track geometry for railway application, by the use of analytical segments.

3.2 Track Characterization

The primary dynamic inputs to railway vehicles come from track geometry variations. In order to study vehicle-track interactions and to evaluate track quality, vehicle performance and loading conditions. It is necessary to represent the track geometry accurately [5]. The track pre-processor uses industry input data such as the curvature, super -elevation and development [28]. Then all the necessary data required as an input informations for the track model, will be provided in an separated input data file, and then the out put data of the track geometry programs will be provided to the dynamic simulation program. This step of obtaining the required data as a pre-processing data provided rapidly.

3.3 Track Geometry

The performance of the railway vehicle is independent, on a great extent, of the track conditions. The loads included on the vehicle by the track and corresponding forces transmitted to the track by the vehicle also depends on the track geometry. In this section, some physical aspects relevant for the design geometry of the track are presented.

3.3.1 Track Gauge

the track gage is defined as the distance G between the inner edges of the rail heads, measured 12 mm below the track plane, as shown in Fig.(3.1). The standard gauge track has a value of 1435 mm, but the Spanish railways use the so called Iberian gauge track of 1668 [mm]

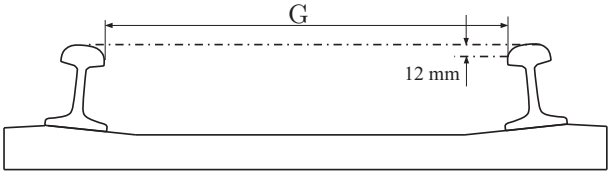

Figure 3.1. *Track gauge description*

3.3.2 Horizontal Curves

The railway tracks are in general composed of straight (or tangent) sections, transition curves and circular curves. The horizontal curves have constant radius and are defined in the tracks described in the horizontal plane. The radius of the curve used is defined with respect to the track centreline as shown in Fig.(3.2).

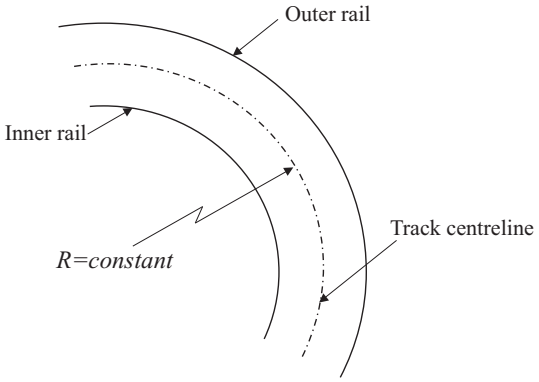

Figure 3.2. *Horizontal circular curve*

3.4 Cant angle definition in the track model

3.4.1 Cant and Equilibrium cant

When traveling in horizontal curves, railway vehicles are influenced by centrifugal forces, which act in a direction a way from the center of the curve to over turn the vehicle. The sum of a vehicle weight and its centrifugal forces produced a resultant force directed to the outer rail. In order to counteract this force, the outer rail in a curve is raised [9, 20, 29]. The difference in hight between th outer and the inner rail plane is called the cant or the super elevation h_t, which can be defined as shown in Fig. (3.3)

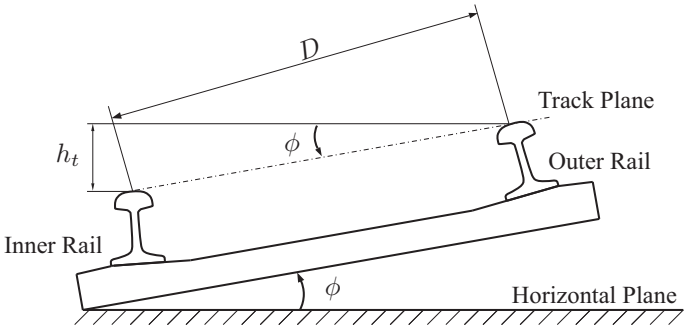

Figure 3.3. *Cant and Cant angle*

Then the cant angle ϕ as shown in the figure can be defined as [20, 29]

$$\phi = \arcsin\left(\frac{h_t}{D}\right) \tag{3.1}$$

The cant angle for zero track plane acceleration, at a given radius of curvature R and vehicle speed V can be defined as equilibrium cant angle [20] which can be found by

$$\phi_{eq} = \arctan\left(\frac{V^2}{R\,g}\right) \tag{3.2}$$

To define the track cant angle we have first to define the plane at which the cant angle is defied in. so in the case of the flat tracks, the horizontal plane is the plane at which the cant angle is defined with respect to. But in case of the full spatial geometry track model it is proposed to use the osculating plane Fig.(3.4), to be the reference plane at which the cant angle should defined [21, 23].

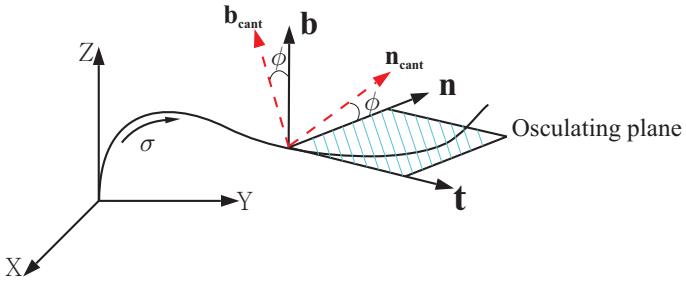

FIGURE 3.4. *Frenet Principle vectors and spatial definition of the cant angle*

in this section we may use the definitions of the principle vectors**(t n b)** [17, 23], which are the tangent, normal, and binormal vector respectively defining Frenet frame that is attached to the spatial curve presenting the track centerline and we find the tangent, normal and binormal unit vectors. Finding the relations between them after the rotation with the cant angle (ϕ), the vectors will be defined as **($\mathbf{t_{cant}}$ $\mathbf{n_{cant}}$ $\mathbf{b_{cant}}$)**. It have to be said that if piecewise cubic interpolation was used to make the parameterization of the spatial curve then the user must set the cant angle corresponds to each one of the nodal points that is used to parameterize the track. and if it supposed to use the analytical representation of the track model using analytical functions the user must set the cant angle at the extremities of each track segment [20, 21]. In the case we have here the cant angle can be defined by the angle of rotation of the track frame of reference about the X_T-axis pointing to the direction of motion of the railway vehicle Fig.(3.5)

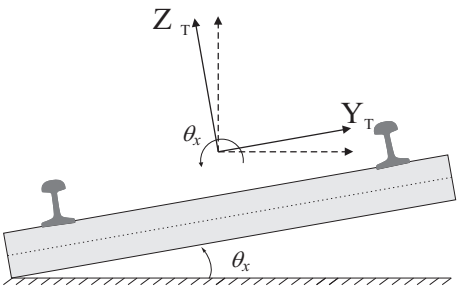

FIGURE 3.5. *Railway track cant angle*

It is supposed here in the analysis to use the transformation matrix **A** which is used to transform from the Track frame to the Fixed frame of reference, this matrix is obtained from a set of successive rotations as defined in chapter.(2). Another analysis was made to use the principal vectors to define the transformation matrix from the fixed frame to the track frame using the transformation matrix obtained in two steps: the first is to define the relative orientation between the fixed frame and the secondary [17] frame by defining the matrix $\mathbf{T_1}$ which can be obtained by knowing the components of the principle vector as follow

$$\mathbf{T}_1 = \begin{bmatrix} t_x & n_x & b_x \\ t_y & n_y & b_y \\ t_z & n_z & b_z \end{bmatrix} \tag{3.3}$$

And the second step is to define the orientation from the secondary frame to the Track frame which can be obtained by defining the transformation matrix $\mathbf{T_2}$ obtained by rotation about X-axis parallel to the rolling direction with the cant angle ϕ as

$$\mathbf{T}_2 = \begin{bmatrix} 1 & 0 & 0 \\ 0 & \cos\phi & -\sin\phi \\ 0 & \sin\phi & \cos\phi \end{bmatrix} \tag{3.4}$$

Then now the transformation matrix obtained to transform from the Track frame to the Fixed frame of reference can be defined as

$$\mathbf{T} = \mathbf{T}_1\mathbf{T}_2 \tag{3.5}$$

comparing this with the transformation matrix **A** with the only difference is that the cant angle ϕ is replaced with the angle θ_x which represent the rotation about the X_T-axis, Fig. (3.5) . It was found that the error matrix obtained representing the difference between the matrix **A** and the matrix **T** take the following value

$$\mathbf{T} - \mathbf{A} = \begin{bmatrix} 6.473e^{-10} & 0 & -7.965e^{-4} \\ 5.848e^{-11} & 0 & -7.196e^{-5} \\ 7.997e^{-4} & 0 & 6.499e^{-10} \end{bmatrix} \tag{3.6}$$

3.4.2 Transition Curves and Super-elevation Ramps

When trains operated at normal speeds, a circular curve with cant cannot be followed directly by a tangent track, and vice-versa [20]. A transition curve is needed to guarantee the curvature continuity and minimize the change in the lateral acceleration of the vehicle. In general transition curves and super-elevation ramps Fig. (3.6), have the same start and the same end points. I.e, the curvature and the cant in transition curves corresponds to each other. The length of the transition curves varies directly with the amount of curve super-elevation required. the maximum allowable rate of change of the super-elevation determines the minimum length of the transition for a given vehicle speed and curve super-elevation. The figure illustrates the main stages

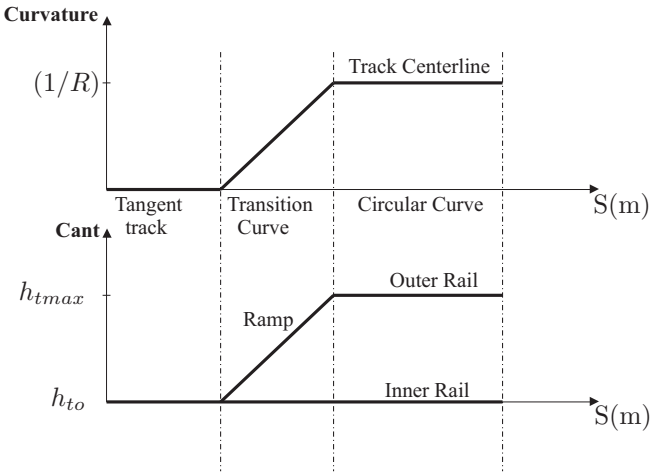

FIGURE 3.6. *Transition Curves and Super-elevation Ramps*

used in the simulation proposed here. R is the radius of curvature used in each stage which has an infinite value for the straight track and increases during the transition stage until it reaches the constant value at the circular curve stage as shown. h_{to} and h_{tmax} are the hight of the track in the straight stage and the final or circular curve stage respectively.

3.5 Track Geometric Description

The dynamic analysis of any railway guided vehicles requires an accurate description for the track geometry [6, 20]. the track is composed of two rails defined in a plane that sits in the track centerline spatial curve, also called the reference path. The basic ingredient to define the track is to define the geometry of the reference path which must includes, vertical gradients, horizontal curves and cant angle. The objective of this part is to introduce a complete description for the geometrics features of the track, and to present their computational implementation in a suitable form for the multibody methodology used in the analysis of the railway systems. For railways and light track vehicles the description of the nominal geometry of the track is generally done by assembling straight and circular segments together, interconnected by transition segments to ensure continuity of the first and second derivatives of the railway in transition points. To ensure smooth variation of the lateral accelerations of the vehicle during the change from the straight, or tangent, track to circular track or the change from circular path to straight one, the complete characterization of the track requires the definition of the cant angle variation along the reference path [9, 29]. For flat tracks, the cant angle is defined as the angle between the horizontal plane and the rails plane, but for spatial geometry, the definition of the cant angle is proposed to be the angle between the osculating plane and the rails plane.

3.5.1 parametrization of the track centerline

3.5.1.1 overview of the track pre-processor

Here we can say that for the parametrization of the track centerline model we have to define first the approach we will use in the parametrization procedure. One of the most commonly approaches is the use of analytical segments [22, 23] for representation of the track parameters, and in this procedure the track has to be defined or build using a combination of tangent track, transition curve and circular curve segments. The second approach that can be used is the parametrization of the track centerline using parametric curve interpolation schemes [20, 23], between the control points that can be used as an input data, defined by the user and the corresponding cant angle at each point. Once we have clearly define the approach that we will use to make the parametrization procedure, we then can easily parameterize the centerline as a function of the distance covered by the vehicle (σ) , also the cant angle parameterized as function of the track distance covered by the vehicle (σ) and the frame of reference associated to the track centerline after the cant angle rotation can be calculated. so the procedure followed can be summarized in the following steps:

- Definition of the approach used for parametrization of the track centerline whether it is analytical segments or piecewise cubic interpolation scheme, this is defined by the user.
- Once the approach is selected then the track centerline is parameterized as function of the covered distance (σ) presenting the distance covered by the railway vehicle during the simulation.
- The cant angle also parameterized also as a function of the distance covered by the vehicle, and then we can define the frame of reference associated to the track centerline after the cant angle rotation.
- An out put database is defined to all the necessary parameters required to define the track centerline geometry stored in it, and this database file is used as an input to the dynamic multibody code.

The method used here in the representation of the track model use the analytical segments [17, 20, 22] approach make parametrization of the track centerline, so the track here as described below in the following context. Using a combination of tangent or straight line segment, followed by transition curve segment to ensure the smooth transition between the tangent part and the circular curve segment.

3.5.1.2 Track Modeling using analytical segments

In this part we will give the specification of the track used in the dynamic simulation, the mathematical presentation of the track at each point represented in the section below to give position vector and then all the kinematic variables at each distance (σ) on the track .The track segments will be selected as the following order:

1. Straight line track, followed by
2. Transition curve, and then
3. Circular curve with constant radius

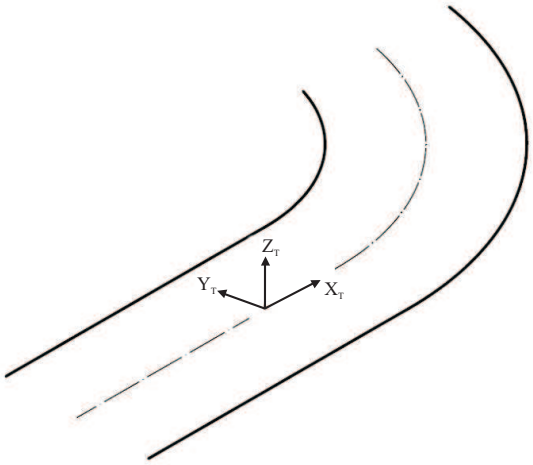

Figure 3.7. *Track model used in the dynamic simulation*

The track reference frame represented by the three orthogonal axes (X_T Y_T Z_T) will be assigned to the centerline between the left rail and the right rail as shown in Fig.(3.7), where the X_T axis is pointing to the rolling direction or the movement direction of the railway vehicle as it was defined in the previous chapter of the definition of the reference frames which can be shown by the following figure.(3.8), representing the steps of the track

1. **Straight line stage**

   The track presented here starts with a straight (or tangent) segment as shown in Fig.(3.9). The starting point of the straight segment of the track is the distance point $\sigma = 0$, and the end point of the straight segment is the point $\sigma = l_1$, This can be represented by the simple straight line equation of first order as

$$x(\sigma) = a_s(\sigma) + b_s \tag{3.7}$$

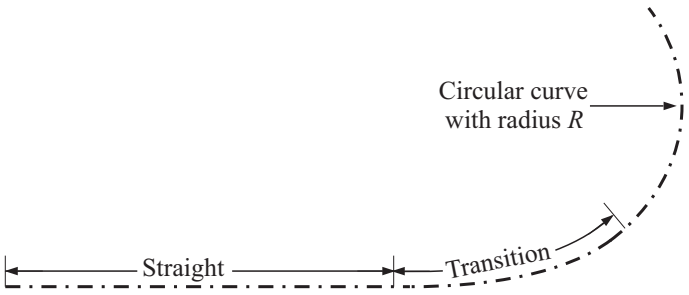

FIGURE 3.8. *Track segments definitions*

Where a_s ,b_s are constants of the straight line equation. This stage was considered to be the first stage in the track simulation. Then the track can be parameterized as a function of the track distance covered as

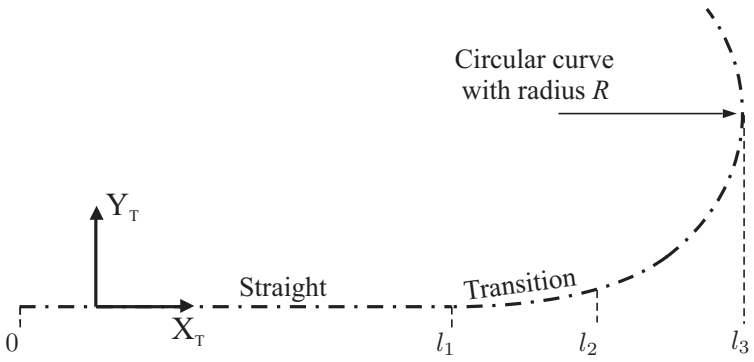

FIGURE 3.9. *Track segment lengths*

$$\mathbf{S}(\sigma) = \begin{bmatrix} x(\sigma) \\ y(\sigma) \\ z(\sigma) \end{bmatrix} \tag{3.8}$$

substituting with the values of $\sigma = 0$ at the beginning of the straight stage and $\sigma = l_1$ at the end of the straight stage we found that, also with substituting with the value of the cant hight for obtaining the z position at the straight track stage we find that

$$x(\sigma) = \sigma \tag{3.9}$$

$$z(\sigma) = h_{to} \tag{3.10}$$

then the position vector of a point on the track in the straight line stage can

described by

$$\mathbf{S}(\sigma) = \begin{bmatrix} \sigma \\ 0 \\ 0 \end{bmatrix} \tag{3.11}$$

2. **Transition curve stage**
The transition curve is called mathematically Euler spiral, fitted between a straight line and circular curve. The transition curve starts with a radius equal to the infinity and ends with a radius equal to the radius of curvature of the adjacent curve. In our analysis here we have used a transition curve of the type clothoid as shown in the Fig.(3.10).

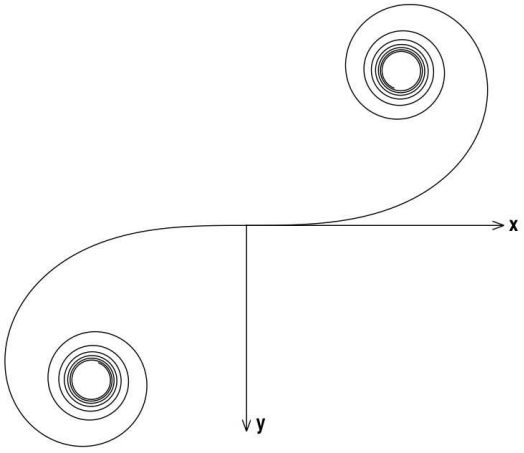

Figure 3.10. *Transition Curve Represented by Clothoid Curve*

The transition curve here represented by the clothoid curve interconnects the straight and circular tracks to ensure the continuity in the first and second derivatives of the railway in the transition points, the transition curves are responsible for smooth variation of the lateral acceleration of the vehicle, when it moves from a straight track to a circular track or between two track segments of the same type with different radius or orientation [23]. To represent the transition between the straight line stage and the circular curve or the circular stage. The tracing method used for the transition curve used is the conserved radius method, which leads to the parabolic equation of the clothoid obtained given by the following expression

$$y = \frac{x^3}{6\, l_{clo}\, R} \tag{3.12}$$

where l_{clo} is the clothoid length, and R is the radius of the circular curve of the following stage. Using Fresnel integral we can represent the coordinates of the clothoid as a function of the distance σ as follow

$$x(\sigma) = \sigma - \frac{1}{10}\frac{\sigma^5}{\pi^2}K^2 \tag{3.13}$$

$$y(\sigma) = \frac{1}{6}\sigma^3 K - \frac{1}{84}\frac{\sigma^7}{\pi^2}K^3 \tag{3.14}$$

Where K is a constant can be calculated as

$$K = \frac{1}{l_{clo}\,R} \tag{3.15}$$

The transition curve in our simulation will start at the point $\sigma = l_1$ and will end at the point of connection to the constant radius curve at the point $\sigma = l_1 + l_2$, where l_2 is the clothoid length l_{clo}. As it was shown it was necessary, for the parameterization method used here in the track parameterization using the analytical segment approach. To define the cant at the starting and at the end of each stage. So for the transition cure stage here represented by the clothoid we find that the hight at the beginning was h_{to} and at the end of the stage was h_{tmax}, and assuming linear cant through the transition stage we find that the elevation of any point on the track can be found by

$$z(\sigma) = h_{to} + \frac{h_{tmax} - h_{to}}{l_{clo}}(\sigma) \tag{3.16}$$

Knowing that the value of h_{to} is equal to zero in case of the straight track, then the position vector of any point on the clothoid curve can be written in matrix form in the planer representation as follow

$$\mathbf{S}(\sigma) = \begin{bmatrix} \sigma - \frac{1}{10}\frac{\sigma^5}{\pi^2}K^2 \\ \frac{1}{6}\sigma^3 K - \frac{1}{84}\frac{\sigma^7}{\pi^2}K^3 \\ \frac{h_{tmax}-h_{to}}{l_{clo}}(\sigma) \end{bmatrix} \tag{3.17}$$

3. **Circular curve stage**
   This is the third stage in the simulation of the track geometry, in this stage the track take a circular path with a constant radius of curvature R, the stage will start at the end point of the clothoid which can be assigned to the point $\sigma = l_1 + l_2$, and will end at the point at which $\sigma = l_1 + l_2 + l_3$, where l_3 is the circular curve length . The circular curve initiation point related to the previous stage as we know that the final point of the clothoid stage is same initiation point of the circular curve stage, so by defining the clothoid angle that can be written as

$$\Phi(\sigma) = \arctan\left(\frac{dy/d\sigma}{dx/d\sigma}\right) \tag{3.18}$$

We can conclude that the initiation angle of the circular curve is the angle of the clothoid when the value of σ is equal to the clothoid length l_{clo} and this can be represented as the following

$$\Phi(\sigma) = \Phi(\sigma = l_{clo}) \tag{3.19}$$

then the angle of the circular curve segment at any point σ on the circular curve, can be calculated from the expression

$$\Phi_P = \Phi(\sigma) + \frac{\sigma}{R} \tag{3.20}$$

Where R is the radius of curvature of the circular curve segment. The position vector of the of the initiation point of the circular curve indicated by the subscript i, so it can be written as

$$x_i(\sigma) = x(l_{clo}) \tag{3.21}$$

$$y_i(\sigma) = y(l_{clo}) \tag{3.22}$$

Finally we can write the components of the position vector of a point on the circular curve indicated by the subscript P as follow

$$x_P(\sigma) = \sin\left(\frac{\sigma}{R} + \Phi_i\right) - \sin(\Phi_i)\ R\ +\ x_i \tag{3.23}$$

$$y_P(\sigma) = -\cos\left(\frac{\sigma}{R} + \Phi_i\right) + \cos(\Phi_i)\ R\ +\ y_i \tag{3.24}$$

$$z_P(\sigma) = h_{tmax} \tag{3.25}$$

$$\mathbf{S}(\sigma) = \begin{bmatrix} x_P(\sigma) \\ y_P(\sigma) \\ z_P(\sigma) \end{bmatrix} \tag{3.26}$$

3.6 Conclusion

The parameterization method used here ensure the representation of all the track geometric properties as a function of the distance covered by the vehicle σ, a pre-processor data file is generated containing all the geometrical properties of the track. This methodology guarantee that the time required for the dynamic simulation of the rail guided vehicle completely independent of the track complexity and the type of the of the scheme used for parameterization. But we have to mention that the use of analytical segments [22, 23] for the parameterization process, specially for the horizontal tracks which not having large complexity, has a great advantage which is it doesn't produce any undesired oscillations in the track model but the only disadvantage of this method is the fact that it can not be used for the geometries which containing vertical curvatures, so it is only applied for horizontal track models. Reaching to this point, one can obtain all the information and the data related to the track designed for the simulation issues, including the the position, velocity and acceleration vector of any point with respect to the fixed frame. Also the transformation matrix required to transform from track to fixed reference frame was obtained, the angular velocities related to the track reference frame also have been obtained at each stage of the track.

Chapter 4

Multibody system methodology

4.1 Introduction

Multibody methodologies are not widely used despite the fact that such methodologies can be applied to develop more detailed and general models for railroad vehicle-track systems [26]. In the proceeding context of this chapter, the geometric, kinematics and dynamic aspects of a general solid system moving along parameterized track representing the railroad were discussed. Equations of motion presenting the multibody systems were formulated for a system consists of multiple rigid bodies each with six DOF, avoiding the use of any kinematic constraint on the motion in order to overcome the difficulties produced when using of the kinematic constraints which appeared in the need to solve a set of differential algebraic equations [20, 23] or the transformation of the system of differential algebraic equations (DAE) to ordinary differential equations (ODE), and then the use of stabilization techniques for the constraint equations in the solution was also avoided. The fundamental component common to all conventional railway vehicles is the wheelset. In general, it consists of two coned wheels rigidly fixed to a common axle. The movement of the wheelset over the track is characterized by a complex interaction where appreciable lateral translations as well as yaw and roll rotations are observed. The simulation of railroad vehicle-track systems using multibody computer algorithms requires the use of a module for the wheel-rail interaction [4, 16]. This interaction, which is due to the rolling and slipping contact between the profiled surfaces of the rail and the wheel, has a significant effect on the vehicle dynamics and stability [26]. Contact point position was detected in the formulation presented in this chapter, the velocity vector of the contact point was calculated and then the creepages introduced at the wheel-rail contact point were determined. Forces due to contact including the normal contact force and the tangential forces are calculated. The moment vector at the contact

patch was calculated, using an alternative technique, in which we replace the contact moment with equivalent pair of forces of equal magnitude and opposite directions, acting on a plane perpendicular to the direction of the moment direction [11], and both supposed to be acting through the longitudinal direction. Then the force vector applied to the wheelset at contact point is determined in order to be implemented in the MBS program used in the dynamic simulation vehicle systems. An important term in the methodology proposed, is the determination of the force vector applied to the bodies produced from the spring element connecting two rigid bodies. Translational force element is used connecting two bodies, this element can consist of a spring, a damper, and an actuator. The coefficients used in this element formulation to define the forces can be linear or non linear functions of the relative motion and velocity of the two bodies connected by this element, in our case here linear functions are used. Lagrangian approach was used here to determine the equation of motions of the system, it is mainly depends on the definition of the generalized coordinates of the system and the determination of the generalized force vector affecting the body under study. Kinematic analysis of a general solid was presented followed by the dynamic analysis of such solid, and then the formulations extended to include the kinematic and dynamic analysis of the wheelset including the definition of the normal contact forces, creepages and tangential contact forces at the contact patch resulting from the wheel-rail interaction.

4.2 Equations of motion of general solid body system

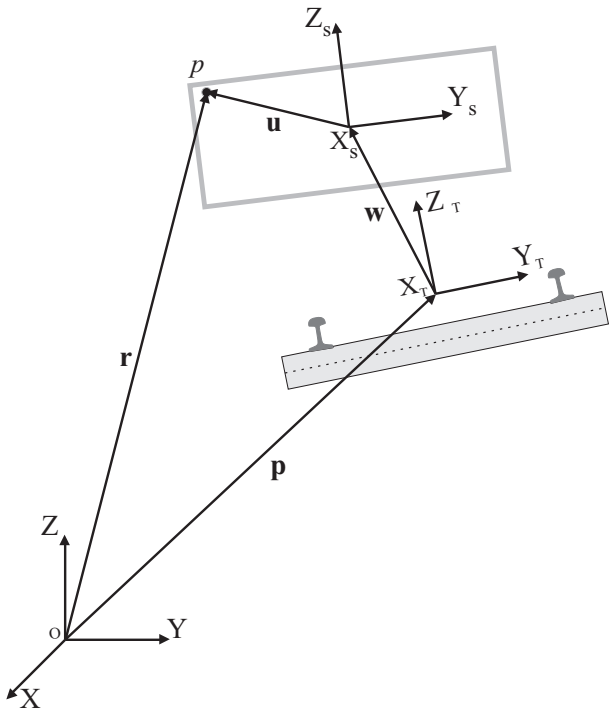

Figure 4.1. *General solid body with respect to global reference frame*

In this part we would present the formulations that can be used to calculate the position vector of arbitrary point located on a solid body using the relations developed in chapter. (2) like the position vector of an arbitrary point on solid or wheelset, the velocity vector and finally we will obtain the equations of motion of the system we have using the formulation developed in the proceeding context. The method that will be used in the calculation of the equations of motion is Lagrangian method for the development of the system equation of motion, and then defining the forces affecting the solid and the determination of the generalized forces associated with the system generalized coordinates [25, 29].

4.2.1 Kinematic analysis of solid body system

The kinematic analysis consists of the study of the motion of the system independently of the forces that cause it. The kinematic analysis is done to obtain the system position and velocity vectors and determination of the generalized coordinates of the system under study [3, 25]. Reaching to this point, we can define the position vector of a

point located on the solid body as shown in Fig. (4.1) using equation (2.6). And by making the first time derivative for the position vector, we can obtain the velocity vector of an arbitrary point located on the solid as

$$\dot{\mathbf{r}}_p = \dot{\mathbf{p}} + \dot{\mathbf{A}}\,\bar{\mathbf{w}} + \mathbf{A}\,\dot{\bar{\mathbf{w}}} + \left(\dot{\mathbf{A}}\,\mathbf{B} + \mathbf{A}\,\dot{\mathbf{B}}\right)\,\bar{\bar{\mathbf{u}}} \tag{4.1}$$

where $\dot{\mathbf{r}}_p$ is the velocity vector of an arbitrary point p, $\dot{\mathbf{p}}$ is the velocity of the origin of the track system of reference, $\dot{\mathbf{A}}$ first time derivative of the transformation matrix required to transform from the track frame of reference to the fixed frame of reference[1], $\dot{\bar{\mathbf{w}}}$ is the velocity of the origin of the solid reference frame which represent the velocity of the CM of the system as the solid reference frame was defined to be coincided with the solid inertial frame of reference located in CM, $\dot{\mathbf{B}}$ is first time derivative of the transformation matrix required to transform from the solid frame of reference to the track frame of reference[1].

4.2.2 Total kinetic energy of the system

Referring to the kinetic energy equation presented in bibliography [25], the kinetic energy of a solid body can be written as

$$T = \frac{1}{2}\int_V \rho\,\dot{\mathbf{r}}^{\mathrm{T}}\,\dot{\mathbf{r}}\,dV \tag{4.2}$$

Where ρ and V are respectively the mass density and the volume of the body, then the kinetic energy can be written as

$$T = \frac{1}{2}\dot{\mathbf{q}}^{\mathrm{T}}\,\mathbf{M_s}\,\dot{\mathbf{q}} \tag{4.3}$$

where $\mathbf{q}$ is the vector of the generalized coordinates of the solid body given by the following equation

$$\mathbf{q} = \begin{bmatrix} \bar{\mathbf{w}} & \boldsymbol{\theta} \end{bmatrix}^{\mathrm{T}} \tag{4.4}$$

where $\bar{\mathbf{w}}$ is the vector of displacements of the solid reference frame, and $\boldsymbol{\theta}$ is the vector of the rotation angles determining the orientation of the solid. According to the portioning of the generalized coordinates of the solid body, the kinetic energy can be found by the following equation

$$T = T_{\bar{\mathrm{w}}\bar{\mathrm{w}}} + T_{\bar{\mathrm{w}}\,\theta} + T_{\theta\theta} \tag{4.5}$$

where T is total kinetic energy of the solid, $T_{\bar{\mathrm{w}}\bar{\mathrm{w}}}$ is the translational kinetic energy term, $T_{\bar{\mathrm{w}}\theta}$ represents the coupling between the translational kinetic energy and the

[1] Appendix **A**

rotational kinetic energy term, and $T_{\theta\theta}$ is the rotational kinetic energy term. But for the solid body system we have in such case, the term that represents the coupling between the translational and rotational kinetic energy $T_{\bar{\mathrm{w}}\theta}$, is null because the solid frame of reference ($\mathrm{X_S}$ $\mathrm{Y_S}$ $\mathrm{Z_S}$) is located at CM of the solid body. Then total kinetic energy of the system in this case will be written as

$$T = T_{\bar{\mathrm{w}}\bar{\mathrm{w}}} + T_{\theta\theta} \tag{4.6}$$

4.2.3 Translational kinetic energy of the system

The translational kinetic energy term of the solid body can be written as

$$T_{\bar{\mathrm{w}}\bar{\mathrm{w}}} = \frac{1}{2}\,\dot{\mathbf{r}}_{CM}^{\mathrm{T}}\,\mathbf{M}_s\,\dot{\mathbf{r}}_{CM} \tag{4.7}$$

where $\mathbf{r}_{CM}$ is the position vector of the center of mass of the solid body represented by

$$\mathbf{r}_{CM} = \mathbf{p} + \mathbf{A}\,\bar{\mathbf{w}} \tag{4.8}$$

and $\mathbf{M}_s$ is the mass matrix of the solid body[1] can be written as

$$\mathbf{M}_s = m_s\,\mathbf{I}_{3\times 3} \tag{4.9}$$

The vector representing the velocity of the center of mass point, can be found through the equation

$$\dot{\mathbf{r}}_{CM} = \dot{\mathbf{p}} + \dot{\mathbf{A}}\,\bar{\mathbf{w}} + \mathbf{A}\,\dot{\bar{\mathbf{w}}} \tag{4.10}$$

substituting in the translational kinetic energy term we obtain

$$\begin{aligned} T_{\bar{\mathbf{w}}\bar{\mathbf{w}}} = {} & \tfrac{1}{2}\dot{\mathbf{p}}^{\mathrm{T}}\,\mathbf{M}_s\,\dot{\mathbf{p}} + \left(\dot{\mathbf{p}}^{\mathrm{T}} + \tfrac{1}{2}\,\dot{\bar{\mathbf{w}}}^{\mathrm{T}}\,\mathbf{A}^{\mathrm{T}} + \bar{\mathbf{w}}^{\mathrm{T}}\,\dot{\mathbf{A}}^{\mathrm{T}}\right)\,\mathbf{M}_s\,\mathbf{A}\,\dot{\bar{\mathbf{w}}} \\ & + \left(\dot{\mathbf{p}}^{\mathrm{T}} + \tfrac{1}{2}\bar{\mathbf{w}}^{\mathrm{T}}\,\dot{\mathbf{A}}^{\mathrm{T}}\right)\,\mathbf{M}_s\,\dot{\mathbf{A}}\,\bar{\mathbf{w}} \end{aligned} \tag{4.11}$$

4.2.4 Rotational kinetic energy of the system

The rotational kinetic energy of the solid can be written as

$$T_{\theta\theta} = \frac{1}{2}\bar{\boldsymbol{\omega}}^{\mathrm{T}}\,\boldsymbol{J}_{\theta\theta}\,\bar{\boldsymbol{\omega}} \tag{4.12}$$

[1] Appendix **A**

where $\boldsymbol{J}_{\theta\theta}$ is the inertia matrix of the solid[1], $\bar{\bar{\boldsymbol{\omega}}}$ is the angular velocity of the solid represented in the solid reference frame which can be written as

$$\bar{\bar{\boldsymbol{\omega}}} = \bar{\bar{\boldsymbol{\tau}}} + \bar{\bar{\boldsymbol{L}}}\,\dot{\boldsymbol{\theta}} \tag{4.13}$$

where $\bar{\bar{\boldsymbol{\tau}}}$ is the track angular velocity vector represented in the solid reference frame, the term $\bar{\bar{\boldsymbol{L}}}\,\dot{\boldsymbol{\theta}}$ represents the relative angular velocity of the solid with respect to the track frame of reference,and $\boldsymbol{L}$ is the matrix containing the vectors acting through the rotation axes Z_S, X_S, and Y_S respectively which are defined in the global reference frame[1] and it represents the matrix that relates the absolute angular velocity vector of the rail to the time derivatives of the orientation parameters [28]. By substitution in the rotational kinetic energy Eq. (4.12) we found that

$$T_{\theta\theta} = \frac{1}{2}\,\bar{\bar{\boldsymbol{\tau}}}^{\mathrm{T}}\,\boldsymbol{J}_{\theta\theta}\,\bar{\bar{\boldsymbol{\tau}}} + \left(\bar{\bar{\boldsymbol{\tau}}}^{\mathrm{T}} + \frac{1}{2}\dot{\boldsymbol{\theta}}^{\mathrm{T}}\,\bar{\bar{\boldsymbol{L}}}^{\,\mathrm{T}}\right)\boldsymbol{J}_{\theta\theta}\,\bar{\bar{\boldsymbol{L}}}\,\dot{\boldsymbol{\theta}} \tag{4.14}$$

By substitution with Eq. (4.11)and Eq. (4.14), the total kinetic energy term represented be found by

$$\begin{aligned} T = {} & \tfrac{1}{2}\dot{\mathbf{p}}^{\mathrm{T}}\,\mathbf{M}_s\,\dot{\mathbf{p}} + \left(\dot{\mathbf{p}}^{\mathrm{T}} + \tfrac{1}{2}\,\dot{\bar{\mathbf{w}}}^{\mathrm{T}}\,\mathbf{A}^{\mathrm{T}} + \bar{\mathbf{w}}^{\mathrm{T}}\,\dot{\mathbf{A}}^{\mathrm{T}}\right)\mathbf{M}_s\,\mathbf{A}\,\dot{\bar{\mathbf{w}}} \\ & + \left(\dot{\mathbf{p}}^{\mathrm{T}} + \tfrac{1}{2}\bar{\mathbf{w}}^{\mathrm{T}}\,\dot{\mathbf{A}}^{\mathrm{T}}\right)\mathbf{M}_s\,\dot{\mathbf{A}}\,\bar{\mathbf{w}} + \tfrac{1}{2}\,\bar{\bar{\boldsymbol{\tau}}}^{\mathrm{T}}\,\boldsymbol{J}_{\theta\theta}\,\bar{\bar{\boldsymbol{\tau}}} + \left(\bar{\bar{\boldsymbol{\tau}}}^{\mathrm{T}} + \tfrac{1}{2}\dot{\boldsymbol{\theta}}^{\mathrm{T}}\,\bar{\bar{\boldsymbol{L}}}^{\,\mathrm{T}}\right)\boldsymbol{J}_{\theta\theta}\,\bar{\bar{\boldsymbol{L}}}\,\dot{\boldsymbol{\theta}} \end{aligned} \tag{4.15}$$

4.3 Dynamic analysis of solid body system

The dynamic analysis of multibody systems consists of the study of their motion as response to the external applied forces and moments [2, 11, 25]. The motion of the system is generally not prescribed, being its calculation one of the principle objectives of the dynamic analysis. This type of analysis also provides a process to estimate external forces that are dependent on the relative position between the system components, such as those type of forces generated by springs, dampers and actuators. Also the external forces generated as a consequence of the interaction between the system and its surrounding environment, such as contact and friction forces are considered [20].

4.3.1 Equations of motion of the solid body

In this section, the dynamic equation of motion of solid body treated as a rigid body is derived. To determine the configuration of the solid body system, it was first necessary to define generalized coordinates $\mathbf{q}$ as defined in the previous section of the kinematic analysis [29], that specify the position and orientation of each point of any body in the multibody system presented by the solid system shown in Fig.(4.1).

[1] Appendix **A**

4.3.2 Lagrange's equation of motion

In the *Lagrangian* approach, scalar quantities such as the virtual work and the kinetic and potential energies are used to develop the equations of motion of the body and in this case there is no need to study the equilibrium of the bodies in the system separately [19, 29]. Due to the linear independency of the generalized coordinates, the application of *D'Alembert- lagrange's* equation leads to *Lagrange's* Equation which is given by the equation

$$\frac{d}{dt}\left(\frac{\partial T}{\partial \dot{\mathbf{q}}}\right) - \frac{\partial T}{\partial \mathbf{q}} - \mathbf{Q} = 0 \tag{4.16}$$

where $\mathbf{q}$, $\dot{\mathbf{q}}$ are vectors of generalized coordinate and velocities respectively. $\mathbf{Q}$ is the generalized force vector associated to the generalized coordinate vector [25, 29], which can be written as follow

$$\mathbf{Q} = \begin{bmatrix} \mathbf{Q}_{\bar{\mathrm{w}}} \\ \mathbf{Q}_{\boldsymbol{\theta}} \end{bmatrix} \tag{4.17}$$

4.3.3 Quadratic velocity vector

By definition of the time derivative of the generalized coordinates vector $\dot{\mathbf{q}}$ associated to the solid body, we can find that the coordinates are the time derivative of the displacements included in the vector $\dot{\bar{\mathbf{w}}}$ and the time derivatives of the rotation angles of the solid included in the vector $\dot{\boldsymbol{\theta}}$. Starting with the translational component of the generalized coordinate vector, we get the derivative of the kinetic energy with respect to the velocity vector $\dot{\bar{\mathbf{w}}}$ we found that

$$\frac{\partial T}{\partial \dot{\bar{\mathbf{w}}}} = \left(\dot{\mathbf{p}}^{\mathrm{T}} + \dot{\bar{\mathbf{w}}}^{\mathrm{T}}\,\mathbf{A}^{\mathrm{T}} + \bar{\mathbf{w}}^{\mathrm{T}}\,\dot{\mathbf{A}}^{\mathrm{T}}\right)\mathbf{M}_s\,\mathbf{A} \tag{4.18}$$

by finding the time derivative term for the previous equation

$$\begin{aligned}\frac{d}{dt}\left(\frac{\partial T}{\partial \dot{\bar{\mathbf{w}}}}\right) =& \ddot{\bar{\mathbf{w}}}^{\mathrm{T}}\,\mathbf{A}^{\mathrm{T}}\,\mathbf{M}_s\,\mathbf{A} + 2\,\dot{\bar{\mathbf{w}}}^{\mathrm{T}}\,\dot{\mathbf{A}}^{\mathrm{T}}\,\mathbf{M}_s\,\mathbf{A} + \dot{\bar{\mathbf{w}}}^{\mathrm{T}}\,\mathbf{A}^{\mathrm{T}}\,\mathbf{M}_s\,\dot{\mathbf{A}} + \\ & \ddot{\mathbf{p}}^{\mathrm{T}}\,\mathbf{M}_s\,\mathbf{A} + \dot{\mathbf{p}}^{\mathrm{T}}\mathbf{M}_s\,\dot{\mathbf{A}} + \bar{\mathbf{w}}^{\mathrm{T}}\,\ddot{\mathbf{A}}^{\mathrm{T}}\,\mathbf{M}_s\,\mathbf{A} + \bar{\mathbf{w}}^{\mathrm{T}}\,\dot{\mathbf{A}}^{\mathrm{T}}\mathbf{M}_s\,\dot{\mathbf{A}}\end{aligned} \tag{4.19}$$

The same with the rotational component of the generalized coordinate vector, we can get the derivative of the kinetic energy with respect to $\dot{\boldsymbol{\theta}}$

$$\frac{\partial T}{\partial \dot{\boldsymbol{\theta}}} = \left(\dot{\boldsymbol{\theta}}^{\mathrm{T}}\,\bar{\bar{\boldsymbol{L}}}^{\mathrm{T}} + \bar{\bar{\boldsymbol{\tau}}}^{\mathrm{T}}\right)\boldsymbol{J}_{\theta\theta}\,\bar{\bar{\boldsymbol{L}}} \tag{4.20}$$

by finding the time derivative term for the previous equation

$$\frac{d}{dt}\left(\frac{\partial T}{\partial \dot{\boldsymbol{\theta}}}\right) = \left(\ddot{\boldsymbol{\theta}}^{\mathrm{T}}\,\bar{\bar{\boldsymbol{L}}}^{\mathrm{T}} + \dot{\boldsymbol{\theta}}^{\mathrm{T}}\,\dot{\bar{\bar{\boldsymbol{L}}}}^{\mathrm{T}} + \dot{\bar{\bar{\boldsymbol{\tau}}}}^{\mathrm{T}}\right)\boldsymbol{J}_{\theta\theta}\,\bar{\bar{\boldsymbol{L}}} + \left(\dot{\boldsymbol{\theta}}^{\mathrm{T}}\,\bar{\bar{\boldsymbol{L}}}^{\mathrm{T}} + \bar{\bar{\boldsymbol{\tau}}}^{\mathrm{T}}\right)\boldsymbol{J}_{\theta\theta}\,\dot{\bar{\bar{\boldsymbol{L}}}} \tag{4.21}$$

4.3.4 Derivatives of the K.E with respect to generalized coordinates

Finding the derivative of the kinetic energy of the system with respect to the displacement $\bar{\mathbf{w}}$ vector we found that

$$\frac{\partial T}{\partial \bar{\mathbf{w}}} = \left(\dot{\mathbf{p}}^{\mathrm{T}} + \bar{\mathbf{w}}^{\mathrm{T}}\,\dot{\mathbf{A}}^{\mathrm{T}} + \dot{\bar{\mathbf{w}}}^{\mathrm{T}}\,\mathbf{A}^{\mathrm{T}}\right)\,\mathbf{M}_s\,\dot{\mathbf{A}} \tag{4.22}$$

In the rotational kinetic energy equation, the term $\bar{\bar{\boldsymbol{\tau}}}$ represented in the solid frame of reference, it can be written in the track frame of reference using the relations defined in chapter. (2), as

$$\bar{\bar{\boldsymbol{\tau}}} \;=\; \mathbf{B}^{\mathrm{T}}\,\bar{\boldsymbol{\tau}} \tag{4.23}$$

Then the kinetic rotational energy can be found by

$$T_{\theta\theta} = \frac{1}{2}\,\bar{\boldsymbol{\tau}}^{\mathrm{T}}\,\mathbf{B}\,\boldsymbol{J}_{\theta\theta}\,\mathbf{B}^{\mathrm{T}}\,\bar{\boldsymbol{\tau}} + \bar{\boldsymbol{\tau}}^{\mathrm{T}}\,\mathbf{B}\,\boldsymbol{J}_{\theta\theta}\,\bar{\bar{\boldsymbol{L}}}\,\dot{\boldsymbol{\theta}} + \frac{1}{2}\dot{\boldsymbol{\theta}}^{\mathrm{T}}\,\bar{\bar{\boldsymbol{L}}}^{\mathrm{T}}\,\boldsymbol{J}_{\theta\theta}\,\bar{\bar{\boldsymbol{L}}}\,\dot{\boldsymbol{\theta}} \tag{4.24}$$

The same for the rotational part, finding the derivative of the kinetic energy of the system with respect to the rotation angles vector $\boldsymbol{\theta}$, we found that the rotation angles are included only in both matrices $\mathbf{B}$ and $\bar{\bar{\boldsymbol{L}}}$ corresponding to the rotation sequence of the solid, we find that

$$\frac{\partial T}{\partial \theta_i} = \bar{\boldsymbol{\tau}}^{\mathrm{T}}\frac{\partial \mathbf{B}}{\partial \theta_i}\left(\boldsymbol{J}_{\theta\theta}\,\bar{\bar{\boldsymbol{\tau}}} + \boldsymbol{J}_{\theta\theta}\,\bar{\bar{\boldsymbol{L}}}\,\dot{\boldsymbol{\theta}}\right) + \left(\bar{\bar{\boldsymbol{\tau}}}^{\mathrm{T}} + \dot{\boldsymbol{\theta}}^{\mathrm{T}}\,\bar{\bar{\boldsymbol{L}}}^{\mathrm{T}}\right)\,\boldsymbol{J}_{\theta\theta}\frac{\partial \bar{\bar{\boldsymbol{L}}}}{\partial \theta_i}\dot{\boldsymbol{\theta}} \tag{4.25}$$

Where

$$\boldsymbol{\theta} = \left[\theta_i\right]^{\mathrm{T}}; i = x, y \text{ and } z. \tag{4.26}$$

4.3.5 Generalized forces associated to the generalized coordinates

The generalized forces are introduced by application of the principle of virtual work [3, 25] in both cases of static and dynamic analysis, then the first step here is to define the virtual work for the system used

1. ***Virtual displacement***
   From equation. (2.6) describing the position vector of an arbitrary point on the solid body, the virtual displacement can be written as

$$\delta\mathbf{r}_p = \mathbf{A}\delta\,\bar{\mathbf{w}} + \mathbf{A}\,\frac{\partial \mathbf{B}}{\partial \boldsymbol{\theta}}\,\bar{\bar{\mathbf{u}}}\,\delta\boldsymbol{\theta} \tag{4.27}$$

2. ***Force vector applied on the solid***
   Assuming that there is an a force vector $\boldsymbol{F}$ affecting the solid body, which represent all the forces affecting the solid, which can be friction forces, external or internal forces generated by force elements such as springs or dampers. This force vector can be written with respect to the track reference frame as

$$\bar{\boldsymbol{F}} = \mathbf{A}^{\mathrm{T}} \boldsymbol{F} \tag{4.28}$$

3. ***Virtual work***
   The virtual work produced from the application of the external force vector can be written as follow

$$\delta W = \boldsymbol{F}^{\mathrm{T}} \mathbf{A}\, \delta \bar{\mathbf{w}} + \boldsymbol{F}^{\mathrm{T}} \mathbf{A}\, \frac{\partial \mathbf{B}}{\partial \boldsymbol{\theta}}\, \bar{\bar{\mathbf{u}}}\, \delta \boldsymbol{\theta} \tag{4.29}$$

   substituting from equation.(4.28) in equation.(4.29) we get the following equation

$$\delta W = \bar{\boldsymbol{F}}^{\mathrm{T}}\, \delta \bar{\mathbf{w}} + \bar{\boldsymbol{F}}^{\mathrm{T}}\, \frac{\partial \mathbf{B}}{\partial \boldsymbol{\theta}}\, \bar{\bar{\mathbf{u}}}\, \delta \boldsymbol{\theta} \tag{4.30}$$

4. ***Generalized force***
   Comparing this expression with the definition of the virtual work [25, 29] that can be expressed as

$$\delta W = \begin{bmatrix} \mathbf{Q}_{\bar{\mathrm{w}}}^{\mathrm{T}} & \mathbf{Q}_{\theta} \end{bmatrix} \begin{bmatrix} \delta \bar{\mathbf{w}} \\ \delta \boldsymbol{\theta} \end{bmatrix} \tag{4.31}$$

   Where $\mathbf{Q}_{\bar{\mathrm{w}}}$ is called the generalized force vector associated to the translational vector $\bar{\mathbf{w}}$, and $\mathbf{Q}_{\theta}$ is the generalized coordinate vector associated to the rotational angles vector $\boldsymbol{\theta}$. Furthermore the generalized forces associated to the mentioned generalized coordinates can be written as:

$$\mathbf{Q}_{\bar{\mathrm{w}}} = \bar{\boldsymbol{F}} \tag{4.32}$$

$$Q_{\theta_x} = \bar{\boldsymbol{F}}^{\mathrm{T}}\, \frac{\partial\, \mathbf{B}}{\partial\, \theta_x}\, \bar{\bar{\mathbf{u}}} \tag{4.33}$$

$$Q_{\theta_y} = \bar{\boldsymbol{F}}^{\mathrm{T}}\, \frac{\partial\, \mathbf{B}}{\partial\, \theta_y}\, \bar{\bar{\mathbf{u}}} \tag{4.34}$$

$$Q_{\theta_z} = \bar{\boldsymbol{F}}^{\mathrm{T}}\, \frac{\partial\, \mathbf{B}}{\partial\, \theta_z}\, \bar{\bar{\mathbf{u}}} \tag{4.35}$$

4.4 Equations of motion development

4.4.1 Translational equation of motion

From equations. (4.19) and (4.22) in Lagrange's formula we get that

$$\ddot{\bar{\mathbf{w}}}^{\mathrm{T}}\,\mathbf{A}^{\mathrm{T}}\,\mathbf{M}_s\,\mathbf{A} + 2\,\dot{\bar{\mathbf{w}}}^{\mathrm{T}}\,\dot{\mathbf{A}}^{\mathrm{T}}\,\mathbf{M}_s\,\mathbf{A} + \ddot{\mathbf{p}}^{\mathrm{T}}\,\mathbf{M}_s\,\mathbf{A} + \bar{\mathbf{w}}^{\mathrm{T}}\,\ddot{\mathbf{A}}^{\mathrm{T}}\,\mathbf{M}_s\,\mathbf{A} - \mathbf{Q}_{\bar{\mathrm{w}}} = 0 \tag{4.36}$$

using the identities explained in the appendix, we replace the first and second time derivative of the track transformation matrix[1], also the mass matrix replaced with its value, we get that

$$m_s\,\ddot{\bar{\mathbf{w}}}^{\mathrm{T}} + m_s\,\ddot{\mathbf{p}}^{\mathrm{T}}\mathbf{A}\; - 2\,m_s\,\dot{\bar{\mathbf{w}}}^{\mathrm{T}}\,\tilde{\bar{\boldsymbol{\tau}}} + m_s\bar{\mathbf{w}}^{\mathrm{T}}\,\tilde{\bar{\boldsymbol{\tau}}}\,\tilde{\bar{\boldsymbol{\tau}}}\; - m_s\bar{\mathbf{w}}^{\mathrm{T}}\,\dot{\tilde{\bar{\boldsymbol{\tau}}}}\; - \mathbf{Q}_{\bar{\mathrm{w}}} = 0 \tag{4.37}$$

Where the term ($\ddot{\bar{\mathbf{w}}}^{\mathrm{T}} + \ddot{\mathbf{p}}^{\mathrm{T}}\mathbf{A}$) represent the local acceleration of origin of the solid body seen by an observer located in the global frame of reference and it is also called the drag acceleration component, the term ($-2\,\dot{\bar{\mathbf{w}}}^{\mathrm{T}}\,\tilde{\bar{\boldsymbol{\tau}}}$) represent Coriolis acceleration component, and the finally the relative acceleration component can be found in the previous equation as ($\bar{\mathbf{w}}^{\mathrm{T}}\,\tilde{\bar{\boldsymbol{\tau}}}\,\tilde{\bar{\boldsymbol{\tau}}}\; - \bar{\mathbf{w}}^{\mathrm{T}}\,\dot{\tilde{\bar{\boldsymbol{\tau}}}}$), also we can recognize both tangential component of the relative acceleration as ($-\bar{\mathbf{w}}^{\mathrm{T}}\,\dot{\bar{\boldsymbol{\tau}}}$) and the normal component as ($\bar{\mathbf{w}}^{\mathrm{T}}\,\tilde{\bar{\boldsymbol{\tau}}}\,\tilde{\bar{\boldsymbol{\tau}}}$)

4.4.2 Rotational equation of motion

The same for the rotational angles vector , from equations.(4.20) and (4.25) in Lagrange's formula we get that

$$\dot{\bar{\boldsymbol{\tau}}}^{\mathrm{T}}\,\boldsymbol{J}_{\theta\theta}\,\bar{\bar{\boldsymbol{L}}} + \bar{\boldsymbol{\tau}}^{\mathrm{T}}\,\boldsymbol{J}_{\theta\theta}\,\dot{\bar{\bar{\boldsymbol{L}}}} + \ddot{\boldsymbol{\theta}}^{\mathrm{T}}\,\bar{\bar{\boldsymbol{L}}}^{\mathrm{T}}\,\boldsymbol{J}_{\theta\theta}\,\bar{\bar{\boldsymbol{L}}} + \dot{\boldsymbol{\theta}}^{\mathrm{T}}\,\dot{\bar{\bar{\boldsymbol{L}}}}^{\mathrm{T}}\,\boldsymbol{J}_{\theta\theta}\,\bar{\bar{\boldsymbol{L}}} + \dot{\boldsymbol{\theta}}^{\mathrm{T}}\,\bar{\bar{\boldsymbol{L}}}^{\mathrm{T}}\,\boldsymbol{J}_{\theta\theta}\,\dot{\bar{\bar{\boldsymbol{L}}}} - \left[\frac{\partial T}{\partial \boldsymbol{\theta}}\right]^{\mathrm{T}} - \mathbf{Q}_{\boldsymbol{\theta}} = 0 \tag{4.38}$$

where the value of the term $\frac{\partial T}{\partial \theta_i}$ can be obtained from equation.(4.25)

[1] Appendix **A**

4.5 Equations of motion of wheelset

The application for studying a solid moving on the track, can be represented here by a wheelset system moving along the track model designed for the simulation of the movement of the general solid system defined in the previous section. The wheelset system should be defined and all the forces acting on the wheelset system including all the contact forces, moments and all applied forces like those forces produced by the force elements like dampers and springs.

4.5.1 Wheelset

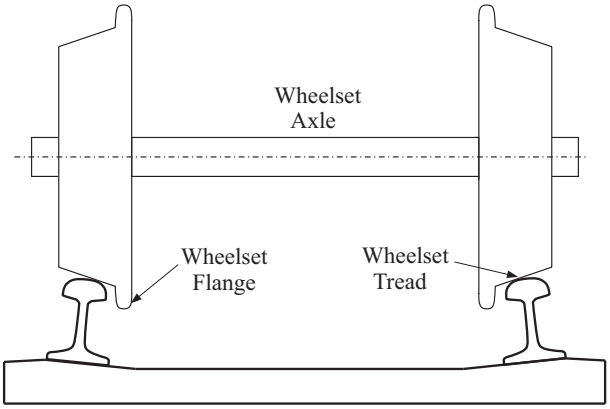

Figure 4.2. *Conventional wheelset*

The fundamental component common in all conventional railway vehicles is the wheelset, it consists of two wheels rigidly fixed to a common axle [26], as shown in Fig.(4.2), since the wheels are not free to rotate independently, they have the same rotational speed and a constant distance between the two wheels is mentioned. The wheels treads are conical and profiled, in order to allow them to negotiate curves with out slipping. The wheelsets have steering capabilities and are on of the most components that affect the vehicle stability and its curving performance [9, 20]. The wheel profile is composed of two parts, the wheel tread and the wheel flange. The wheel tread is usually conned at 1/20 or 1/40 and is in contact with the rail head. The wheel flange is provided on the inside edge of the tread and, for lateral displacement, it becomes in contact with the rail edge, limiting the wheel lateral motion and reducing the probability to derailment.

4.5.2 Wheelset frame of reference

For the wheelset system represented here, it was considered to use an intermediate system of reference represented before making the final rotation about the Y- axis which is the axis of rotation of the wheelset, so the considered intermediate system of reference will be defined after two consecutive rotations about Z-axis and X-axis respectively. The importance of the use of the intermediate system of reference appeared in the definition of the contact forces and the angular velocity vectors before making the rotation of the wheelset about Y-axis to provide the simplicity of the representation of the angular velocity vector[25], which is a non linear function of Euler angles, in the intermediate reference frame. Fig.(4.3) shows a description of the intermediate reference frame, which consists of three orthogonal coordinates ($\underline{X}$ $\underline{Y}$ $\underline{Z}$), where the $\underline{Z}$-axis is pointing to the vertical direction, $\underline{Y}$-axis is parallel to the axis of rotation of the wheelset, and finally the $\underline{X}$-axis is normal to the two other axes and pointing to the direction of motion of the wheelset.

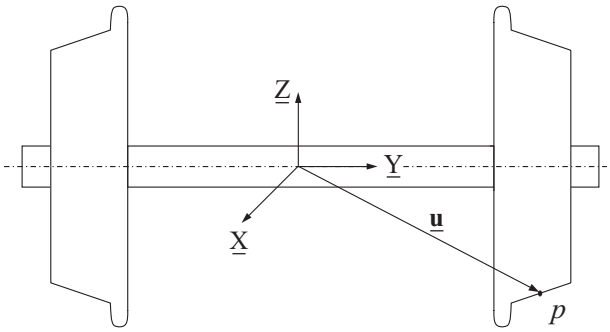

FIGURE 4.3. *Intermediate reference system associated to wheelset system*

For an arbitrary point located on the wheel profile, the position vector be written as follow

$$\underline{\mathbf{u}} = \begin{bmatrix} \underline{u}_x & \underline{u}_y & \underline{u}_z \end{bmatrix}^{\mathrm{T}} \tag{4.39}$$

The lower bar sign appeared in the equation means here that the quantity represented in the intermediate frame of reference. Then by defining the wheelset frame of reference in combination with the track and fixed reference frames Fig.(4.4), all the kinematic and dynamic quantities calculated for the wheelset can be represented in the global reference frame as well as the track reference frames.
Contact problem for the wheel rail interaction forms a crucial part in the simulation of the MBS representing the wheelset and this problem can be divided in three distinct but correlated tasks [17]. The first is the contact geometry which is the problem of finding the location of the contact points on the profiled surfaces taking into account the relative displacements and orientation of the contact bodies, the second is the contact kinematics in which the creepages are defined at the point of contact, and

finally the contact mechanics in which the contact tangential creep forces and spin moments are calculated.

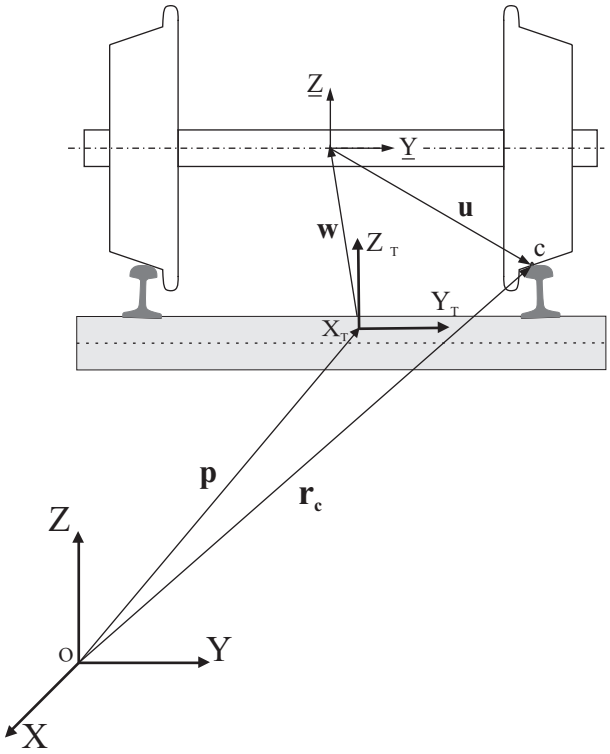

Figure 4.4. *Representation of the Wheelset, Track and Fixed reference frame combination*

4.6 Kinematic analysis of wheelset system

The kinematic analysis is done to obtain the system position and velocity vectors and determination of the generalized coordinates of the system under study. Reaching to this point, we can define the position vector of a point located on the wheelset system, the most important points in the study of the wheelset systems is the points of contact between the wheel and rail, where all the forces of contact and moments are represented. So in the following section the selected point for the analysis is the contact point located on the wheel tread as demonstrated in Fig.(4.4).

4.6.1 Position vector of the contact point

The position vector of the point of contact can be written with respect to the global reference frame as

$$\mathbf{r}_c = \mathbf{p} + \mathbf{A}\,\bar{\mathbf{w}} + \mathbf{A}\,\mathbf{B}_{zx}\,\underline{\mathbf{u}}_c \tag{4.40}$$

where $\mathbf{B}_{zx}$ is the intermediate transformation matrix required to transform from the intermediate to track reference frame, it is the matrix produced from two successive rotations about Z-axis and X-axis respectively, $\underline{\mathbf{u}}_c$ is the position vector of the contact point with respect to the intermediate reference frame. By defining the over all motion of the wheelset with making the final rotation about Y-axis, the transformation from the intermediate transformation reference frame to the general solid reference frame can defined by introducing the transformation matrix $\mathbf{B}_y$. Now all the transformation matrices are introduced between all the system of references used in the formulation of the wheelset system, and these can be explained by the Fig.(4.5).

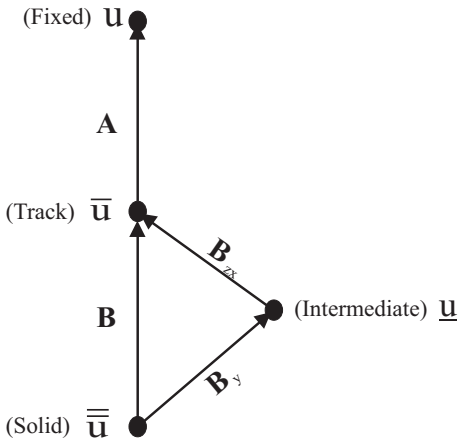

FIGURE 4.5. *Transformation schema between the different reference frames*

The figure.(4.5) shows that, to transform from the track reference frame to the fixed reference frame it was necessary to define the transformation matrix $\mathbf{A}$, to transform from the solid reference frame to the track reference frame the matrix $\mathbf{B}$ was defined, the transformation from between the solid to track reference frame was achieved by two steps in which the intermediate reference system was defined. The first step is to make a transformation from Solid to intermediate by defining the transformation matrix $\mathbf{B}_y$ and then the second step was defined in the definition of the matrix $\mathbf{B}_{zx}$ required to transform from intermediate to track reference frame. Finally the position vector of the contact point can be expressed by the equation

$$\mathbf{r}_c = \mathbf{p} + \mathbf{A}\,\bar{\mathbf{w}} + \mathbf{A}\,\mathbf{B}\,\bar{\bar{\mathbf{u}}}_{\mathbf{c}} \tag{4.41}$$

Where $\bar{\bar{\mathbf{u}}}_{\mathbf{c}}$ is the local position vector of the contact point defined in the solid reference frame.

4.6.2 Velocity vector of contact point

By making the first time derivative for the position vector Eq. (4.40), we can obtain the velocity vector of the contact point as

$$\mathbf{V}_c = \dot{\mathbf{p}} + \dot{\mathbf{A}}\,\bar{\mathbf{w}} + \mathbf{A}\,\dot{\bar{\mathbf{w}}} + \left(\dot{\mathbf{A}}\,\mathbf{B} + \mathbf{A}\,\dot{\mathbf{B}}\right)\,\bar{\bar{\mathbf{u}}}_c \tag{4.42}$$

The velocity of a point on the wheel profile consists of the summation of the total velocity of the wheelset and the circumferential velocity of the point. The total velocity of the wheelset which represent the velocity of the origin of the wheelset reference frame is equal to the velocity of the railway vehicle, it can be written as

$$\mathbf{V} = \dot{\mathbf{p}} + \dot{\mathbf{A}}\,\bar{\mathbf{w}} + \mathbf{A}\,\dot{\bar{\mathbf{w}}} \tag{4.43}$$

The circumferential velocity of a point on the wheel profile can be written as

$$\mathbf{V}_{Cir} = \left(\dot{\mathbf{A}}\,\mathbf{B} + \mathbf{A}\,\dot{\mathbf{B}}\right)\,\bar{\bar{\mathbf{u}}}_c \tag{4.44}$$

$$\mathbf{V}_{Cir} = \left(\mathbf{A}\,\tilde{\bar{\boldsymbol{\tau}}}\,\mathbf{B} + \mathbf{A}\,\dot{\mathbf{B}}_{zx}\,\mathbf{B}_y + \mathbf{A}\,\mathbf{B}_{zx}\,\dot{\mathbf{B}}_y\right)\,\bar{\bar{\mathbf{u}}}_c \tag{4.45}$$

$$\mathbf{V}_{Cir} = \mathbf{A}\,\tilde{\bar{\boldsymbol{\tau}}}\,\mathbf{B}_{zx}\,\underline{\mathbf{u}}_c + \mathbf{A}\,\dot{\mathbf{B}}_{zx}\,\underline{\mathbf{u}}_c + \mathbf{A}\,\mathbf{B}_{zx}\,\dot{\mathbf{B}}_y\,\bar{\bar{\mathbf{u}}}_c \tag{4.46}$$

By recalling the identities used in the calculation of the time derivative of the transformation matrices $\mathbf{A}$ and $\mathbf{B}_{zx}$ [1], the global velocity vector of the contact point can be written as

$$\mathbf{V}_c = \dot{\mathbf{p}} + \mathbf{A}\,\tilde{\bar{\boldsymbol{\tau}}}\,\bar{\mathbf{w}} + \mathbf{A}\,\dot{\bar{\mathbf{w}}} + \mathbf{A}\,\tilde{\bar{\boldsymbol{\tau}}}\,\mathbf{B}_{zx}\,\underline{\mathbf{u}}_c + \mathbf{A}\,\dot{\mathbf{B}}_{zx}\,\underline{\mathbf{u}}_c + \mathbf{A}\,\mathbf{B}_{zx}\,\frac{\partial\,\mathbf{B}_y}{\partial\,\theta_y}\,\dot{\theta_y}\,\mathbf{B}_y^{\mathrm{T}}\,\underline{\mathbf{u}}_c \tag{4.47}$$

which can be written in with respect to the intermediate reference frame in the form

$$\begin{aligned}\underline{\mathbf{V}}_c &= \mathbf{B}_{zx}^{\mathrm{T}}\,\mathbf{A}^{\mathrm{T}}\,\mathbf{V}_c \qquad (4.48)\\ &= \mathbf{B}_{zx}^{\mathrm{T}}\,\mathbf{A}^{\mathrm{T}}\dot{\mathbf{p}} + \mathbf{B}_{zx}^{\mathrm{T}}\,\tilde{\bar{\boldsymbol{\tau}}}\,\bar{\mathbf{w}} + \mathbf{B}_{zx}^{\mathrm{T}}\,\dot{\bar{\mathbf{w}}} + \mathbf{B}_{zx}^{\mathrm{T}}\,\tilde{\bar{\boldsymbol{\tau}}}\,\mathbf{B}_{zx}\,\underline{\mathbf{u}}_c + \mathbf{B}_{zx}^{\mathrm{T}}\,\dot{\mathbf{B}}_{zx}\,\underline{\mathbf{u}}_c + \frac{\partial\,\mathbf{B}_y}{\partial\,\theta_y}\,\dot{\theta_y}\,\mathbf{B}_y^{\mathrm{T}}\,\underline{\mathbf{u}}_c.\end{aligned}$$

[1] Appendix **A**

4.6.3 Wheel-Rail contact forces

In the presentation of the wheel and rail models used in the formulations. Both of them was considered to be a rigid body, so that the contact zone could be reduced to a contact point. In reality when two bodies are in contact, the elastic deformation of both surfaces causes the contact to be spread over a finite area, rather than to be concentrated in a point. This finite area is known as the contact patch. In railway vehicle dynamics, when a wheel rolls over the rails exists a micro-slip in the contact zone, which called creep. This micro-slip together with the normal contact forces, cause the tangential contact forces, known as creep forces [5, 6, 20]. In the wheel-rail contact problem, the dimension of the contact area is small when compared with the typical dimensions of the contacting bodies. Hence, the normal contact force developed in the contact area can be reduced to a single normal force. According to Hertz theory proposed here to study the wheel-rail contact problem, the dimension of the contact area are only dependent of the normal force, the material properties and the surface curvature of the contact bodies, being independent of the tangential forces that developed in the contact interface. The normal and tangential contact problems are decoupled and their solutions are treated sequentially.

4.6.4 Normal contact force

Generally in the wheel-rail interaction problem, if there is no penetration between the wheel and the rail, there is no contact and then the contact forces are null. the occurrence of the penetration is used as the basis to develop a procedure to evaluate the local deformation of the bodies in contact. These forces are calculated as being equivalent to those that would appear if the bodies in contact were pressed against each other by external static force [20, 24, 28]. This means that the contact forces are treated as elastic forces expressed as functions of the co-ordinates and velocities of the two bodies. The procedure proposed here for the calculation of the normal contact force depends on Hertz contact model for calculating the normal force applied at the contact point between the wheel and the rail. The direction of the normal force is determined from the normal vector to the wheel and rail surfaces at the point of contact.

4.6.4.1 Hert'z normal contact force

The figure below Fig. (4.6), shows the interaction between the rail and the wheel, and the radius of curvature of both the wheel and the rail was defined as shown in the figure below. The principle rolling radius of the wheel is R_1, R_3 is the transversal radius of curvature of the wheel at the point of contact, R_2 is the transversal radius of curvature of the rail which usually has infinity value, and R_4 is the principal rolling radius of the rail at point of contact. The normal contact force produced at the point of contact can be calculated through the following expression

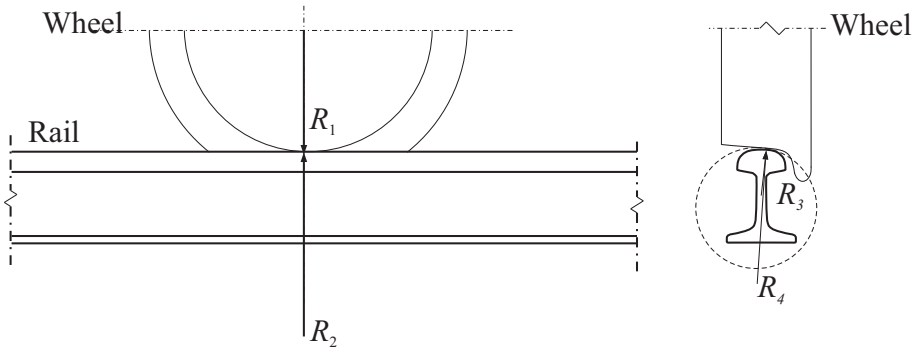

FIGURE 4.6. *Wheel and rail radii of curvatures*

$$F_z = \left(\frac{\delta^3}{r^3 \left(\frac{3}{4} \ (K_w + K_r)\right)^2 \left(\frac{A-B}{2}\right)} \right)^{0.5} \tag{4.49}$$

where F_z is the normal contact force, δ is the amount of indentation or the penetration between the wheel and the rail, K_w and K_r are the material parameters of the wheel and the rail respectively, and can be calculated through the expression

$$K_w = \frac{1 - \nu_w^2}{E_w} \quad ; \quad K_r = \frac{1 - \nu_r^2}{E_r} \tag{4.50}$$

where ν_w and ν_w are the poisson's ratio for the wheel and rail materials respectively, E_w and E_R are young's modulus of elasticity of the wheel and rail materials. The parameter r in Eq. (4.49) can be found from Hertz's table [2], by interpolation between the values of the angular parameter Θ [20, 29], which can be calculated by the following expression

$$\Theta \ = \ \arccos\left(\frac{A-B}{A+B}\right) \tag{4.51}$$

where A and B are geometrical functions related to the principle and transversal radii of curvature of the wheel and the rail, which can be found by

$$\left.\begin{aligned} A = & \ \frac{1}{2} \ (\kappa_3 \ + \kappa_4) \\ B = & \ \frac{1}{2} \ (\kappa_1 \ + \kappa_2) \end{aligned}\right\} \tag{4.52}$$

Where κ is the curvature which can be calculated through the following equation

[2] Appendix **B**

$$\kappa = \frac{1}{R_n} \quad ; \; n = 1, 2, 3 \text{ and } 4 \tag{4.53}$$

4.6.4.2 Size and shape of the contact patch

When two elastic bodies are pressed against each other by normal force, a contact region is formed around the point contact. The shape and size of the contact patch between the two bodies are given by Hertz contact theory [6, 9, 15, 20]. In this section we will describe the necessary expressions required to calculate the size of the contact patch. According to Hertz theory and the assumptions proposed by in it which considered to be one of the most realistic ways of analyzing of normal wheel-rail contact. In most of the railway applications the contact ellipse is a good approximation of the real contact patch, and in our simulation here it was sufficient to use Hertz theory in the analysis of the normal contact problem. The contact patch takes the shape of an ellipse shown in Fig. (4.7)

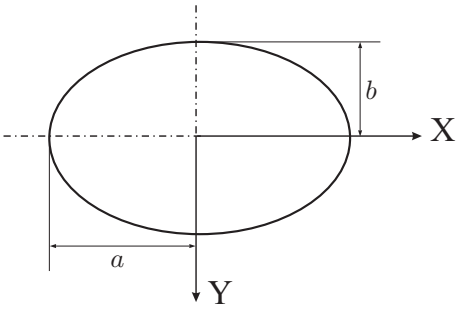

FIGURE 4.7. *Longitudinal and transversal semi axes of the contact ellipse*

The longitudinal and transversal semi axis of the contact ellipse can be calculated by knowing the radii of curvature, the properties of the both wheel and the rail, and the normal contact force between them. The formulations used in the bibliography [5, 9], to calculate the contact ellipse semi axes can be written as

$$a = m \sqrt[3]{\frac{3}{4} F_z \left(\frac{K_w + K_r}{A + B} \right)} \tag{4.54}$$

$$b = n \sqrt[3]{\frac{3}{4} F_z \left(\frac{K_w + K_r}{A + B} \right)} \tag{4.55}$$

where m and n are constants can be found by the interpolation between the values illustrated in Hertz table [2], for the corresponding values of the angle Θ which vary from 0 to 180 °.

[2] Appendix **B**

4.6.5 Tangential contact forces

In the study of the wheel rail interaction phenomenon, it was found that lateral instability, hunting motion, ride quality and derailment problems are directly affected by the creep forces that occur at the contact patch. In the proceeding part, a three dimensional rolling contact model illustrated, presenting the wheel rail interaction, to calculate the creep forces at the contact patch [20]. According to Hertz theory, an elliptical contact area was produced due to the contact between the wheel and the rail, normal stress distribution was formed. Due to the rotation of the wheel over the rail, a friction is assumed to be presented in addition to the normal stress, shear stress may occur in the contact area which result a longitudinal and lateral tangential forces. The axis of rotation of the wheel is not required to be parallel to the rail lateral axis, so a relative angular velocity about the normal axis is produced. So the contact interface tends to twist which leads to tangential stress and slip, due to the spin produced due to angular velocity at the contact area [26].

4.6.5.1 Creepage phenomena

The creep phenomenon, also known as creepages, exists when two bodies are pressed against each other with normal forces and are allowed to roll over each other. Creep may be described as a part elastic and part frictional behavior in which an elastic body, rolls over another elastic body, shares an area of contact where both slip and adhesion occur simultaneously.Therefore, a creep region of contact may be regarded as transition stat between pure rolling and pure sliding. The creepages are crucial in the calculation of the creep forces and moments that develop in the wheel rail contact region, for this purpose the accurate description of the creep phenomenon associated to the wheel-rail interaction is essential. In railway vehicle dynamics, the creep is used to characterize the relative difference in velocities between ideally rolling wheel [8, 18], having no slip in the contact, and the real one. The slip velocity between the wheel and the rail can be defined as a function of the longitudinal, lateral and spin creep which known as the creepages. For better understanding of the creep phenomenon, a wheel rolling over a rail was presented in the figure below, illustrating the longitudinal and lateral creepages as shown in Fig. (4.8)

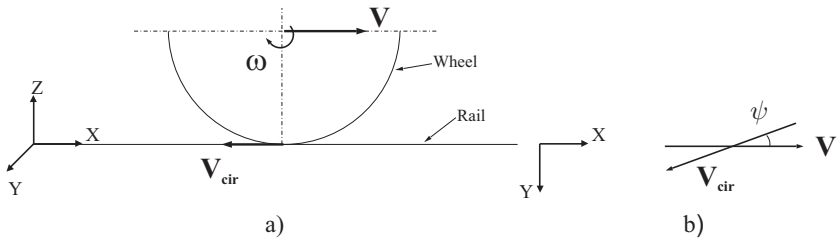

Figure 4.8. *Wheel rolling over rail:a) Longitudinal creepage; b) Lateral creepage*

4.6.5.2 Longitudinal Creepage

In case of rolling with out slipping, the distance traveled by the wheel in one revolution is equal to the circumference of the wheel. But when torque is applied to the wheel, the distance traveled by the wheel in the forward direction is less than the circumference. Since the wheel profile is conned then the longitudinal creep is arises when there is a difference in the rolling radii of the two wheels of the wheelset. The longitudinal creepage can be defined as [28].

$$\xi_x = \frac{\textit{Forward velocity of the wheel - Forward velocity of the rail}}{\textit{Pure rolling forward velocity}} \tag{4.56}$$

by finding the velocity vector of the point of contact represented by Eq.(4.48). The longitudinal creepage can be written as

$$\xi_x = \frac{\underline{\mathbf{V}}_c^{\mathrm{T}}\,\underline{\boldsymbol{l}}}{\mathbf{V}} \tag{4.57}$$

where $\underline{\mathbf{V}}_c$ is the velocity vector of the contact point represented in the intermediate system of reference associated with the wheelset, $\mathbf{V}$ is the rolling velocity [18], $\underline{\boldsymbol{l}}$ is the principle vector in the longitudinal direction at the point of contact on the wheel profile as shown in Fig. (4.9).

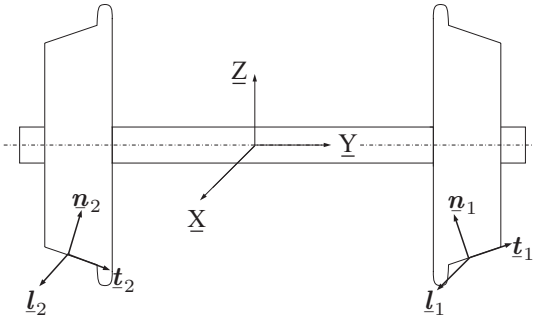

FIGURE 4.9. *The principle tangent, normal, and longitudinal vector at the left wheel represented by number(1) and at the right wheel represented by number(2)*

4.6.5.3 Lateral Creepage

The lateral creepage ξ_y occurs when the wheelset is forced to move in a direction that makes a yaw angle ψ with respect to the rolling plane Fig.(4.8), it is defined as the quotient between the lateral component of the relative velocity of the contact points, i.e the lateral slip velocity, and the wheel forward velocity [20], lateral creepage generally can be defined as

$$\xi_y = \frac{\textit{Lateral velocity of the wheel - Lateral velocity of the rail}}{\textit{Pure rolling forward velocity}} \tag{4.58}$$

lateral creepage has a significant influence on the rails corrugations caused by the lateral creepage forces. Furthermore, the stick -slip phenomenon can be supposed to be induced between a resultant of mainly lateral and longitudinal creepage force [7]. Lateral creepage is thus likely to exist in combination with longitudinal creepage and the influence of longitudinal creepage on the mechanism of squeal noise behaviour, specifically the creepage/creep force relationship, is of interest [18]. to calculate the lateral creepage for the model we use here in the dynamic simulation of the wheelset system, the following expression is used

$$\xi_y = \frac{\mathbf{V}_c^{\mathrm{T}}\, \underline{\boldsymbol{t}}}{\mathbf{V}} \tag{4.59}$$

where $\underline{\boldsymbol{t}}$ is the tangential unit vector at the point of contact on the wheel profile as shown in Fig. (4.8).

4.6.5.4 Spin Creepage

The spin creepage is due to the component of the relative angular velocity of the two bodies normal to the contact surfaces. Generally speaking, the angular velocity of a wheel relative to the rail can be decomposed into three components; one of them is perpendicular to the contact plane, while the other two are tangent to the plane of contact [26]. However pure rolling occurred when the rolling occurs with out sliding or spin [20]. The normal angular velocity is the instantaneous rate at which the wheel turns on the contact plane relative to rail, the normal component of the relative angular velocity acting through the normal direction to the contact surface represented by the unit normal vector $\vec{\mathbf{n}}$ shown in Fig.(4.10), causes the spin (or yaw). Since the wheel profiles are coned, the rolling angular velocity of the wheel $\vec{\boldsymbol{\omega}}$ is not

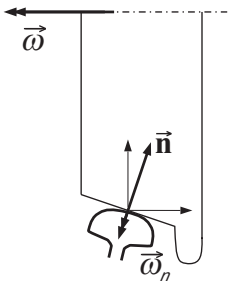

FIGURE 4.10. *Spin creepage*

perpendicular to the vector normal to the contact area $\vec{\mathbf{n}}$ as shown in Fig. (4.10) the consequence is that the wheel has an angular velocity $\vec{\boldsymbol{\omega}}_n$ relative to the rail in the

contact patch. The spin creepage is given by the angular velocity of the wheel, about the normal to the contact region and can be defined by the following equation

$$\xi_{sp} = \frac{Wheel\ \ angular\,velocity\ \text{-}Rail\ \ angular\,velocity}{Pure\ \ rolling\ \ forward\ \ velocity} \tag{4.60}$$

which can be written in the form

$$\xi_{sp} = \frac{\underline{\boldsymbol{\omega}}^{\mathrm{T}}\,\underline{\boldsymbol{n}}}{\mathbf{V}} \tag{4.61}$$

Where $\underline{\boldsymbol{\omega}}$ is the angular velocity of the wheelset represented in the intermediate reference frame and $\underline{\boldsymbol{n}}$ is the unit normal vector at the contact point. Longitudinal and lateral creepages are dimensionless, but the spin creep has the dimension of $\left(length^{-1}\right)$. The longitudinal creepage ξ_x is related with the difference between the rolling forward velocity and the circumferential velocity $|\mathbf{V} - \mathbf{V_{cir}}|$, the lateral creepage ξ_y characterize the non alignment of the wheel with respect to the rail, while the spin creepage ξ_{sp} is related with the concity of the wheel[14].

4.7 Contact forces resulting from the wheel-rail interaction

In addition to the normal contact forces acting on the contact patch, the tangential forces acting at the contact area must be determined. The creep forces and the spin creep moment result from the tangential motion of the wheel relative to the rail in the contact region, therefore they depends on the creepages. The dimension of the contact ellipse and the normal contact force calculated by Hertz formulation expressed by Eq(4.49), are required to calculate the creep forces. The relationship between the creepages quantities, longitudinal creepage ξ_x and lateral creepage ξ_y and the spin creep moment ξ_{sp} and the creep forces can be determined by the creep force law [8, 12, 15]. Various theories was used to solve the problem of the rolling contact and calculation of the creepage forces namely, *saturation of the tangential contact forces; the simplified theory of the rolling contact; linear steady state rolling contact; Heuristic non linear creep force model.* It was proposed to use the *linear steady state rolling contact* to calculate the tangential contact forces at the contact patch, the name linear is directly joined to the application of Coulomb's law and the application of the conditions of Coulomb's theory for the saturation of the tangential stress. Then the linear theory is an approximation, because for large creepages, the tangential traction expressed by Coulomb's law can be violated[15, 18, 20]. For small creepages ξ_x and ξ_y and spin ξ_{sp}, the area of slip is so small that its influence can be neglected. The adhesion zone, therefore, can be assumed to cover the area of contact. Kalker's linear creep force-creepages relation [5, 8, 21, 24] are given for the longitudinal creep force as

$$F_x = -f_{33}\,\xi_x \tag{4.62}$$

and for the lateral creep force

$$F_y = -f_{11}\,\xi_y - f_{12}\,\xi_{sp} \tag{4.63}$$

finally for the spin creep moment can be expressed as

$$M_{sp} = f_{12}\,\xi_y - f_{22}\,\xi_{sp} \tag{4.64}$$

The minus sign indicates that the creep force acts in the opposite direction to the creepages [15, 18], where the coefficients appeared in equations(4.62), (4.63) and (4.64), f_{11}, f_{12}, f_{22} and f_{33} are Kalker's creep coefficient which can be determined by the following expressions.

$$\left.\begin{array}{ll} f_{11} = Ga\,b\,c_{22} & f_{12} = G\sqrt{a^3b^3}\,c_{23} \\ f_{22} = Ga^2b^2c_{22} & f_{33} = Ga\,b\,c_{11} \end{array}\right\} \tag{4.65}$$

Then the creep force law can be written in matrix form as

$$\left\{\begin{array}{c} F_x \\ F_y \\ M_{sp} \end{array}\right\} = -G\,a\,b \left[\begin{array}{ccc} c_{11} & 0 & 0 \\ 0 & c_{22} & \sqrt{a\,b}\,c_{23} \\ 0 & -\sqrt{a\,b}\,c_{23} & a\,b\,c_{33} \end{array}\right] \left\{\begin{array}{c} \xi_x \\ \xi_y \\ \xi_{sp} \end{array}\right\} \tag{4.66}$$

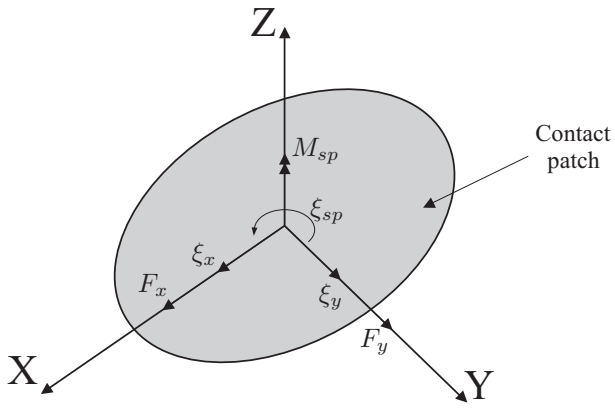

FIGURE 4.11. *Creepages velocities and tangential forces on the contact patch*

where G is the combined shear modulus of rigidity of rail and wheel materials, c_{ij} are the creepage and spin coefficients which are calculated for the exact theory can be obtained from Kalker table, and these coefficients depend on the combined poisson's ratio and the ratio between the longitudinal and transversal axis (a/b) of the contact

ellipse[2]. The coefficients c_{ij} are valid for dry friction, which, according to Kalker, corresponds to a friction coefficient of $\mu = 0.6$. All these forces are acting in local normal and tangential coordinate directions defined by the orientation of the contact ellipse Fig. (4.11) By appropriate transformations they may be expressed as acting and counter acting forces on the wheel and the rail in their interference systems. Finally the contact loads can mainly divided into contact forces and contact moments shown in the equation of motion for the wheel set and the track [4].

4.8 Dynamic analysis of wheelset

The same as the dynamic analysis for a solid body explained in section.(4.3) we can find the equations of motion for the wheelset defined in the previous part, the only difference is the values of the generalized force associated to the wheelset generalized coordinates. For calculating the generalized force, it was supposed to use the virtual work principle [3, 25, 29] as it was explained, in the previous sections, for the calculations of the generalized forces associated to the generalized coordinates of the solid. The virtual work can be found for a wheelset system by determining the virtual displacement of a point on the the wheel profile, then the calculation of the force applied at this point. Reaching to the end of the determination of the contact forces and moments at the contact patch resulting from wheel-rail interaction, also the force applied to the wheelset system due to the spring element mounted between the wheel axle and the bogie, one can find the virtual work due to these types of forces as it can be illustrated in the following sections.

4.8.1 Virtual work due to contact forces

For the contact forces applied at the contact patch, including the normal contact force, longitudinal and lateral creepage forces, with knowing the virtual displacement that can be calculated from the position vector of the contact point represented by Eq. (4.40) which can be written as

$$\delta \mathbf{r}_{\mathrm{c}} = \frac{\partial \mathbf{r}_{\mathrm{c}}}{\partial \bar{\mathbf{w}}} \delta \bar{\mathbf{w}} + \frac{\partial \mathbf{r}_{\mathrm{c}}}{\partial \boldsymbol{\theta}} \delta \boldsymbol{\theta} \tag{4.67}$$

$$\delta \mathbf{r}_{\mathrm{c}} = \mathbf{A} \delta \bar{\mathbf{w}} + \mathbf{A} \frac{\partial \mathbf{B}_{zx}}{\partial \boldsymbol{\theta}} \underline{\mathbf{u}}_{\mathrm{c}} \delta \boldsymbol{\theta} \tag{4.68}$$

where

$$\frac{\partial \mathbf{B}_{zx}}{\partial \boldsymbol{\theta}} = \left[\frac{\partial \mathbf{B}_{zx}}{\partial \theta_i} \right]^{\mathrm{T}} \quad , i = x, y \text{ and } z \tag{4.69}$$

Then the virtual work due to the contact force can be found by

[2] Appendix **B**

$$\delta W = \boldsymbol{F}_c^{\mathrm{T}}\, \delta\, \mathbf{r}_{\mathrm{c}} \tag{4.70}$$

$$\delta W = \boldsymbol{F}_c^{\mathrm{T}}\, \mathbf{A}\, \delta\, \bar{\mathbf{w}} + \boldsymbol{F}_c^{\mathrm{T}}\, \mathbf{A}\, \frac{\partial\, \mathbf{B}_{zx}}{\partial\, \boldsymbol{\theta}}\, \underline{\mathbf{u}}_{\mathrm{c}}\, \delta\, \boldsymbol{\theta} \tag{4.71}$$

by defining the contact force vector resulting from the wheel-rail interaction and determined by Eq. (4.62), Eq. (4.63) and Eq. (4.49), which can be written as

$$\boldsymbol{F}_c = \begin{bmatrix} F_x & F_y & F_z \end{bmatrix}^{\mathrm{T}} \tag{4.72}$$

From equation.(4.31), the generalized forces due to the contact force can be written as

$$\mathbf{Q}_{\bar{\mathrm{w}}} = \bar{\boldsymbol{F}}_c \tag{4.73}$$

$$Q_{\theta_x} = \underline{\boldsymbol{F}}_c^{\mathrm{T}}\, \mathbf{B}_{zx}^{\mathrm{T}}\, \frac{\partial\, \mathbf{B}_{zx}}{\partial\, \theta_x}\, \underline{\mathbf{u}}_c \tag{4.74}$$

$$Q_{\theta_y} = \underline{\boldsymbol{F}}_c^{\mathrm{T}}\, \mathbf{B}_{zx}^{\mathrm{T}}\, \frac{\partial\, \mathbf{B}_{zx}}{\partial\, \theta_y}\, \underline{\mathbf{u}}_c \tag{4.75}$$

$$Q_{\theta_z} = \underline{\boldsymbol{F}}_c^{\mathrm{T}}\, \mathbf{B}_{zx}^{\mathrm{T}}\, \frac{\partial\, \mathbf{B}_{zx}}{\partial\, \theta_z}\, \underline{\mathbf{u}}_c \tag{4.76}$$

Where $\underline{\boldsymbol{F}}_c$ is the contact force vector represented in the intermediate coordinate system associated to the wheelset and $\mathbf{B}_{zx}$ is the transformation matrix from intermediate to fixed or global frame of reference.

4.8.2 Virtual work due to contact moment

The contact moment at the contact patch, produce from the spin creepage momoent $\boldsymbol{M}_{sp}$. The virtual work due to this moment $\boldsymbol{M}_c$ may be replaced by an equivalent pair of forces, $\boldsymbol{f}_1$ and $\boldsymbol{f}_2$, of equal magnitude and opposite directions, acting on a plane perpendicular to the direction of $\boldsymbol{M}_c$ [11] and both supposed to be acting through the longitudinal direction defined by the unit vector $\underline{\boldsymbol{l}}$, and separated by the lateral unit vector $\underline{\boldsymbol{t}}$, Fig. (4.12) which represent the lateral vector.If the two forces applied at the contact point can be found by:

$$\left.\begin{aligned} \underline{\boldsymbol{f}}_1 &= -f\, \underline{\boldsymbol{l}} \\ \underline{\boldsymbol{f}}_2 &= f\, \underline{\boldsymbol{l}} \end{aligned}\right\} \tag{4.77}$$

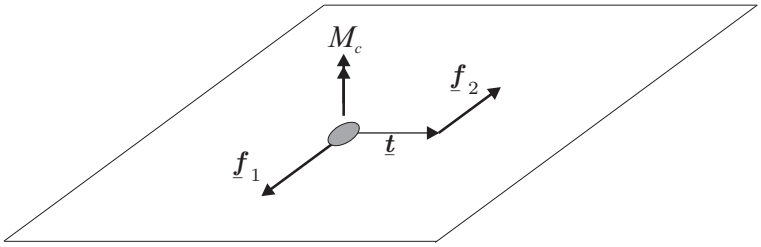

FIGURE 4.12. *Concentrated contact moment $\boldsymbol{M}_c$ acting on contact area*

Then the moment at the contact point can be found by

$$\underline{\boldsymbol{M}}_c = \underline{\boldsymbol{t}} \times \underline{\boldsymbol{f}}_2 \tag{4.78}$$

Furthermore the virtual work due to the contact moment can be now found by the following expression

$$\delta W = \underline{\boldsymbol{f}}_1 \delta \mathbf{r}_{f1} + \underline{\boldsymbol{f}}_2 \delta \mathbf{r}_{f2} \tag{4.79}$$

From Eq. (4.78), we find that

$$\underline{\boldsymbol{f}}_2 = -M\underline{\boldsymbol{l}} \tag{4.80}$$

but we know that $\boldsymbol{f}_1 = -\boldsymbol{f}_2$, then the virtual work due to these forces reduced to

$$\delta W = -M\underline{\boldsymbol{l}}^{\mathrm{T}} \mathbf{B}_{zx}^{\mathrm{T}} \frac{\partial \mathbf{B}_{zx}}{\partial \boldsymbol{\theta}} \mathbf{t}_c \, \delta \boldsymbol{\theta} \tag{4.81}$$

4.8.3 Virtual work due to internal forces

The internal forces that may affect the wheelset such as the spring element forces acting on the wheelset connection with the bogie frame through the primary suspension springs. These Springs are elements capable of storing elastic potential energy and of exerting forces that are a function of their positions[11]. In addition, springs play an important role in all but the kinematic problems. Modeling of the suspension element is a crucial part in the multibody dynamic program used for the simulation of the railway vehicle. To represent the forces transmitted by the suspension element we have to define the amount of change in the relative position vector between the two connection points which represent the amount of change between the undeformed and deformed spring length, and for this issue we use the model shown in Fig. (4.13) , which represent a suspension element connecting two rigid bodies i and j.

The suspension is attached to the body i at the point **1** and to the body j through the point **2**. By defining the position vector of the reference frame of each body we

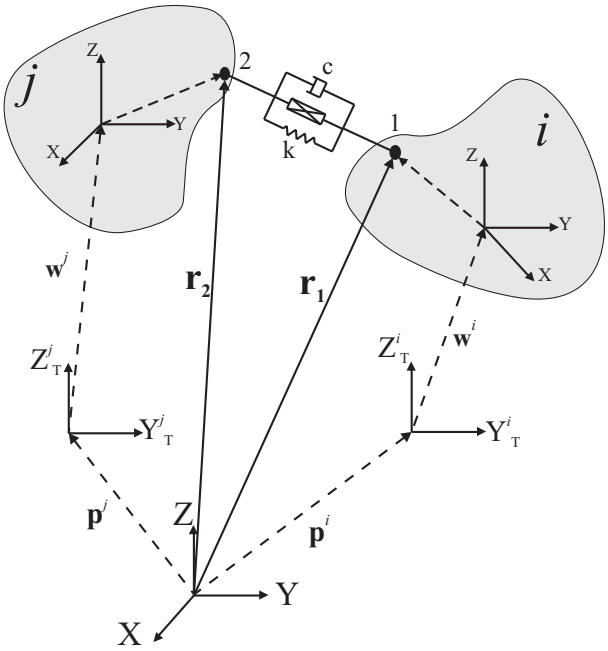

FIGURE 4.13. *Position vector of two connection points of a spring element between two bodies i and j.*

found that, the position vector of the origin of the frame of reference of the solid i can be found by the following expression

$$\mathbf{r}^i_{CM} = \mathbf{p}^i + \mathbf{A}^i \, \bar{\mathbf{w}}^i \tag{4.82}$$

and the position vector of the origin of the reference frame of the solid j can be written as follow

$$\mathbf{r}^j_{CM} = \mathbf{p}^j + \mathbf{A}^j \, \bar{\mathbf{w}}^j \tag{4.83}$$

the position vector of the first connection point of the spring with the solid body i can be written as

$$\mathbf{r}_1 = \mathbf{r}^i_{CM} + \mathbf{A}^i \, \mathbf{B}^i \, \bar{\bar{\mathbf{u}}}^i_1 \tag{4.84}$$

the position vector of the first connection point of the spring with the solid body j can be written as

$$\mathbf{r}_2 = \mathbf{r}^j_{CM} + \mathbf{A}^j \, \mathbf{B}^j \, \bar{\bar{\mathbf{u}}}^j_2 \tag{4.85}$$

the relative position vector representing the deformed length of the spring element from point **1** to point **2** can be written as

$$\mathbf{r}_{12} = \mathbf{r}_2 - \mathbf{r}_1 \tag{4.86}$$

$$\mathbf{r}_{12} = \ \mathbf{r}^j_{CM} \ - \mathbf{r}^i_{CM} + \mathbf{A}^j \, \mathbf{B}^j \, \bar{\bar{\mathbf{u}}}^j_2 \ - \mathbf{A}^i \, \mathbf{B}^i \, \bar{\bar{\mathbf{u}}}^i_1 \tag{4.87}$$

Where $\mathbf{A}^i$ and $\mathbf{A}^j$ are the transformation matrices required to transform from the track frame corresponding to the body i and body j respectively, to the fixed frame of reference. $\mathbf{B}^i$ and $\mathbf{B}^j$ are the transformation matrices required to transform from the local frame of of body i and body j to each corresponding track frame of reference, $\bar{\bar{\mathbf{u}}}^i_1$ is the position vector of the first connection point **1** with respect to the local frame of reference of body i and $\bar{\bar{\mathbf{u}}}^j_2$ is the position vector of the second connection point **2** with respect to the local frame of reference of body j. And by the relative position vector between the spring connection points with respect to the local frame of reference of the first body i the we find that it can be written as

$$\bar{\bar{\mathbf{r}}}^i_{12} = {\mathbf{B}^i}^{\mathrm{T}} \, {\mathbf{A}^i}^{\mathrm{T}} \left(\mathbf{r}^j_{CM} - \mathbf{r}^i_{CM} + \mathbf{A}^j \, \mathbf{B}^j \, \bar{\bar{\mathbf{u}}}^j_2 \right) - \bar{\bar{\mathbf{u}}}^i_1 \tag{4.88}$$

The relative vector between the two connection points can be written with respect to the second body j as follow

$$\bar{\bar{\mathbf{r}}}^j_{21} = {\mathbf{B}^j}^{\mathrm{T}} \, {\mathbf{A}^j}^{\mathrm{T}} (\mathbf{r}^i_{CM} \ - \mathbf{r}^j_{CM} + \mathbf{A}^i \, \mathbf{B}^i \, \bar{\bar{\mathbf{u}}}^i_1) - \bar{\bar{\mathbf{u}}}^j_2 \tag{4.89}$$

From equation.(4.84) the velocity vector of the point **1** can be written as

$$\dot{\mathbf{r}}_1 = \dot{\mathbf{r}}^i_{CM} + \dot{\mathbf{A}}^i \, \mathbf{B}^i \, \bar{\bar{\mathbf{u}}}^i_1 + \mathbf{A}^i \, \dot{\mathbf{B}}^i \, \bar{\bar{\mathbf{u}}}^i_1 \tag{4.90}$$

The same from equation.(4.85) the velocity vector of the point **2** can be written as

$$\dot{\mathbf{r}}_2 = \dot{\mathbf{r}}^j_{CM} + \dot{\mathbf{A}}^j \, \mathbf{B}^j \, \bar{\bar{\mathbf{u}}}^j_2 + \mathbf{A}^j \, \dot{\mathbf{B}}^j \ \bar{\bar{\mathbf{u}}}^j_2 \tag{4.91}$$

Also the relative velocity vector between the two connection points can be expressed with respect to the local frame of reference of body i as follow

$$\dot{\bar{\bar{\mathbf{r}}}}^i_{12} = {\mathbf{B}^i}^{\mathrm{T}} \, {\mathbf{A}^i}^{\mathrm{T}} \left(\dot{\mathbf{r}}^j_2 - \dot{\mathbf{r}}^i_1 \right) \tag{4.92}$$

The same can be found with respect to the reference frame of the second solid body j as

$$\dot{\bar{\bar{\mathbf{r}}}}^j_{21} = {\mathbf{B}^j}^{\mathrm{T}} \, {\mathbf{A}^j}^{\mathrm{T}} \left(\dot{\mathbf{r}}^i_1 - \dot{\mathbf{r}}^j_2 \right) \tag{4.93}$$

By knowing the undeformed vector between the two connection points $\bar{\bar{\mathbf{r}}}_{12\mathrm{O}}$, the force vector of the spring element can be calculated at the first connection point on the body i, by knowing the stiffness vector $\mathbf{k}$ and the damping coefficient vector $\mathbf{c}$ of the

spring element which will have a constant values if the spring and the damper are linear, in addition to the force vector representing the actuator force $\mathbf{f_a}$, as follow

$$\bar{\bar{\mathbf{F}}}_{\mathrm{s}}^{i} = \mathbf{k}\left(\bar{\bar{\mathbf{r}}}_{12}^{i} - \bar{\bar{\mathbf{r}}}_{12\mathrm{O}}\right) + \mathbf{c}\left(\dot{\bar{\bar{\mathbf{r}}}}_{12}^{i}\right) + \mathbf{f}_{\mathrm{a}} \tag{4.94}$$

and the same for the force vector of spring element affecting the body j can be written with respect to its local frame as

$$\bar{\bar{\mathbf{F}}}_{\mathrm{s}}^{j} = \mathbf{k}\left(\bar{\bar{\mathbf{r}}}_{21}^{j} - \bar{\bar{\mathbf{r}}}_{21\mathrm{O}}\right) + \mathbf{c}\left(\dot{\bar{\bar{\mathbf{r}}}}_{21}^{j}\right) - \mathbf{f}_{\mathrm{a}} \tag{4.95}$$

Then, after the calculation of the element forces. We can apply the same virtual work principle defined by equation (4.29) to calculate the generalized force vector associated to the spring element force

4.9 Conclusion

In this chapter a methodology for the railway vehicle modeling was improved, using multibody formulations depending on the modeling of the railway vehicle components as rigid bodies. The Cartesian coordinates was used to present the kinematic structure of the rigid bodies forming the model used int the analysis. The kinematic and dynamic analysis of a solid body and a wheelset was presented and the equation of motions of the system was developed using Lagrangian approach. It was necessary to completely define the contact problem which can be divided in three main problems namely: the geometry problem, the kinematic problem and finally the dynamic problem. The normal contact forces was determined using the elastic approach and the relative velocities between the contact surfaces was calculated and then implemented in Kalker's linear model for calculating the tangential forces at the contact zone. The tangential forces include: longitudinal creep forces, lateral or transversal creep forces and spin creep moment. It was supposed to use the virtual work principle to calculate the generalized force vector associated to the generalized coordinates. The spin creep moment in the modeling replaced by an equivalent pair of forces, of equal magnitude and opposite directions, acting on a plane perpendicular to the direction of the moment, and both supposed to be acting through the longitudinal direction defined by the unit vector, and separated by the lateral unit vector. Then the analysis included a definition the formulations used in the modeling of the connection elements connecting these rigid bodies to complete the analysis proposed by the methodology illustrated in this chapter.

Chapter 5

Case study and obtained results

5.1 Introduction

In this chapter, the vehicle model used in the multibody program developed in this work , was described and its dynamic behavior is studied in different operation scenarios. First the exact values for the input data required for the track pre-processing step was provided, then the complete definition of the model used in the study is presented including all the assumptions proposed in the modeling of the railway vehicle. Afterwards the construction of the multibody program implemented in MATLAB environment was described. The model performance is analyzed through the different track stages. The vehicle multibody model, consists of four wheelset and two bogie frames supporting a car body, was explained emphasizing the mechanical elements that are relevant to the studies carried out here in this work. This chapter conclude the method and verify the implementation of the developed multibody program which supposed to be used for the dynamic analysis of railway vehicle systems in different operation conditions.

5.2 Track pre-processing stage

For the proposed track model used in this work, which consisting of a straight segment having a length of $1000\,m$, followed by a transition curve connecting the straight line stage to the plane curve stage, with a length of $200\,m$, then the plane curve stage which present the final stage in the designed track model having a length of $3000\,m$. It was proposed to put the fixed frame of reference at which can be the position of an observer located at the starting point of the transition curve stage as it was illustrated

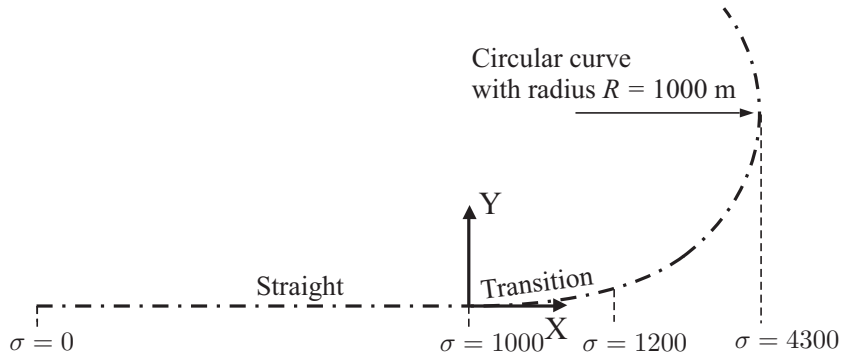

FIGURE 5.1. *Track segments data for the designed track*

in Fig. (5.1). For the complete definition of the track parametrization step in this part, it was necessary to define the cant angle at each track stage, for this issue we define the track hight at the start and end of the track stage under study as shown in Fig. (5.2)

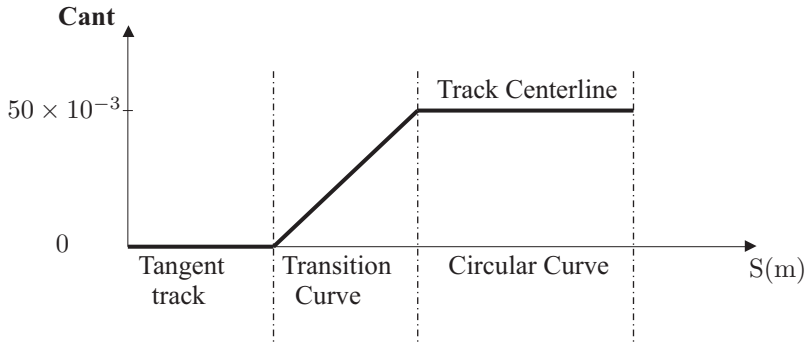

FIGURE 5.2. *Track Super-elevation Ramps*

The track hight for the straight curve stage is defined as $h_{t,o} = 0$, and the maximum hight of the track was defined as $h_{t,max} = 50 \times 10^{-3}$, taking into account that the value of the equilibrium cant angle can be obtained from the equation

$$\phi_{eq} = \arctan(\frac{V^2}{R\,g}) \tag{5.1}$$

Where V is the velocity of the vehicle, R is the radius of curvature of the plane curve stage, g is the gravitational acceleration.

5.3 Multibody model of the vehicle used

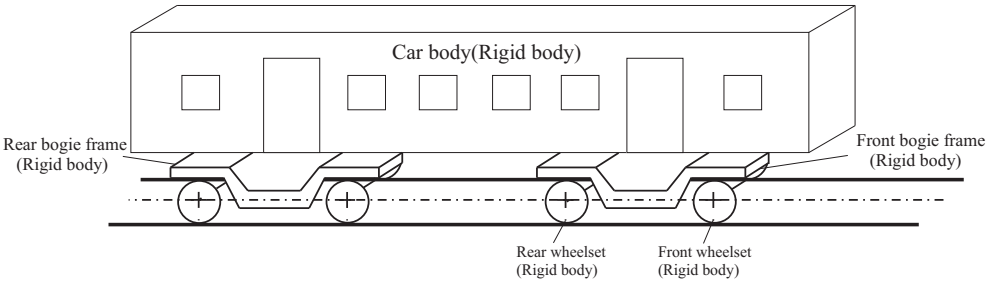

Figure 5.3. *Three dimensional model of railway vehicle*

Generally, a railway vehicle consists of a collection of bodies and mechanical elements moving along the track. In the analysis proposed here in this work it was supposed to deal with only rigid bodies, then the car body, bogie frames, wheelsets Fig. (5.3) all treated as rigid bodies due to their high structural stiffness. The connection between these bodies is presented here by means of spring elements. A schematic diagram Fig. (5.4) representing the rigid bodies connection presenting the multibody vehicle model used in the dynamic analysis proposed in this work.

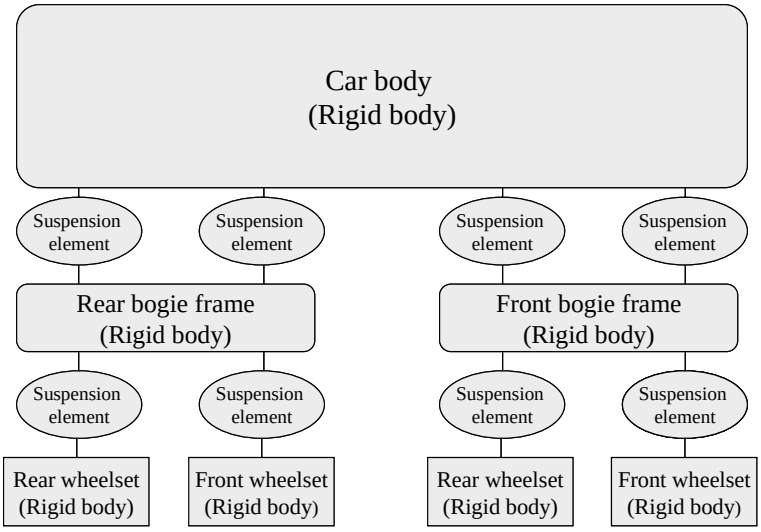

Figure 5.4. *Schematic diagram of the rigid bodies used in the dynamic analysis*

According to the the schematic diagram represented in Fig. (5.4), the car body is connected to the bogie frames by means of suspension elements usually known as the primary suspensions, then the bogie frames are connected to the wheelsets by means of other spring elements defined as the secondary suspensions. The forces applied to the wheelset is transmitted upwards through these elements. The vehicle performance and dynamic behavior are affected by the characteristics of these elements.

5.3.1 Model description

According to the three-dimensional model representing the vehicle proposed here Fig. (5.3).It can be shown the the model consists of 7 rigid bodies, 1 car body;2 pairs of bogie frames; 4 wheelsets. Each rigid body has a 6 DOF, that means that there is no restrictions made for the movement of the body in what ever direction. Then for the system used here in the analysis has 42 DOF.
The system of reference of each solid ($X_s\, Y_s\, Z_s$) is attached to the CM of the solid. The number of the solid frame of reference used coincides with the number of the solids, and the number of track reference frames used is equal to the number of the wheelsets, because in the analysis we toke the track reference frame of the bogie to coincides with the track frame of the front wheelset of each bogie connection, and for the car body it was considered to be represented with respect to the track frame of the the front wheelset attached to the front bogie frame. The position of each track frame was considered to be centered with the frame of reference of the solid frame of reference at a height equal to the nominal radius of the wheel profile, taking in to account the symmetry characteristics for the wheelset and solids which are not wheelset, then the initial position of the each body is given by the location of its center of mass CM with respect to the corresponding track frame of reference and also with respect to the global reference frame. To represent the geometry properties and other inertia parameters for the solids used, it was used to identify the solid with numbers to facilitate the analysis implemented in the multibody program used, for this issue the identification number of each solid was illustrated as shown in Fig.(5.5)

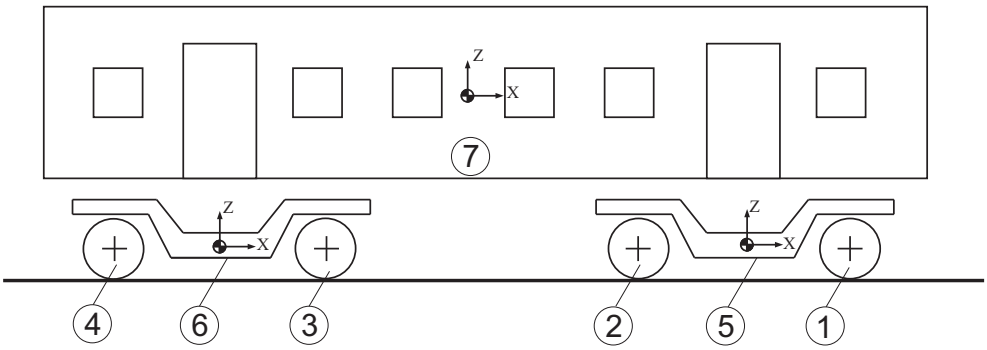

Figure 5.5. *Identification of the solids numbers*

The solids modeled here have a inertia and geometric properties as it can be shown in the following tables

ID	Rigid body	Mass (Kg)	Inertia properties (kg.m2) $\boldsymbol{J}_x$	$\boldsymbol{J}_y$	$\boldsymbol{J}_z$
1	Front wheelset Front bogie	1500	799,35	93,75	799,35
2	Rear wheelset Front bogie	1500	799,35	93,75	799,35
3	Front wheelset Rear bogie	1500	799,35	93,75	799,35
4	Rear wheelset Rear bogie	1500	799,35	93,75	799,35
5	Front bogie frame	3020	2130,912	4063,712	4063,712
6	Rear bogie frame	3020	2130,912	4063,712	4063,712
7	Car body	43200	69677,28	2430000	2430000

Table 5.1. *Mass and inertia properties of rigid bodies*

The initial position vector of each rigid body can be determined here by knowing the initial position vector of the moving track frame with respect to the fixed or the global frame of reference and this will be assigned to only the X-component representing the the distance covered by the solid on the track (σ), and then the initial position vector of the solid frame of reference with respect to the corresponding track frame of reference as shown in the following table.

ID	Corresponding Track F.O.R	I.P of the Track F.O.R w.r.t the Fixed F.O.R (X)	(Y)	(Z)	I.P of the Solid F.O.R w.r.t the Track F.O.R (X)	(Y)	(Z)
1	1	$\sigma = 600$	0	0	0	0	0,45
2	2	$\sigma = 597$	0	0	0	0	0,45
3	3	$\sigma = 580.65$	0	0	0	0	0,45
4	4	$\sigma = 577.65$	0	0	0	0	0,45
5	1	–	–	–	-1,5	0	1,0575
6	3	–	–	–	-1,5	0	1,0575
7	1	–	–	–	-11,175	0	2,5175

Table 5.2. *Initial position vectors of the rigid bodies*

5.3.2 Special elements

In addition to the geometry problems and the definition of the bodies used in the model, there are some special elements that distinguish railway vehicle from other multibody system application. In this part we define the spring elements existing in the model, which can be translational spring, damper, and actuator. The coefficients used in this element formulation define the type of this elements to be linear functions of the relative motion and velocity between the two connected bodies by the spring elements. Table. (5.4)define the stiffness and the damping coefficients of the spring

elements connecting the wheelsets with the bogie frames as it can be shown by spring topology table .(5.5)

spring number	First body	Second body
1	1	5
2	1	5
3	2	5
4	2	5
5	3	6
6	3	6
7	4	6
8	4	6

Table 5.3. *Topology of the springs connecting the wheelsets with the bogie frames*

spring number	Stiffness (N.m)			Damping Coefficients ($\frac{N.s}{m}$)		
	k_x	k_y	k_z	c_x	c_y	c_z
1	3.90×10^7	7.85×10^6	9.75×10^5	0	0	1.08×10^4
2	3.90×10^7	7.85×10^6	9.75×10^5	0	0	1.08×10^4
3	3.90×10^7	7.85×10^6	9.75×10^5	0	0	1.08×10^4
4	3.90×10^7	7.85×10^6	9.75×10^5	0	0	1.08×10^4
5	3.90×10^7	7.85×10^6	9.75×10^5	0	0	1.08×10^4
6	3.90×10^7	7.85×10^6	9.75×10^5	0	0	1.08×10^4
7	3.90×10^7	7.85×10^6	9.75×10^5	0	0	1.08×10^4
8	3.90×10^7	7.85×10^6	9.75×10^5	0	0	1.08×10^4

Table 5.4. *Springs stiffness and Damping coefficients for elements connecting the wheelsets with the bogie frames*

The same for the spring elements connecting the car body with the bogie frames, the connection topology and the coefficients values of the springs and dampers used can be shown in the following tables

spring number	First body	Second body
9	5	7
10	5	7
11	6	7
12	6	7

Table 5.5. *Topology of the springs connecting the bogie frame with the car body*

spring number	Stiffness (N.m)			Damping Coefficients ($\frac{N.s}{m}$)		
	k_x	k_y	k_z	c_x	c_y	c_z
9	1.73×10^5	1.73×10^5	5.3×10^5	0	3.5×10^4	1.50×10^4
10	1.73×10^5	1.73×10^5	5.3×10^5	0	3.5×10^4	1.50×10^4
11	1.73×10^5	1.73×10^5	5.3×10^5	0	3.5×10^4	1.50×10^4
12	1.73×10^5	1.73×10^5	5.3×10^5	0	3.5×10^4	1.50×10^4

Table 5.6. *Springs stiffness and Damping coefficients for elements connecting the bogie frames with the car body*

The most common part in conventional railway vehicles is the wheelset, the wheel set used in the model here composed of two conical wheels rigidly connected by the wheel axle. The used wheelset-rail interaction used here in the simulation is the Knife Edge model defining the shape and type of the interaction between the two surfaces of the wheel and rail profiles as it can be shown in Fig. (5.6)

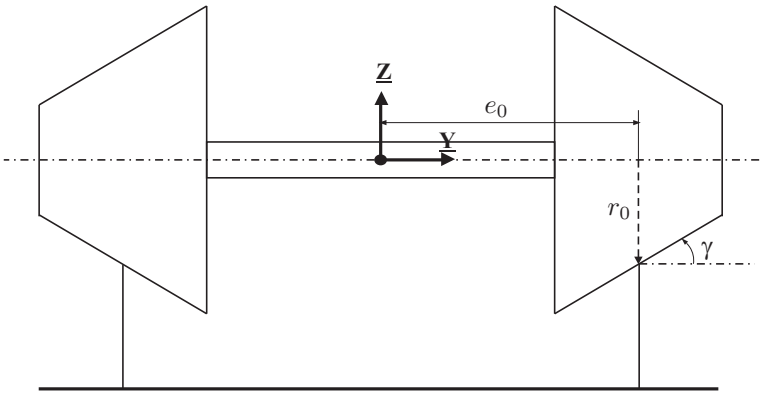

Figure 5.6. *Knife edge model of the wheel-rail interaction*

To represent the contact points and determine the geometry of the contact as an important step in the contact problem, the geometric parameter and contact parameters that represent the model used here in the simulation Fig. (5.7) can be obtained from the following table

The simplified model as described in the figure having the reference frame (X Y Z) in the center of mass of the axle and the shown parameters shown on the figure can be defined as follow

- e_0: is the lateral distance from the wheelset reference associated to the center of mass of the axle frame to the nominal contact point
- r_0: is the nominal radius of rotation.
- γ : is the conicity angle of the wheel.
- y : is the lateral displacement of the wheelset.

Parameter	Symbol	Value	unite
Conicity angle	γ	0.1	rad
Semi distance	e_0	0.75	m
Nominal radius	r_0	0.45	m
Poisson's ratio of wheel material	ν_w	0.25	
Modulus of elasticity of wheel material	E_w	2.10×10^{11}	Pa
Poisson's ratio of rail material	ν_r	0.25	
Modulus of elasticity of rail material	E_r	2.10×10^{11}	Pa

Table 5.7. *Geometry and contact parameters of the wheelset*

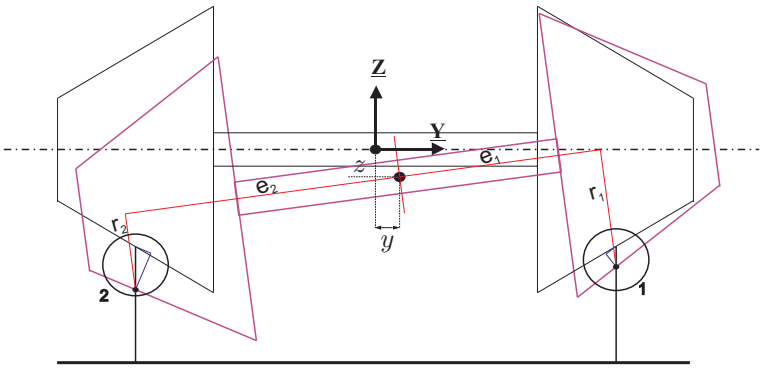

Figure 5.7. *Contact penetration produced from the movement of the wheelset*

- z : is the vertical displacement of the wheelset.
- δ: is the amount of the approach
- ϕ : is the angle of rotation about the longitudinal x-axis
- e_1 : is the normal distance between the rolling radius r_1 and CM
- r_1 : is the new left wheel rolling radius. r_1 and CM
- r_2 : is the new right wheel rolling radius.

after shifting the wheelset with a lateral distance y to the right the position of the center of mass of the axle is now changed and another point of contact produced due to the rotation of the axle about its center with an angle of rotation ϕ about the x-axis, producing change in the rolling radius for the left and right wheel as shown in Fig. (5.7)
we can now analyze the surfaces of contact after making the lateral shift with a displacement y and the rotation angle ϕ with making a magnification for the contact zone for the left wheel contact at point **1** and also the same for the right wheel contact at point **2** as shown in Fig. (5.8)

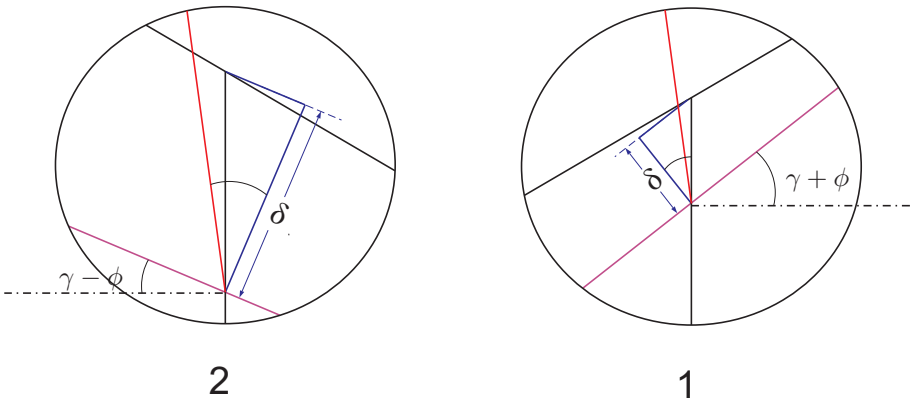

Figure 5.8. *Contact penetration calculation for the left and right wheel*

Left wheel

The contact geometry and amount of approach of the left wheel can be determined by the following equations

$$e_0 = \mathrm{y} + \mathrm{e}_1 \ \cos\phi + \mathrm{r}_1 \ \sin\phi \tag{5.2}$$

$$-\ r_0 = z + e_1 \ \sin\phi - \ r_1 \ \cos\phi \ + \ \delta \ \cos\left(\gamma + \phi\right) + \delta \ \tan\left(\gamma + \phi\right) \ \sin\left(\gamma + \phi\right) \tag{5.3}$$

$$\tan\gamma = \frac{r_1 - r_0}{e_0 - e_1} \tag{5.4}$$

Right wheel

The contact geometry and amount of approach of the right wheel can be determined by the following equations

$$e_0 = \ y \ - e_2 \ \cos\phi + r_2 \ \sin\phi \tag{5.5}$$

$$-\ r_0 = \ z \ - e_2 \ \sin\phi - r_2 \ \cos\phi + \ \delta \ \cos\left(\gamma - \phi\right) + \delta \ \tan\left(\gamma - \phi\right) \ \sin\left(\gamma - \phi\right) \tag{5.6}$$

$$\tan\gamma = \frac{r_0 - r_2}{e_2 - e_0} \tag{5.7}$$

5.4 Main structure of the program.

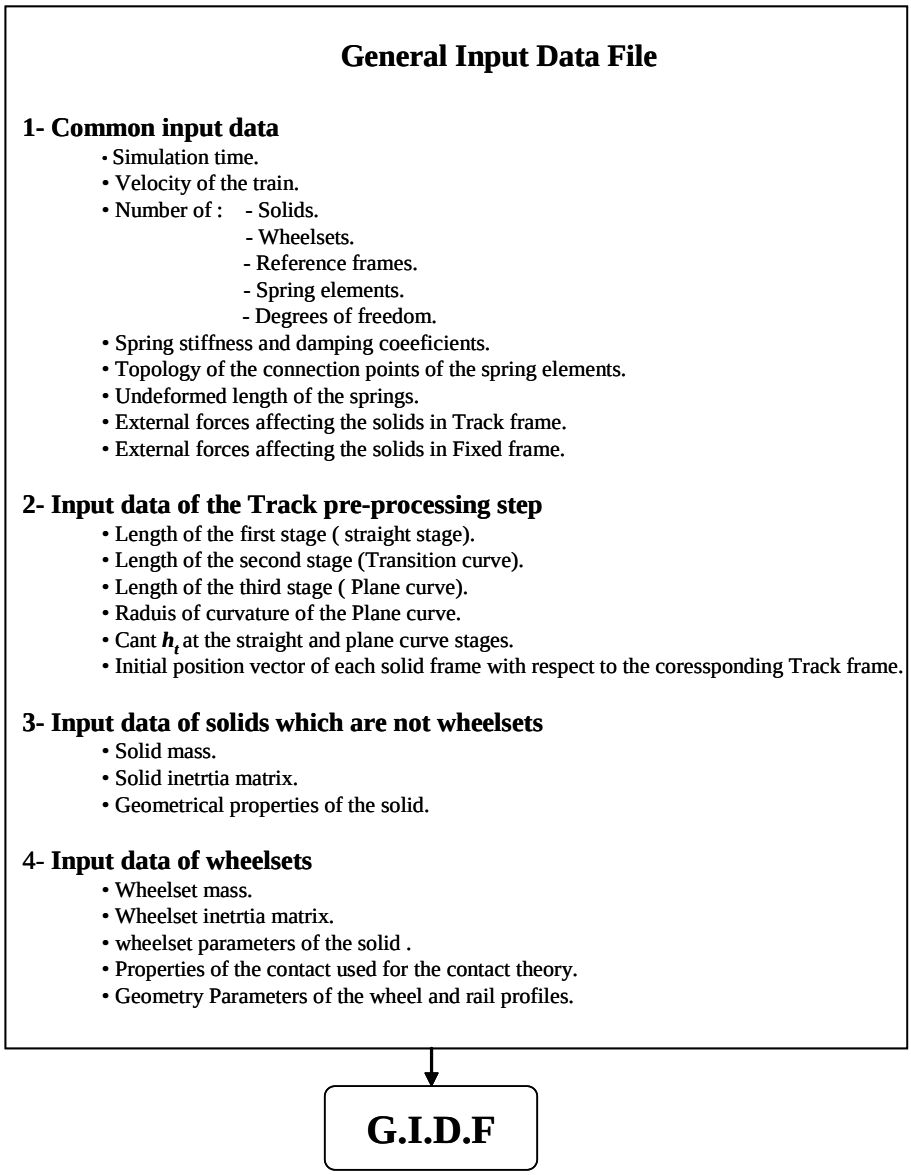

Figure 5.9. *Multibody program flow chart*

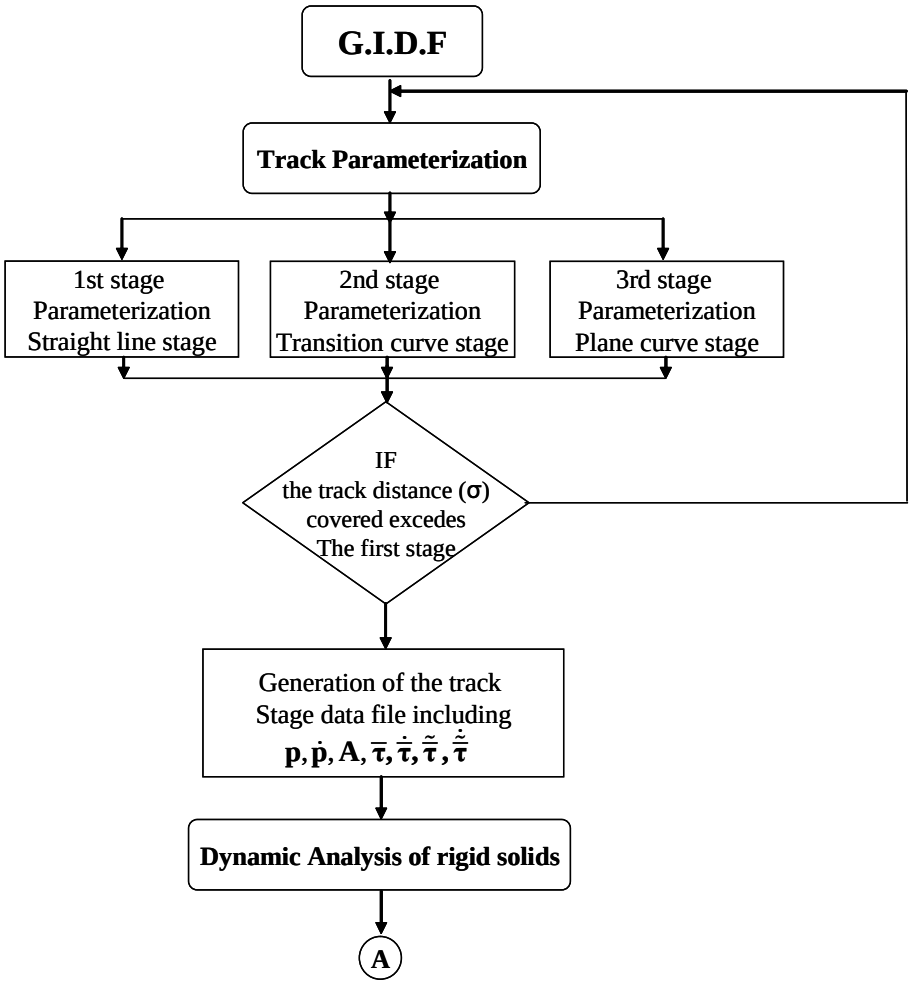
G.I.D.F
Track Parameterization
1st stage
Parameterization
Straight line stage
2nd stage
Parameterization
Transition curve stage
3rd stage
Parameterization
Plane curve stage
IF
the track distance (σ)
covered excedes
The first stage
Generation of the track
Stage data file including
p, ṗ, A, τ̄, τ̇, τ̃, τ̈̃
Dynamic Analysis of rigid solids
A

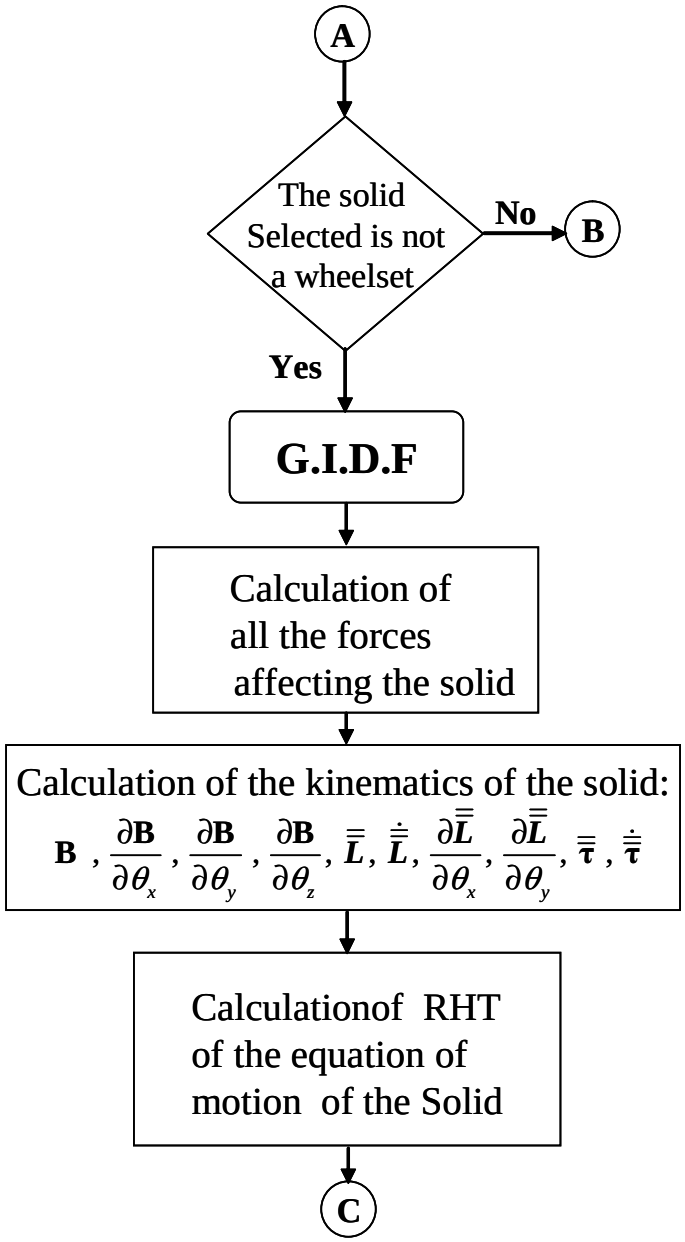
A
The solid Selected is not a wheelset
No
B
Yes
G.I.D.F
Calculation of all the forces affecting the solid
Calculation of the kinematics of the solid:
$\mathbf{B}$, $\frac{\partial \mathbf{B}}{\partial \theta_x}$, $\frac{\partial \mathbf{B}}{\partial \theta_y}$, $\frac{\partial \mathbf{B}}{\partial \theta_z}$, $\bar{\bar{L}}$, $\dot{\bar{\bar{L}}}$, $\frac{\partial \bar{\bar{L}}}{\partial \theta_x}$, $\frac{\partial \bar{\bar{L}}}{\partial \theta_y}$, $\bar{\bar{\tau}}$, $\dot{\bar{\bar{\tau}}}$
Calculationof RHT of the equation of motion of the Solid
C

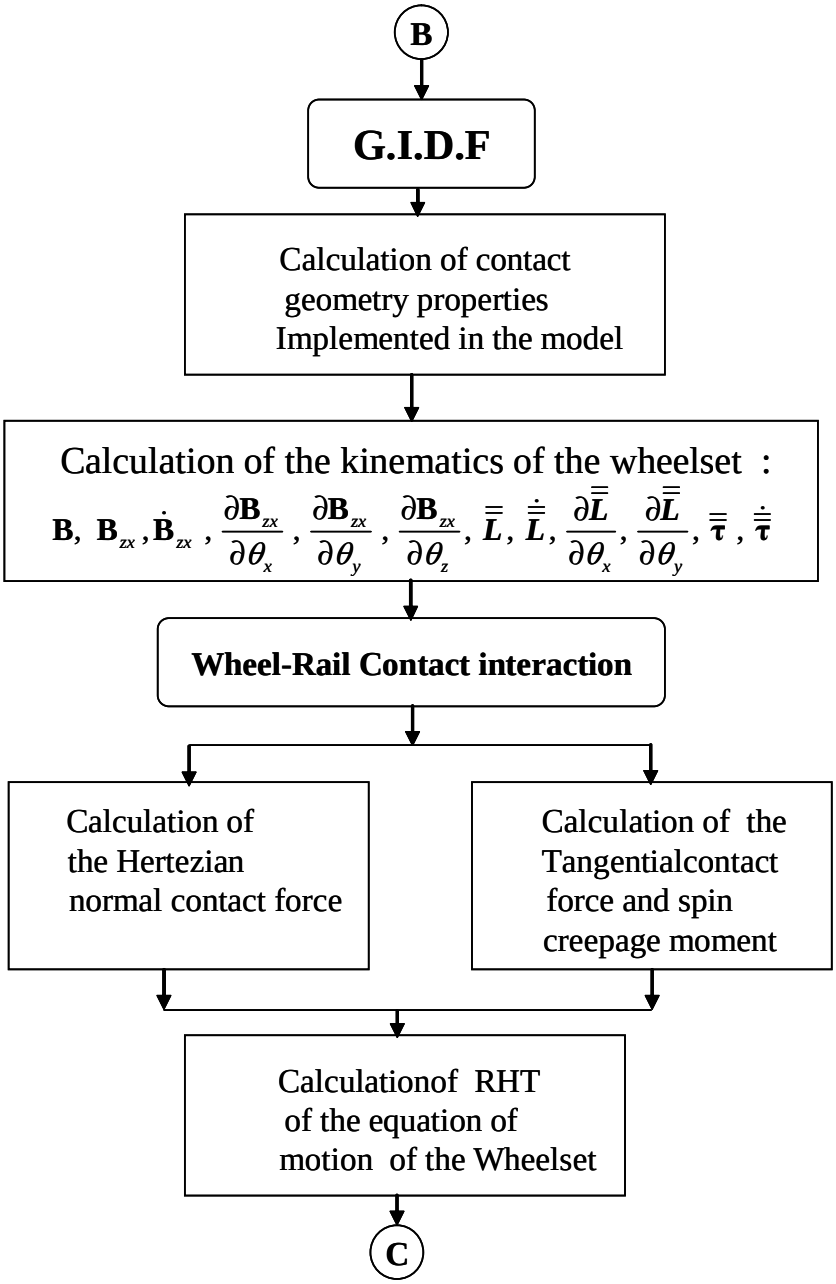
B
G.I.D.F
Calculation of contact geometry properties Implemented in the model
Calculation of the kinematics of the wheelset :
$\mathbf{B},\ \mathbf{B}_{zx},\dot{\mathbf{B}}_{zx},\ \frac{\partial \mathbf{B}_{zx}}{\partial \theta_x},\ \frac{\partial \mathbf{B}_{zx}}{\partial \theta_y},\ \frac{\partial \mathbf{B}_{zx}}{\partial \theta_z},\ \bar{\bar{L}},\ \dot{\bar{\bar{L}}},\ \frac{\partial \bar{\bar{L}}}{\partial \theta_x},\ \frac{\partial \bar{\bar{L}}}{\partial \theta_y},\ \bar{\bar{\tau}},\ \dot{\bar{\bar{\tau}}}$
Wheel-Rail Contact interaction
Calculation of the Hertezian normal contact force
Calculation of the Tangentialcontact force and spin creepage moment
Calculationof RHT of the equation of motion of the Wheelset
C

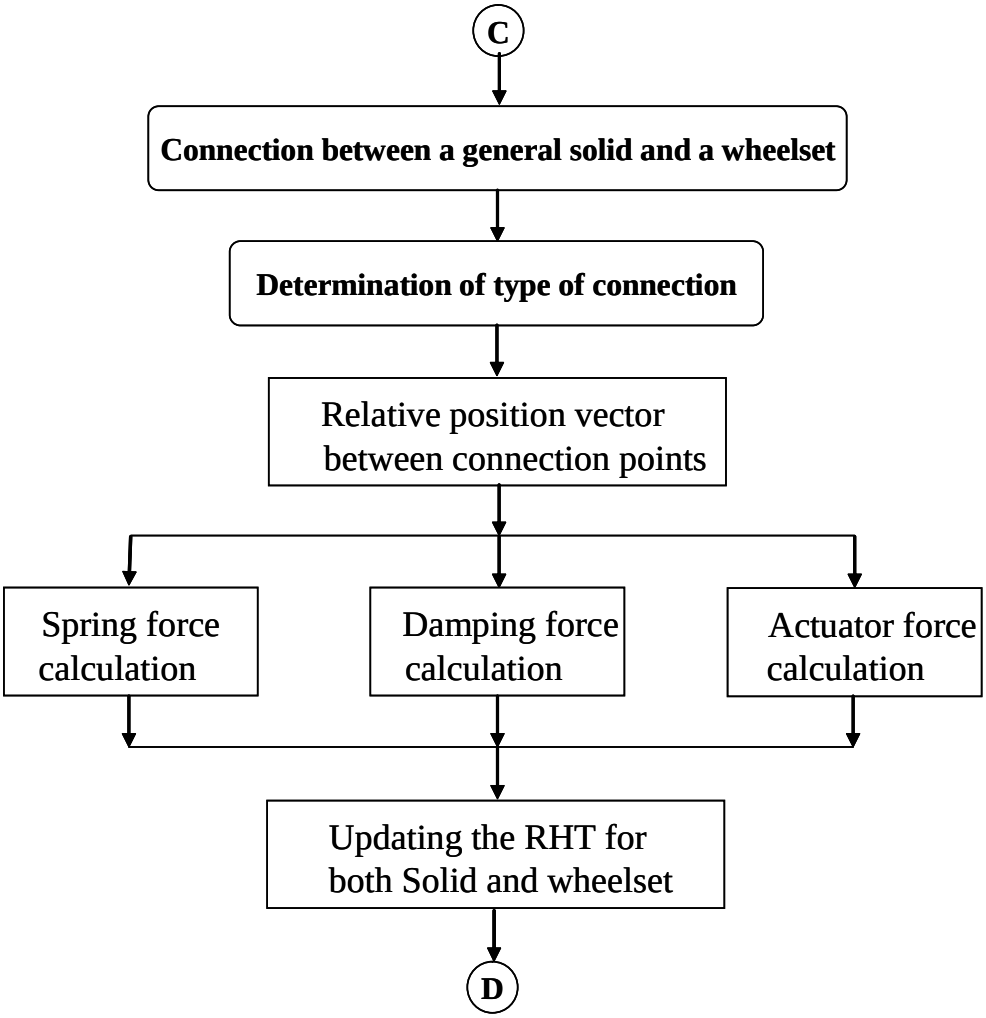
C
Connection between a general solid and a wheelset
Determination of type of connection
Relative position vector between connection points
Spring force calculation
Damping force calculation
Actuator force calculation
Updating the RHT for both Solid and wheelset
D

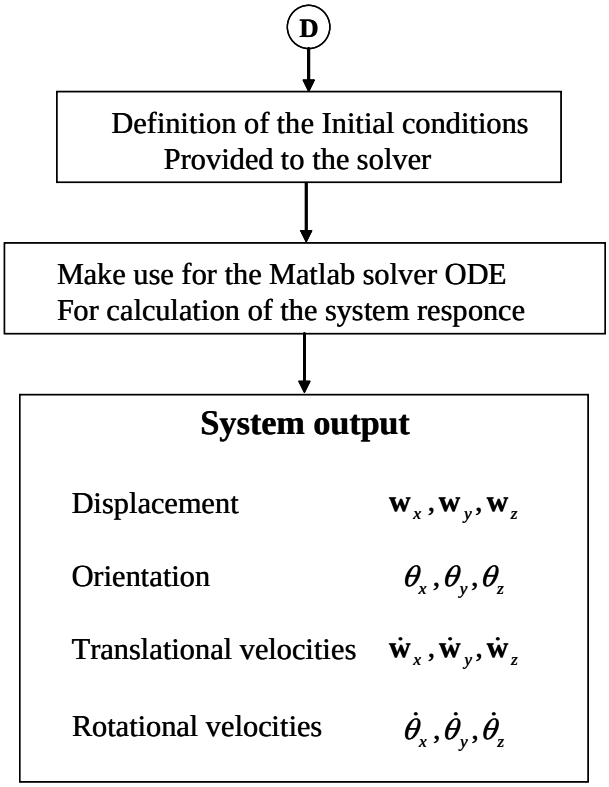
D
Definition of the Initial conditions
Provided to the solver
Make use for the Matlab solver ODE
For calculation of the system responce
System output
Displacement
$\mathbf{w}_x, \mathbf{w}_y, \mathbf{w}_z$
Orientation
$\theta_x, \theta_y, \theta_z$
Translational velocities
$\dot{\mathbf{w}}_x, \dot{\mathbf{w}}_y, \dot{\mathbf{w}}_z$
Rotational velocities
$\dot{\theta}_x, \dot{\theta}_y, \dot{\theta}_z$

5.5 Simulation results

The simulation conditions used here for the track model used in the pre-processing step is defined for the simulation of a single bogie frame negotiating the proposed track and then it was supposed to make the analysis and the simulation for a complete vehicle negotiating the designed track also.

5.5.1 Single bogie frame simulation

5.5.1.1 Single bogie negotiating straight track

The simulation condition for the Bogie frame can be defined primary by the description of the track geometry which include here a straight line stage with a length of 1000 [m] then followed by a transition curve stage with a length of 200 [m], finally the circular curve with a constant radius of 1000 [m]. The fixed frame of reference presenting the observer of the body was located at the point of the beginning of the transition curve. The bogie Fig. (5.10) including the bogie frame as a solid body and two wheelsets, was located initially on the track with out any initial misalignments or rotation that may develop any initial disturbance in the results.

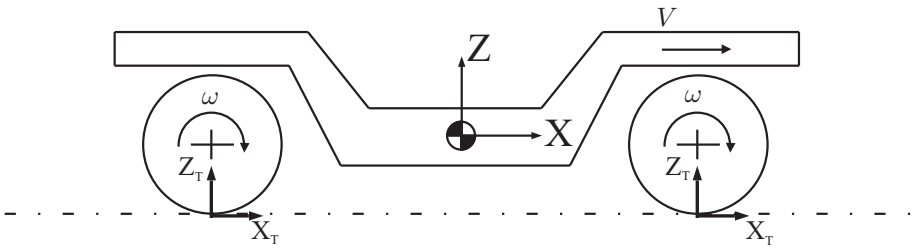

Figure 5.10. *Single bogie frame used in the simulation*

The bogie frame here was studied at the conditions of, forward velocity 20 [m/s], the angular velocity of each wheel was calculates by the following expression

$$\omega = \frac{V}{r_0} \tag{5.8}$$

where r_0 is the wheel nominal rolling radius. For the model shown of the bogie, a dynamic analysis was made to study the dynamic response of the bogie firstly moving through straight line section. The model exhibits stable response during the motion when it was moving with a velocity of 20 [m/s]. Then it was supposed to change the forward velocity to higher values to study the instability of the model and hunting motion produced during the simulation.

Fig.(5.11) shows the lateral displacement and the yaw angle of the first wheelset of the bogie frame under study. An initial misalignment with a value of 1 [mm] was given

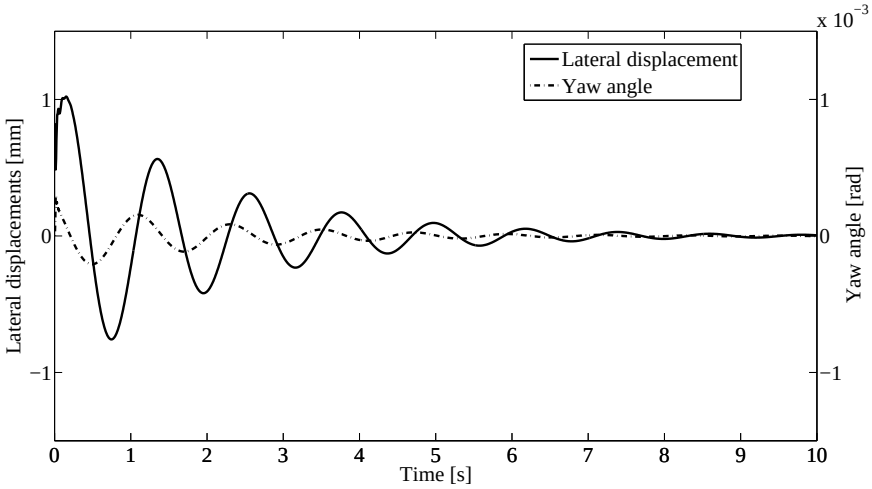

Figure 5.11. *Lateral displacement and yaw angle of 1st wheelset*

to first wheelset, and it is noted that the system returns to its stable position after 15 seconds,also this can be noted in Fig. (5.12) representing the lateral displacements of front and rear wheelsets.

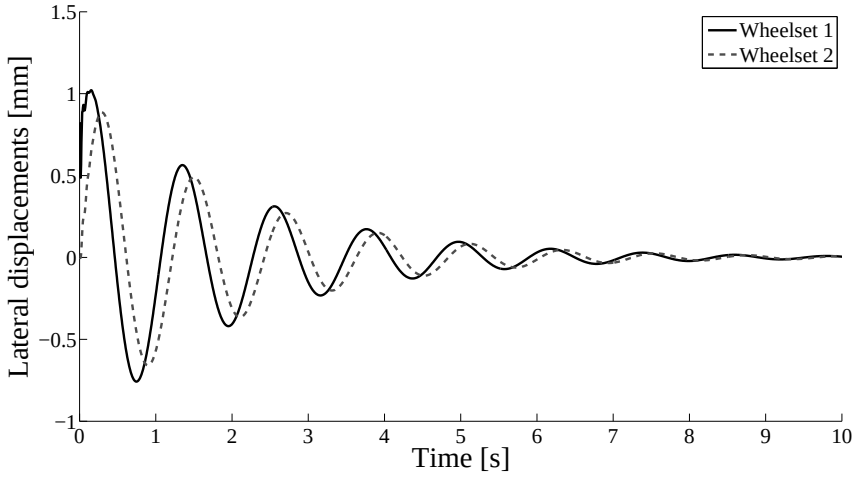

Figure 5.12. *Lateral displacement of the front and rear wheelset of the bogie*

It can be seen that the lateral displacement of the rear wheelset is shifted from the frontal one with an amount representing the distance between the center of mass of the front wheelset and the rear wheelset.

To study the instability of the system of the wheelsets, it was considered to increase the velocity to 40 [m/s] with the same value of the initial misalignment.

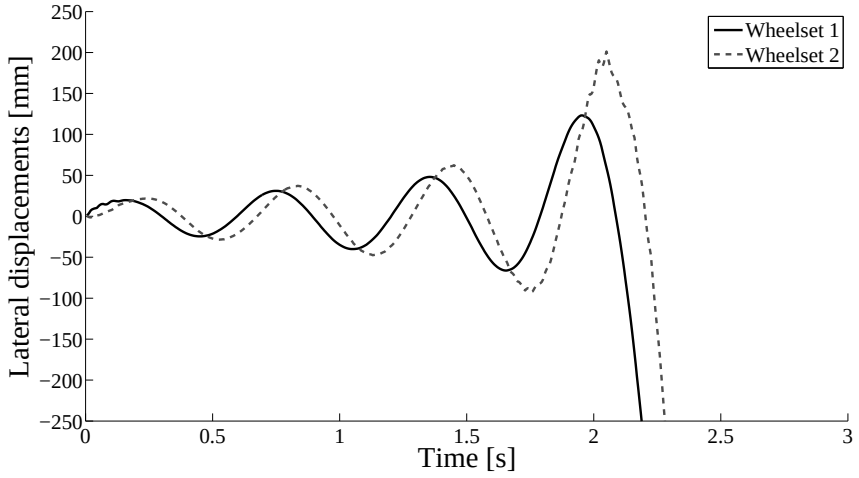

Figure 5.13. *Lateral displacement of first wheelset and second wheelset*

We can not in Fig. (5.13) that the lateral displacement of first and second wheelset, is increasing with the time and doesn't return to its stable position. This means that the system exceeds the critical velocity entering to the instability stage.

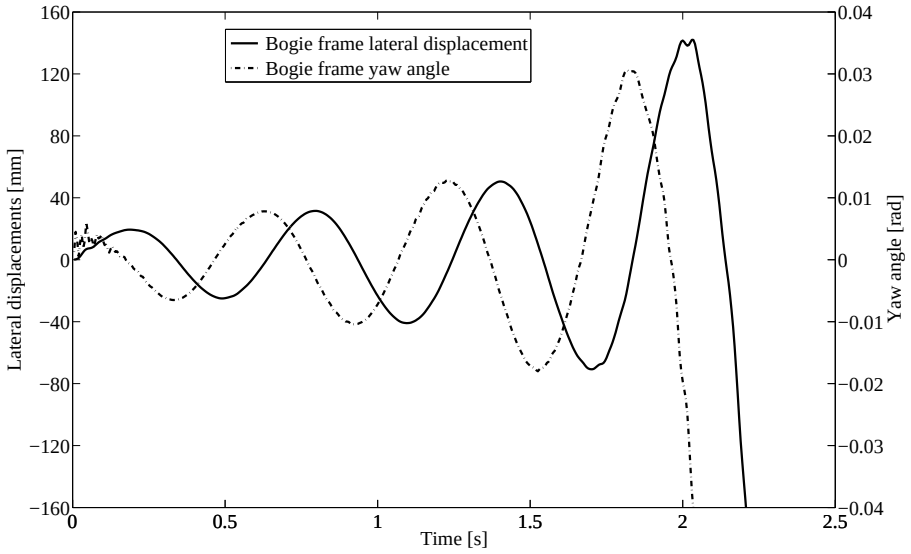

Figure 5.14. *Lateral displacement and yaw angle of the bogie frame*

Fig. (5.14) shows the lateral displacement and the yaw angle change for the bogie frame as it represent a different type of analysis for a solid which is not wheelset.

5.5.1.2 Single bogie negotiating curved track

The second scenario here in the simulation is defined for a bogie frame moving through a curved track, then it was necessary to define the transition curve stage connecting the tangent track to the constant radius circular track. The transition curve stage here taking the form of a clothoid curve with a length of 200 [m]. the transition curve here was designed to connect the tangent track defined in the previous to a canted curve with a constant radius equal to 1000 [m]. The cant was designed here for a velocity of 100 [m/s] and the equilibrium cant angle can be defined by knowing this velocity using equation (3.2).

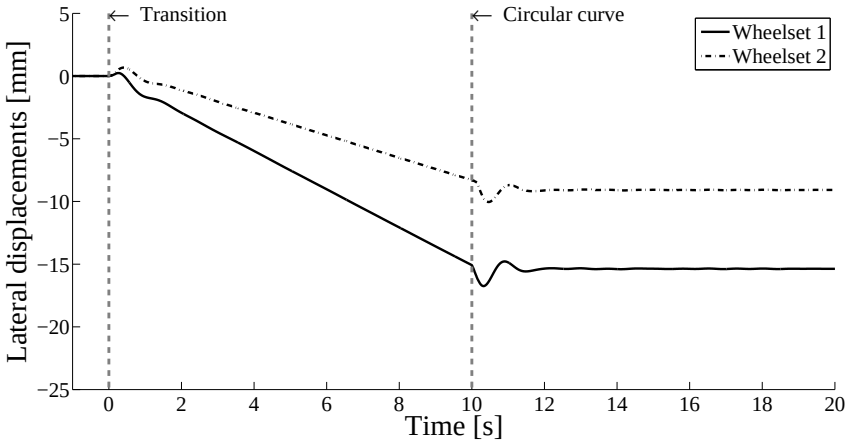

Figure 5.15. *Lateral displacement of front and rear wheelset negotiating transition curve stage*

Fig. (5.15) shows that the wheelset displaced toward the outer rail during the motion of the through the transition curve stage. The wheelsets systems return to the stability positions after they enter the constant radius circular curve stage. Fig. (5.16) shows the change in the roll angle of both wheelsets during the motion in the curved tracks provided by the used track segments in this work

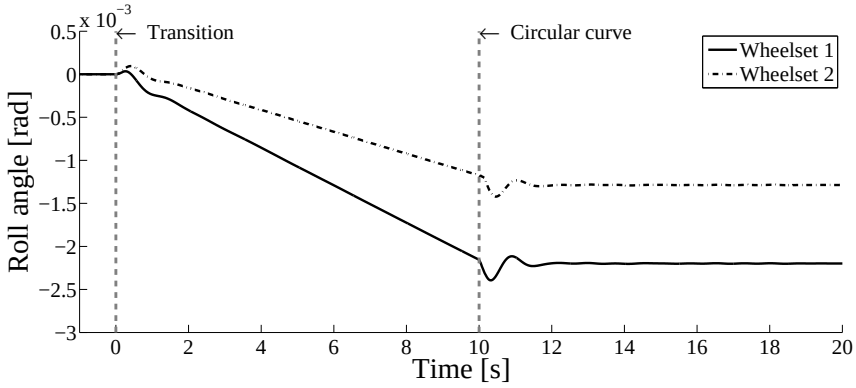

Figure 5.16. *Roll angle of the front and rear wheelset of the bogie frame*

5.5.2 Complete vehicle simulation

5.5.2.1 Complete vehicle negotiating straight track

The multibody program used for the simulation issue here, was applied for the case of a complete railway vehicle Fig. (5.3), composed as it was shown,of two bogie frames and a car body. Each bogie frame contains front and rear wheelset. The same analysis was defined here to represent the dynamic response of the complete vehicle in different simulation scenarios, starting with the motion of the vehicle systems through tangent track stage. The stability conditions for the motion was studied and with the increase in the velocity produces unstable response of the vehicle.

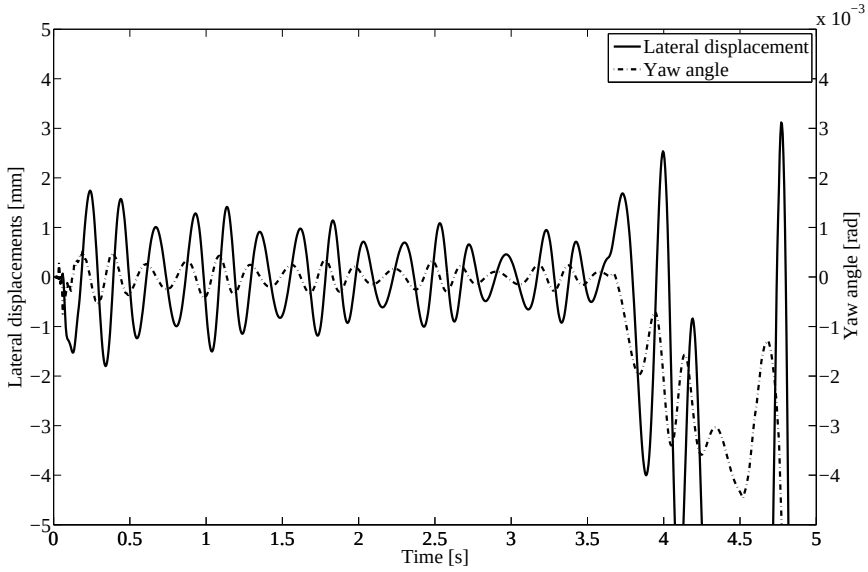

Figure 5.17. *Lateral displacement and yaw angle of the front wheelset of the front bogie frame of the complete vehicle model*

Fig. (5.17) shows unstable response for the lateral displacement of the front wheelset of the frontal bogie presented in the vehicle model.

5.5.2.2 Complete vehicle negotiating curved track

The same analysis made for a single bogie frame along the transition curve stage, was applied here for the case of complete vehicle. The lateral displacements of the wheelsets was determined for the front and rear wheelset attached to both front and rear bogie frames. We can not that the behavior of the 1^{st} wheelset of the front bogie exhibits the same as the 3^{rd} wheelset which attached to the rear bogie frame. And the same for both wheelset number 2 and wheelset number 4. It is also clear that there is a shift between the response of each wheelset from the first wheelset, this is because the wheelset enters the curved track primary and then followed by the other wheelsets separated with the amount of time required to move from the origin of the system of reference of the first wheelset to the following one.

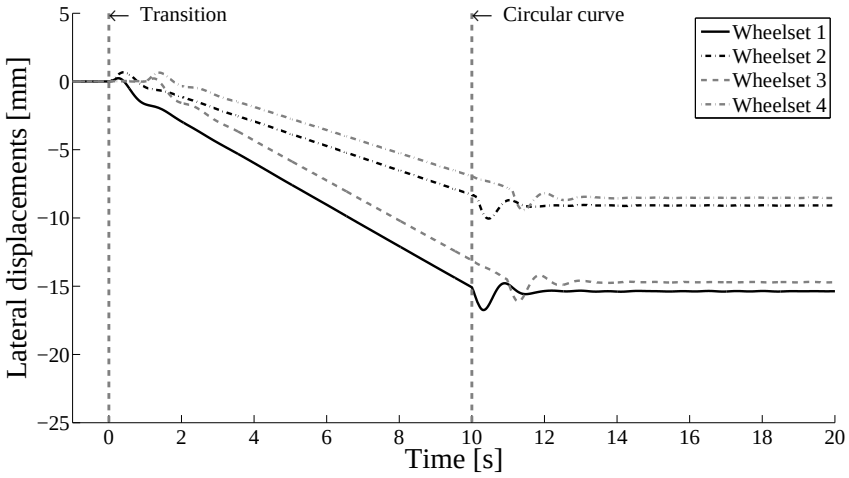

Figure 5.18. *Lateral displacement of the wheelsets attached to the front and rear bogie frames*

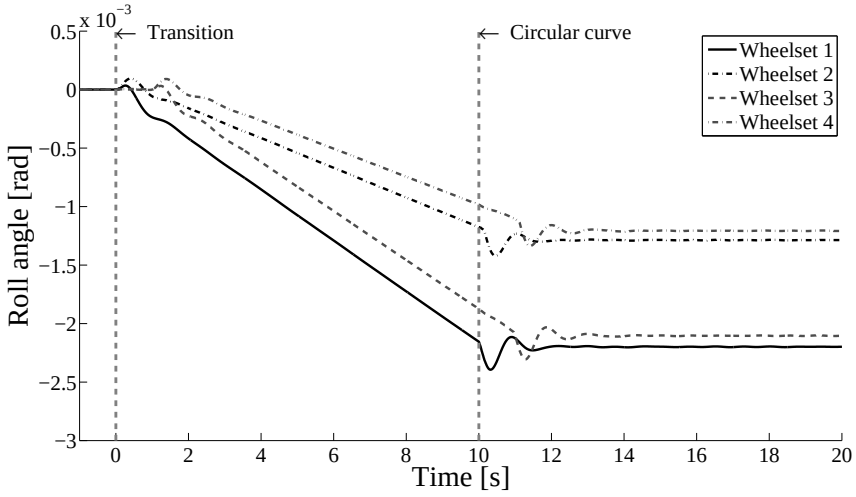

Figure 5.19. *Lateral displacement of the wheelsets attached to the front and rear bogie frames*

Fig. (5.18) and Fig. (5.19) shows the lateral displacement and the roll angle change, respectively for the front and rear wheelset systems of the vehicle during the motion through the transition curve.

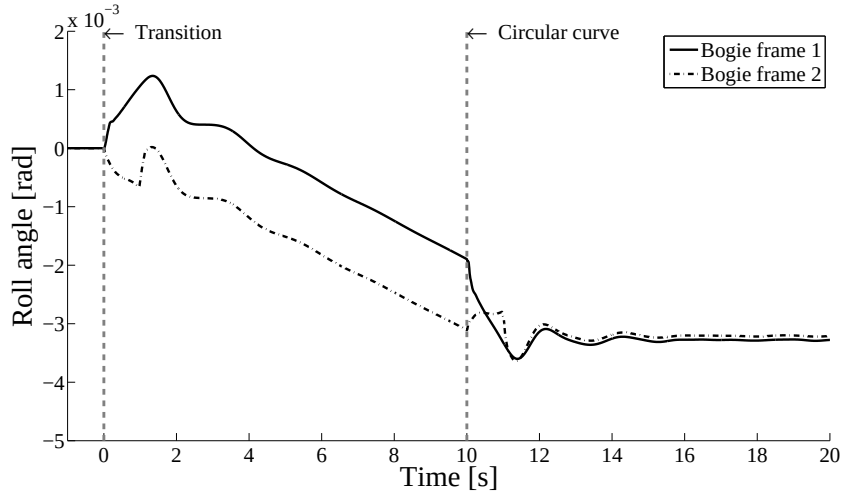

Figure 5.20. *Roll angle change of front and rear bogie frames*

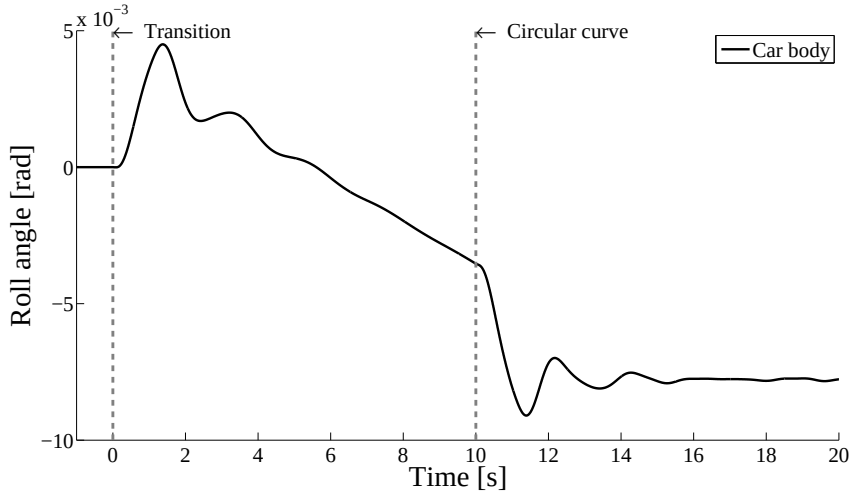

Figure 5.21. *Roll angle change of car body*

The same for the bogie frames ad the car body, the change in the roll angle Fig. (5.20) and Fig. (5.21), can be shown for both systems during the period covered by the vehicle through the transition curve stage which extends to 10 [sec] with a velocity of 20 [m/s].

Chapter 6

Conclusions and Future developments

6.1 Conclusions

In this work, a computational tool used for the dynamic analysis of railway vehicle systems was developed using mutlibody formulations. This techniques of multibodies permit the precise analysis grand displacements between the solids that compose the railway vehicle systems with out the models based on linearization. The computer program used for the analysis general multibody code is developed in MATLAB environment. It was designed to be a flexible program to have the possibility to change and incorporate different contact models and including the irregularities in the future modifications. The developed methodology for the analysis of railway vehicles using the multibody systems formulation was studied before by other authors like A. Shabana en U. Illinois, J.L.Escalona en U. Sevilla, J. Pombo en I.S.T. Lisboa and P. Fisette em U.C. Lovaina. Those authors developed other techniques based on dependent coordinates just like *Euler parameters* and *Rodriguez formula* with principal advantage which is avoiding singularity configurations. We can overcome the singularity problem as it was mentioned by the selection of the sequence of rotations applied by *Euler angles*. The selection of the intermediate reference frame associated to the wheelset systems, provides more precise definition for the contact problem. A pre-processing step was made for the track analysis to ensure the efficiency and fast calculation. a parametrization method for the track centerline was used based on the the definition of the track segments analytically. A simple model for the wheel-rail contact was used in the analysis, consists of the definition of the wheels surfaces as a conical surfaces and the rails as wires and this model is known as *knife edge model* as a first step for the determination of the position of the contact points geometrically. The study of the railway systems involves the construction of three independent models: the model of the vehicle, the model of the contact, and the track model. All

these models are implemented in the multibody computer program in order to study the dynamic analysis of the railway vehicles. Several analysis was carried out for different operation scenarios of the railroad vehicle negotiating the presented track model. The model of the vehicle was built, using only rigid bodies interconnected by force elements as it was shown in the model description section. The creepages are calculated at the wheel-rail interaction surface and the creep forces are determined using Kalker linear model. The change of the stability of the of the vehicle model used here was noted here and it was noted that for high forward velocity, the misalignment affect the stability of the vehicle. The analysis of a single bogie frame negotiating tangent track followed by the transition curve and finally to a constant circular curve, presenting the change in the lateral displacement of the wheelsets and the solid frame of the bogie during the motion through the transition curve stage. The stability of the bogie frame was changed with introducing high velocities with initial misalignments. The same computational model used in the analysis of single bogie frame, was applied to make the simulation for a complete vehicle model as it was shown in the previous section. The model was tested here with the two different type of analysis of a wheelset system and for a solid body system and both of them was treated as a rigid body in order to be implemented in the program. Further enhancements will be added to the program in with the issue of the improvement of the computational efficiency and computational time cost.

6.2 Future developments

The development of advanced railway vehicles is a complex research field that requires new ideas and novel design solutions. So the future work in the field of railway dynamics will not finish comparing with the large challenges can be faced by the research efforts in the enhancement of passenger comfort and rapid transportation using railway transportation methods. But the future work proposed by the end of this work for the improvement of the vehicle models and enhancement methodologies, can be summarized in the following points

- Including the track irregularities in the parametrization of the track, in order to provide realistic representation of the track perturbations, which affect the dynamic performance of the railway systems.
- The use of a flexible multibody approach, in which the vehicle components can be modeled as flexible bodies, can be an alternative technique to be used in the future.
- The inclusion of nonlinear spring elements, with defined stiffness characteristics and clearance, could lead to an important improvements when modeling the primary and secondary suspension elements.
- The use of other techniques for the calculations of the wheel-rail interaction problem, and choosing the suitable form of determination of the contact point positions, including two points of contact analysis.
- The inclusion of track flexibility modeling of the track also seen as future goal for this work.

Appendix A

Kinematic and Dynamic Background

A.1 Introduction

In this appendix, all the matrices used in the mathematical formulations of the models used in the kinematic presentation of the wheelset and general solid body, are presented with accurate description for all the identities and variables used in each. The calculation of each transformation matrix used in the formulation is explained in this part, its time derivative is also derived, detailed description for the and inertia matrices of the solids are also included.

A.2 Rotation matrix

A.2.1 Rotation matrix definition

In multibody systems, the components may undergo large relative translational and rotational displacements. To define the configuration of a body in the multibody system in space, one must be able to determine the location of every point on the body with respect to a selected inertial frame of reference. To this end, it is more convenient to assign for every body in the multibody system a body reference in which the position vectors of the material points can be easily described. The position vectors of these points can then be found in other coordinate systems by defining the relative position and orientation of the body coordinate system with respect to the other coordinate systems. Six variables are sufficient for definition of the position and orientation of one coordinate system X_i Y_i Z_i with respect to another coordinate system X Y Z. As shown in Fig. (A.1), three variables define the relative translational

motion between the two coordinate systems. This relative translational motion can be measured by the position vector of the origin O_i of the coordinate system X_i Y_i Z_i with respect to the coordinate system X Y Z. The orientation of one coordinate system with respect to another can be defined in terms of three independent variables[25].

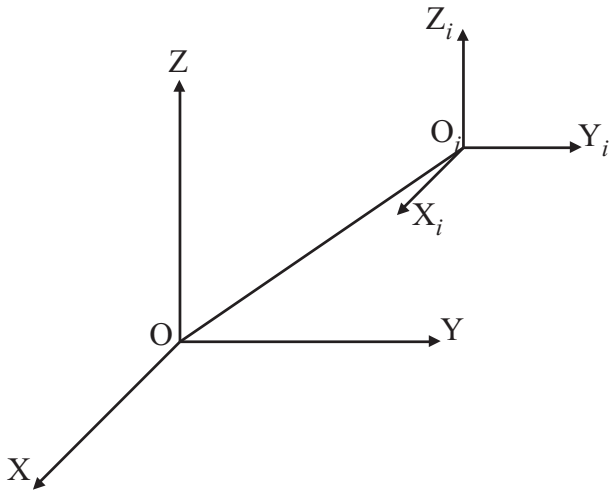

Figure A.1. *Two different coordinate systems* X Y Z *and* X_i Y_i Z_i

A.2.2 Derivation of the rotation matrix

There are several formulations used to represent the rotation matrix such as *Rodriguez formula* ,*Euler parameters* and finally *Euler angles formulations*. These forms used to determine the rotation matrix and here we use the last method depending on the definition of Euler angles representing the required transformation

A.2.3 Euler angles

The third formulation that can be used for the representation of the rotation matrix is using *Euler angles*. These angles are used to carry out the transformation from one coordinate system to another using successive rotations performed in a known sequence. Furthermore these angles used to determine the successive rotations about three axes which are not orthogonal in general, so we consider the coordinate system Z,Y and X, which represent our global frame of reference and we will show the rotation matrices produced from rotation about X-axis with an angle θ_x, which can be defined in the railway application field with by the an angle ϕ which represent the cant angle, rotation about Y-axis with angle θ_y that can be defined in the railway application by the pitch angle θ, and finally rotation about Z-axis with an angle θ_z that can be defined in the railway application by the angle of attack ψ.

A.2.4 Basic rotations

As it was introduced the orientation of a body in the space may be defined by knowing the rotations made by the body with respect to the spatial coordinates. In the following part the rotation matrices about the main spatial coordinates are represented

A.2.4.1 Rotation about X-axis

In notations used in the following context we will define the rotation matrix with the symbol $\mathbf{A}_i$, where i represents the corresponding axis of rotation (i.e $i = x$, y, and z). The rotation matrix produced from the rotation about X-axis with an angle θ_x, Fig. (A.2), can be defined as

$$\mathbf{A}_x = \begin{bmatrix} 1 & 0 & 0 \\ 0 & \cos\theta_x & -\sin\theta_x \\ 0 & \sin\theta_x & \cos\theta_x \end{bmatrix} \tag{A.1}$$

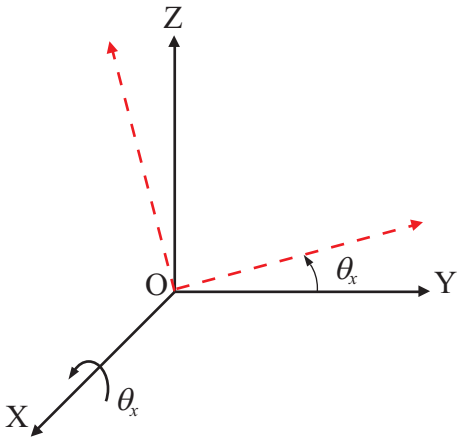

FIGURE A.2. *Rotation about* X*-axis with angle* θ_x

A.2.4.2 Rotation about Y-axis

The rotation matrix produced from the rotation about Y-axis with an angle θ_y Fig. (A.3), can be defined as

$$\mathbf{A}_y = \begin{bmatrix} \cos\theta_y & 0 & \sin\theta_y \\ 0 & 1 & 0 \\ -\sin\theta_y & 0 & \cos\theta_y \end{bmatrix} \tag{A.2}$$

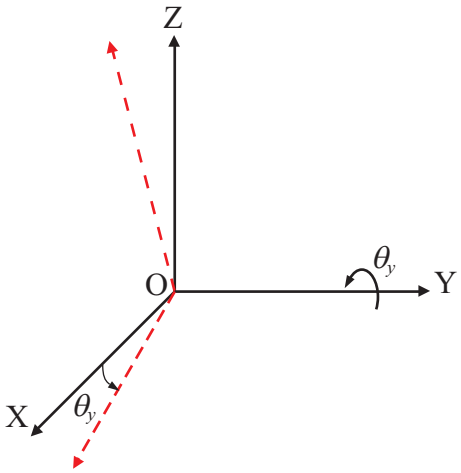

FIGURE A.3. *Rotation about* Y*-axis with angle* θ_y

A.2.4.3 Rotation about Z-axis

The rotation matrix produced from the rotation about Z-axis with an angle θ_z Fig. (A.4), can be defined as

$$\mathbf{A}_z = \begin{bmatrix} \cos\theta_z & -\sin\theta_z & 0 \\ \sin\theta_z & \cos\theta_z & 0 \\ 0 & 0 & 1 \end{bmatrix} \tag{A.3}$$

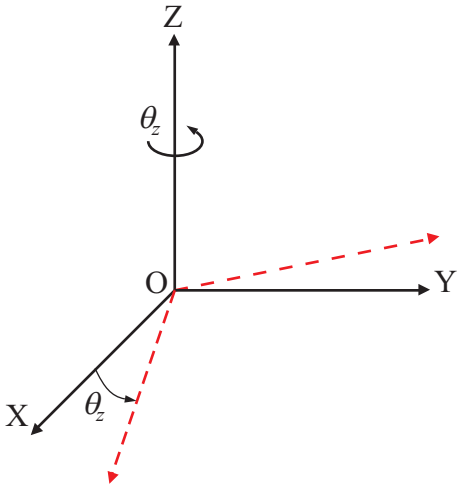

FIGURE A.4. *Rotation about* Z*-axis with angle* θ_z

A.3 Successive rotations

In this part we will represent the final rotation matrix produced from a known sequence of successive rotations, here in this part we should have to know that there are two procedures for the representation of the successive rotations, the first called *single-frame* method and the other is called *multiframe* method.

A.3.1 Single-Frame method

In this method fixed frame of reference is defined and after each rotation we define the rotational axes and the unite vectors with respect to the fixed coordinate system. Now if we consider a set of consecutive rotations using the following rotation angles θ_1, θ_2... θ_n about the unite vectors v_1, v_2... v_n respectively, the rotation matrices produced after each rotation can be calculated using any formulation from the mentioned methods used to derive the rotation matrix and denoted as $\mathbf{A}_1$, $\mathbf{A}_2$... $\mathbf{A}_n$. After n successive rotations we can calculate the final transformation matrix as

$$\mathbf{A} = \mathbf{A}_n \, \mathbf{A}_{n-1} ... \mathbf{A}_2 \, \mathbf{A}_1 \tag{A.4}$$

Where $\mathbf{A}_1$ is equal to the identity matrix.

A.3.2 Multiframe method

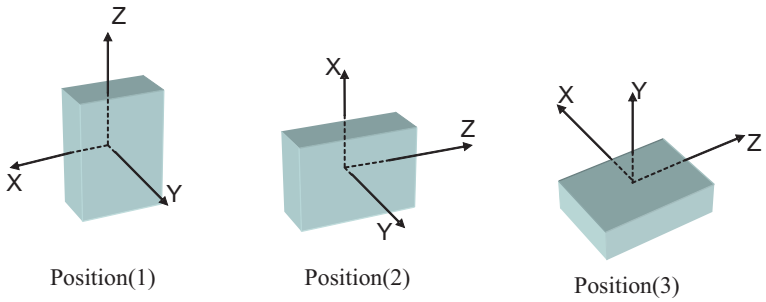

FIGURE A.5. *Successive rotation of a solid body about its reference coordinates*

This method can be discussed by this simple example. Consider that the body shown in Fig.(A.5) is subjected to two successive rotations, the first rotation is with an angle θ_1 about Y-axis producing the configuration of coordinates shown in position(2), and the second rotation with an angle θ_2 about Z-axis producing the configuration of the coordinate system shown in position(3).The orientation of coordinate system of position(2) with respect to coordinate system shown in position(1) can be described by defining the matrix $\mathbf{A}_{21}$, also the orientation of the coordinate system shown in position(3) with respect to the coordinate system shown in position(2)by defining the matrix $\mathbf{A}_{32}$,Where n is the number of position

A.4 Transformation matrices

A.4.1 Transformation matrix definition

It is the matrix required to present the different identities such as the kinematics identities and the dynamic identities of a specified reference system with respect to another frame of reference .

A.4.2 Track transformation matrix

This matrix is the matrix required to transform from the track reference frame to the global reference frame and it is calculated here by making three consecutive rotation, first rotation about Z-axis and then about Y-axis and finally about X-axis

$$\mathbf{A} = \mathbf{A}_z \, \mathbf{A}_y \, \mathbf{A}_x \tag{A.5}$$

$$\mathbf{A} = \begin{bmatrix} \cos\theta_z \, \cos\theta_y & -\sin\theta_z \, \cos\theta_x + \cos\theta_z \, \sin\theta_y \, \sin\theta_x & \sin\theta_z \, \sin\theta_x + \cos\theta_z \, \sin\theta_y \, \cos\theta_x \\ \sin\theta_z \, \cos\theta_y & \cos\theta_z \, \cos\theta_x + \sin\theta_z \, \sin\theta_y \, \sin\theta_x & -\cos\theta_z \, \sin\theta_x + \sin\theta_z \, \sin\theta_y \, \cos\theta_x \\ -\sin\theta_y & \cos\theta_y \, \sin\theta_x & \cos\theta_y \, \cos\theta_x \end{bmatrix} \tag{A.6}$$

A.4.3 Solid transformation matrix

This matrix is the matrix required to transform from the track reference frame to the solid reference frame and it is calculated here by making three consecutive rotation, first rotation about Z-axis and then about X-axis and finally about Y- axis.

$$\mathbf{B} = \mathbf{B}_z \, \mathbf{B}_x \, \mathbf{B}_y \tag{A.7}$$

$$\mathbf{B} = \begin{bmatrix} \cos\theta_z \, \cos\theta_y - \sin\theta_z \, \sin\theta_x \, \sin\theta_y & -\sin\theta_z \, \cos\theta_x & \cos\theta_z \, \sin\theta_y + \sin\theta_z \, \sin\theta_x \, \cos\theta_y \\ \sin\theta_z \, \cos\theta_y + \cos\theta_z \, \sin\theta_x \, \sin\theta_y & \cos\theta_z \, \cos\theta_x & \sin\theta_z \, \sin\theta_y - \cos\theta_z \, \sin\theta_x \, \cos\theta_y \\ -\cos\theta_x \, \sin\theta_y & \sin\theta_x & \cos\theta_x \, \cos\theta_y \end{bmatrix} \tag{A.8}$$

A.4.4 Intermediate transformation matrix

This matrix is the matrix required to transform from the track reference frame to the intermediate reference frame and it is calculated here by making three consecutive rotation, first rotation about Z-axis and then about X-axis.

$$\mathbf{B} = \mathbf{B}_z \, \mathbf{B}_x \tag{A.9}$$

$$\mathbf{B}_{zx} = \begin{bmatrix} \cos\theta_z & -\sin\theta_z \cos\theta_x & \sin\theta_z \sin\theta_x \\ \sin\theta_z & \cos\theta_z \cos\theta_x & -\cos\theta_z \sin\theta_x \\ 0 & \sin\theta_x & \cos\theta_x \end{bmatrix} \tag{A.10}$$

A.5 Angular velocity matrices

A.5.1 Absolute angular velocity matrix

$$\boldsymbol{\omega} = \boldsymbol{\tau} + \boldsymbol{L}\dot{\boldsymbol{\theta}} \tag{A.11}$$

where $\boldsymbol{\tau}$ is the absolute angular velocity of the track and it can be calculated knowing the value of the angular velocity $\bar{\boldsymbol{\tau}}$ represented in the track reference frame. The value of $\bar{\boldsymbol{\tau}}$ can be calculated by defining the skew symmetric matrix of the track angular velocity vector represented in the track reference frame $\tilde{\bar{\boldsymbol{\tau}}}$

A.5.2 Skew symmetric matrix of the track angular velocity vector

$$\tilde{\bar{\boldsymbol{\tau}}} = \mathbf{A}^{\mathrm{T}} \, \dot{\mathbf{A}} \tag{A.12}$$

$$\tilde{\bar{\boldsymbol{\tau}}} = \begin{bmatrix} 0 & -\cos\theta_y \, \dot{\theta}_z \, \cos\theta_x + \sin\theta_x \, \dot{\theta}_y & \cos\theta_y \, \dot{\theta}_z \, \sin\theta_x + \cos\theta_x \, \dot{\theta}_y \\ \cos\theta_y \, \dot{\theta}_z \, \cos\theta_x - \sin\theta_x \, \dot{\theta}_y & 0 & -\dot{\theta}_x + \sin\theta_y \, \dot{\theta}_z \\ -\cos\theta_y \, \dot{\theta}_z \, \sin\theta_x - \cos\theta_x \, \dot{\theta}_y & \dot{\theta}_x - \sin\theta_y \, \dot{\theta}_z & 0 \end{bmatrix} \tag{A.13}$$

A.5.3 Track angular velocity vector represented in track frame

$$\bar{\boldsymbol{\tau}} = \begin{bmatrix} \dot{\theta}_x - \sin\theta_y \, \dot{\theta}_z \\ \cos\theta_y \, \dot{\theta}_z \, \sin\theta_x + \cos\theta_x \, \dot{\theta}_y \\ \cos\theta_y \, \dot{\theta}_z \, \cos\theta_x - \sin\theta_x \, \dot{\theta}_y \end{bmatrix} \tag{A.14}$$

A.5.4 Absolute relative angular velocity of the solid

The value of the matrix **L** depends on the rotation sequence. It represents the matrix that relates the absolute angular velocity vector of the rigid body defined in the global reference frame to the time derivative of the orientation parameters[shabana, chamarro- shabana railroad]. Then by definition of the unite vectors v_1, v_2, and v_3 acting along the three axes of rotations Z, X, and Y respectively with respect to the global reference frame Fig. (A.6), we can define the matrix $\bar{\mathbf{L}}$ as it is represented in the track reference frame

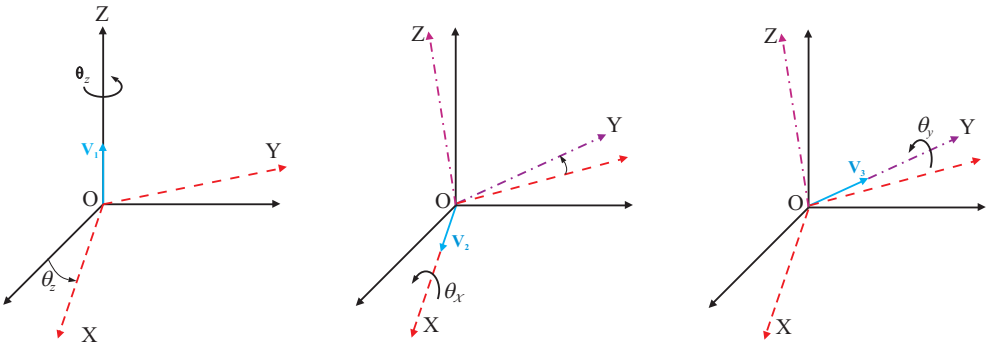

FIGURE A.6. *Consecutive rotations of the solid*

$$\mathbf{v}_1 = \begin{bmatrix} 0 & 0 & 1 \end{bmatrix}^{\mathrm{T}} \tag{A.15}$$

$$\mathbf{v}_2 = \begin{bmatrix} \cos\theta_z & \sin\theta_z & 0 \end{bmatrix}^{\mathrm{T}} \tag{A.16}$$

$$\mathbf{v}_3 = \begin{bmatrix} -\sin\theta_z \cos\theta_x & \cos\theta_z \cos\theta_x & \sin\theta_x \end{bmatrix}^{\mathrm{T}} \tag{A.17}$$

then the relative angular velocity matrix can be defined corresponding to Fig.(A.6) as follow

$$\bar{\boldsymbol{L}}\dot{\boldsymbol{\theta}} = \begin{bmatrix} \mathbf{v}_2 & \mathbf{v}_3 & \mathbf{v}_1 \end{bmatrix} \dot{\boldsymbol{\theta}} \tag{A.18}$$

the matrix $\bar{\boldsymbol{L}}$ defined in the track reference frame can be found by

$$\bar{\boldsymbol{L}} = \begin{bmatrix} \cos\theta_z & -\sin\theta_z \cos\theta_x & 0 \\ \sin\theta_z & \cos\theta_z \cos\theta_x & 0 \\ 0 & \sin\theta_x & 1 \end{bmatrix} \tag{A.19}$$

By knowing the transformation matrix **B** we can express the matrix $\boldsymbol{L}$ in the solid frame of reference as follow

$$\bar{\bar{\boldsymbol{L}}} = \mathbf{B}^{\mathrm{T}} \bar{\boldsymbol{L}} \tag{A.20}$$

$$\bar{\bar{\boldsymbol{L}}} = \begin{bmatrix} \cos\theta_y & 0 & -\cos\theta_x \sin\theta_y \\ 0 & 1 & \sin\theta_x \\ \sin\theta_y & 0 & \cos\theta_x \cos\theta_y \end{bmatrix} \tag{A.21}$$

A.6 Inertia properties of the solid body

A.6.1 Mass matrix of solid

$$\mathbf{M}_s = m_s \, \mathbf{I}_{3\times 3} \tag{A.22}$$

where m_s is the mass of the solid and $\mathbf{I}$ is 3×3 identity matrix

A.6.2 Inertia matrix of solid

$$\boldsymbol{J}_{\theta\theta} = \begin{bmatrix} J_{xx} & 0 & 0 \\ 0 & J_{yy} & 0 \\ 0 & 0 & J_{zz} \end{bmatrix} \tag{A.23}$$

The elements J_{ij} represent the mass moment of inertia of the solid body and for rigid bodies these terms are constants, also when $i \neq j$ then it called the product of inertia, but for deformable bodies these terms are time independent

A.7 Time derivative of transformation matrices

A.7.1 Time derivative of the Track transformation matrix

recalling the expression of the transformation matrix in the track frame of reference

$$\mathbf{A} = \mathbf{A}_z \, \mathbf{A}_y \, \mathbf{A}_x \tag{A.24}$$

the time derivative of the matrix $\mathbf{A}$ can be written as

$$\dot{\mathbf{A}} = \frac{\partial \mathbf{A}}{\partial t} \tag{A.25}$$

but the matrix $\mathbf{A}$ is not a function of the time, then by using the chain rule , the time derivative of the matrix $\mathbf{A}$ can be written as

$$\dot{\mathbf{A}} = \frac{\partial \mathbf{A}}{\partial \theta} \, \frac{\partial \theta}{\partial t} \tag{A.26}$$

$$\dot{\mathbf{A}} = \frac{\partial \mathbf{A}}{\partial \theta_z}\,\dot{\theta}_z + \frac{\partial \mathbf{A}}{\partial \theta_y}\,\dot{\theta}_y + \frac{\partial \mathbf{A}}{\partial \theta_x}\,\dot{\theta}_x \tag{A.27}$$

the partial derivative of the matrix $\mathbf{A}$ with respect to the three rotation angles as follow

$$\frac{\partial \mathbf{A}_x}{\partial \theta_x} = \begin{bmatrix} 0 & 0 & 0 \\ 0 & -\sin\theta_x & -\cos\theta_x \\ 0 & \cos\theta_x & -\sin\theta_x \end{bmatrix} \tag{A.28}$$

$$\frac{\partial \mathbf{A}_y}{\partial \theta_y} = \begin{bmatrix} -\sin\theta_y & 0 & \cos\theta_y \\ 0 & 0 & 0 \\ -\cos\theta_y & 0 & -\sin\theta_y \end{bmatrix} \tag{A.29}$$

$$\frac{\partial \mathbf{A}_z}{\partial \theta_z} = \begin{bmatrix} -\sin\theta_z & -\cos\theta_z & 0 \\ \cos\theta_z & -\sin\theta_z & 0 \\ 0 & 0 & 0 \end{bmatrix} \tag{A.30}$$

A.7.2 Time derivative of Solid transformation matrix

The same can be done for the transformation matrix $\mathbf{B}$ between the solid frame of reference and the track frame of reference

$$\mathbf{B} = \mathbf{B}_z\,\mathbf{B}_x\,\mathbf{B}_y \tag{A.31}$$

$$\dot{\mathbf{B}} = \frac{\partial \mathbf{B}}{\partial t} \tag{A.32}$$

$$\dot{\mathbf{B}}_{zx} = \frac{\partial \mathbf{B}_{zx}}{\partial \theta_z}\,\dot{\theta}_z + \frac{\partial \mathbf{B}_{zx}}{\partial \theta_x}\,\dot{\theta}_x \tag{A.33}$$

A.7.3 Time derivative of Intermediate transformation matrix

The same for the transformation matrix $\mathbf{B_{zx}}$

$$\mathbf{B}_{zx} = \mathbf{B}_z\,\mathbf{B}_x \tag{A.34}$$

$$\dot{\mathbf{B}}_{zx} = \frac{\partial \mathbf{B}_{zx}}{\partial t} \tag{A.35}$$

$$\dot{\mathbf{B}}_{zx} = \frac{\partial \mathbf{B}_{zx}}{\partial \theta_z}\,\dot{\theta}_z + \frac{\partial \mathbf{B}_{zx}}{\partial \theta_x}\,\dot{\theta}_x \tag{A.36}$$

Appendix B

Tables Used

	c_{11}			c_{12}			c_{23}			c_{33}		
g	$\nu = 0$	0.25	0.5	$\nu = 0$	0.25	0.5	$\nu = 0$	0.25	0.5	$\nu = 0$	0.25	0.5
(a/b)												
0.1	2.51	3.31	4.85	2.51	2.52	2.53	0.334	0.473	0.731	6.42	8.28	11.7
0.2	2.59	3.37	4.81	2.59	2.63	2.66	0.483	0.603	0.809	3.46	4.27	5.66
0.3	2.68	3.44	4.80	2.68	2.75	2.81	0.607	0.715	0.889	2.49	2.96	3.72
0.4	2.78	3.53	4.82	2.78	2.88	2.98	0.720	0.823	0.977	2.02	2.32	2.77
0.5	2.88	3.62	4.83	2.88	3.01	3.14	0.827	0.929	1.07	1.74	1.93	2.22
0.6	2.98	3.72	4.91	2.98	3.14	3.31	0.930	1.03	1.18	1.56	1.68	1.86
0.7	3.09	3.81	4.97	3.09	3.28	3.48	1.03	1.14	1.29	1.43	1.50	1.60
0.8	3.19	3.91	5.05	3.19	3.41	3.65	1.13	1.25	1.40	1.34	1.37	1.42
0.9	3.29	4.01	5.12	3.29	3.54	3.82	1.23	1.36	1.51	1.27	1.27	1.27
(b/a)												
1.0	3.40	4.12	5.20	3.40	3.67	3.98	1.33	1.47	1.63	1.21	1.19	1.16
0.9	3.51	4.22	5.30	3.51	3.81	4.16	1.44	1.59	1.77	1.16	1.11	1.06
0.8	3.65	4.36	5.42	3.65	3.99	4.39	1.58	1.75	1.94	1.10	1.04	0.954
0.7	3.82	4.54	5.58	3.82	4.21	4.67	1.76	1.95	2.18	1.05	0.965	0.852
0.6	4.06	4.78	5.80	4.06	4.50	5.04	2.01	2.23	2.50	1.01	0.892	0.751
0.5	4.37	5.10	6.11	4.37	4.90	5.56	2.35	2.62	2.96	0.958	0.819	0.650
0.4	4.84	5.57	6.57	4.84	5.48	6.31	2.88	3.24	3.70	0.912	0.747	0.549
0.3	5.57	6.34	7.34	5.57	6.40	7.51	3.79	4.32	5.01	0.868	0.674	0.446
0.2	6.96	7.78	8.82	6.96	8.14	9.79	5.72	6.63	7.89	0.828	0.601	0.341
0.1	10.7	11.7	12.9	10.7	12.8	16.0	12.2	14.6	18.0	0.795	0.526	0.228

Table B.1. *Kalker's creepage and spin coefficients*

Bibliography

[1] H. Akima. A new method of interpolation and smooth curve fitting based on local procedures. *Journal of the Association for Computational Machinery*, 17 (4), 1970.

[2] J. Ambrósio. *Advances in Computational Multibody Systems*. Springer, Dordrecht, Netherland, 2005.

[3] F. M. L. Amirouche. *Fundamentals of Multibody Dynamics: Theory and Applications*. Birkhäuser, Boston, 2006.

[4] C. Andersson and T. Abrahamsson. Simulation of interaction between a train in general motion and track. *Vehicle System Dynamics*, 38(6), 2002.

[5] R V . Dukkipati. *Vehicle Dynamics*. CRC Press, New York, 2000.

[6] V K. Grag and R V . Dukkipati. *Dynamics of Railway Vehicle Systems*. Academic Press, New York, 1984.

[7] M. Ishida, T. Moto, and M. Takikawa. The effect of lateral creepage force on rail corrugation on low rail at sharp curves. *Journal of Wear*, 253, 2002.

[8] S. Iwnicki. Simulation of wheel-rail contact forces.

[9] S. Iwnicki. *Handbook of Railway Vehicle Dynamics*. CRC Press, New York, 2006.

[10] S. Iwnicki and A. H Wickens. Validation of a matlab railway vehicle simulation using a scale roller rig. *Vehicle System Dynamics*, 30, 1998.

[11] J. Jalon and E. Bayo. *Kinematic and Dynamic Simulation of Multibody Systems : The Real-Time Challenge*. Springer-Verlage, New York, 1994.

[12] J. J. Kalker. Survey of wheel-rail rolling contact theory. *Vehicle System Dynamics*, 8(4), 1979.

[13] J. J. Kalker. Wheel-rail rolling contact. *Journal of Wear*, 144, 1979.

[14] J. J. Kalker. A fast algorithm for the simplified theory of rolling-contact. *Vehicle System Dynamics*, 11(1), 1982.

[15] J. J. Kalker. Three dimensional elastic bodies in rolling contact. *Kluwer Academic publishers, Dordrecht*, 1990.

[16] E. Kassa, C. Andersson, and J. C. O. Nielsen. Simulation of dynamic interaction between trainand railway turnout. *Vehicle System Dynamics*, 44(3), 2006.

[17] E. Meli, M. Malvezzi, S. Papini, L. Pugi, and A. Rindi. A railway vehicle multibody model for real-time application. *Vehicle System Dynamics*, 46(2), 2008.

[18] A. D. Monk-Steel, D. J. Thompson, F. G. de Beer, and M. H. A. Janssens. An investigation into the influence of longitudinal creepage on railway squeal noise due to lateral creepage. *Journal of Sound and Vibration*, 293, 2006.

[19] Parviz E. Nikravesh. *Computer-Aided Analysis of Mechanical Systems*. Parentice Hall, Engelwood cliffs, New York, 1988.

[20] J. Pombo. *A multibody methodology for railway dynamics applications*. PhD thesis, Instituto Superior Técnico, Universidad Técnica de Lisboa, 2004.

[21] J. Pombo and J. Ambrósio. A computational efficient general wheel-rail contact detection method.

[22] J. Pombo and J. Ambrósio. Development of Roller Coaster Model. In *Proceeding of the Métodos Numéricos en Ingeniería V,(J. Goicolea et al Eds.)*. SEMNI, Madrid, Spain, 2002.

[23] J. Pombo and J. Ambrósio. General spatial curve joint for rail guided vehicles: kinematics and dynamics. *Multibody System Dynamics*, 9, 2003.

[24] J. Pombo and J. Ambrósio. A new wheel-rail contact model for railway dynamics. *Vehicle System Dynamics*, 45(10), 2007.

[25] A. A. Shabana. *Dynamics of Multibody Systems, Second Edition*. Cambridge University Press, Cambridge, United Kingdom, 1998.

[26] A. A. Shabana and J. R. Sany. A survey of rail vehicle track simulation and flexible multibody dynamics. *Nonlinear Dynamics*, 26, 2001.

[27] A. A. Shabana, K. E. Zaazaa, J. L. Escalona, and J. R. Sany. Development of elastic force model for wheel/rail contact problems. *Journal of Sound and Vibration*, 269, 2004.

[28] A. A. Shabana, R. Chamorro, and C. Rathod. A multi-body system approach for finite-element modelling of rail flexibility in railroad vehicle applications. *Proc. IMechE, Part K: Journal of Multi-body*, 222(1), 2008.

[29] A. A. Shabana, K. E. Zaazaa, and H. Sugiyam. *Rail Road Vehicle Dynamics : A Computational Approach*. CRC Press, Taylor and Francis group, New York, 2008.

[30] W. Zhai, K. Wang, and C. Cai. Fundamentals of vehicle-track coupled dynamics. *Vehicle System Dynamics*, 47(11), 2009.